



**SEISMIC STUDY OF THE ORANGE BASIN, OFFSHORE NAMIBIA AND  
ITS RELEVANCE FOR HYDROCARBON SYSTEM ANALYSIS**

A THESIS SUBMITTED IN FULFILLMENT OF THE REQUIREMENT FOR

THE DEGREE OF

MASTER OF SCIENCE IN GEOLOGY

OF

THE UNIVERSITY OF NAMIBIA

By

**Victoria Sibeya**

**Student Number: 9819509**

November 2014

Main Supervisor: Dr. Ansgar Wanke

**ABSTRACT**

The Orange Basin is located on the South-west African continental margin adjacent to the boundary between South Africa and Namibia. The interpretation of the existing 2D seismic and well data using Petrel software provided a structural and stratigraphic analysis of the Orange Basin. The objective of the study is to identify and characterize the regional petroleum systems and reveal the sequence of depositional events and structural developments which occurred in the Basin. Four major tectonostratigraphic units separated by three major unconformities were identified as Pre-rift (Carboniferous to early Permian), Syn-rift (late Jurassic to Hauterivian), Early drift (Barremian to Cenomanian) and Late Cretaceous (Turonian to recent). The stratigraphic analysis of seismic data revealed a number of depositional features such as clinoforms, channels and palaeo highs which were used to depict different depositional environments in the Basin.

Onshore analogues such as the aeolian/lava deposits of the Huab Basin, Kalkrand Formation, Ganigobis Shale Member, Whitehill Formation and Orange River Mouth deposits provides an insight into the depositional history of the Orange Basin.

There is a complete petroleum system in Orange Basin which consists of a lacustrine Synrift section, succeeded by Barremian to early Aptian and Cenomanian-Turonian source rocks. Three potential reservoir intervals have been identified, one in the lacustrine Synrift section, the second in aeolian/lava deposits of the Barremian section and the youngest one in Tertiary sandstones. The Orange Basin exhibits both, stratigraphic and structural traps. Deep marine Cretaceous to Tertiary shales are

predicted to act as seals in the Pre-rift, Syn-rift and Drift sequences. Less faulted Cretaceous and Tertiary shales reveal a good quality seal. Faulting augments the migration pathway of hydrocarbons in the Basin. The southern part of the Basin is considered to be more prospective because it attains thick sediment accumulations which augment source rock maturity and contains most of the stratigraphic and structural closures in the Basin.

## **ACKNOWLEDGEMENT**

I would first like to express my most sincere gratitude to my supervisor Dr. Ansgar Wanke, for his support and supervision offered in every aspect of my studies towards this Thesis. The encouragements and assistance rendered with many constructive discussions contributed greatly to the success of this study.

A special thank you goes to the National Petroleum Corporation of Namibia (NAMCOR) Ltd, for supplying data used in this study and also partially funding the Orange River field-trip.



Finally, I would like to thank Schlumberger for donating Petrel software to the University of Namibia which was used for this study.



**DECLARATION**

I, Victoria Sibeya, declare hereby that this study is a true reflection of my own research, and that this work, or part thereof has not been submitted for a degree in any other institution of higher education.

No part of this thesis may be reproduced, stored in any retrieval system, or transmitted in any form, or by means (e.g. electronic, mechanical, photocopying, recording or otherwise) without the prior permission of the author, or The University of Namibia in that behalf.

I, Victoria Sibeya, grant the University of Namibia the right to reproduce this thesis in whole or in part, in any manner or format, which the University of Namibia may deem fit, for any person or institution requiring it for study and research; providing that The University of Namibia shall waive this right if the whole thesis has been or is being published in a manner satisfactory to the University.

.....  
Victoria Sibeya

.....  
Date

## **TABLE OF CONTENTS**

<b>ABSTRACT .....</b>	<b>ii</b>
<b>ACKNOWLEDGEMENT .....</b>	<b>iv</b>
<b>DECLARATION.....</b>	<b>v</b>
<b>LIST OF FIGURES .....</b>	<b>x</b>
<b>LIST OF TABLES .....</b>	<b>xx</b>
<b>CHAPTER 1: INTRODUCTION.....</b>	<b>1</b>
1.1 BACKGROUND TO THE RESEARCH .....	1
1.2 EXPLORATION HISTORY .....	3
1.3 STATEMENT OF THE PROBLEM.....	8
1.4 OBJECTIVES OF THE STUDY .....	8
<b>CHAPTER 2: LITERATURE REVIEW.....</b>	<b>10</b>
<b>CHAPTER 3: MATERIAL AND METHODOLOGY.....</b>	<b>22</b>
3.1 AVAILABLE DATA.....	22
3.2 INTERPRETATION APPROACH .....	25
3.2.1 <i>Data analysis</i> .....	25
3.2.2 <i>Seismic to well tie</i> .....	28
3.2.3 <i>Stratigraphic analysis</i> .....	32
i. Seismic Facies Analysis.....	36
ii. Identification of System Tracts .....	41
3.2.4 <i>Structural Analysis</i> .....	44

3.2.5 Petroleum System.....	45
3.2.6 Onshore Analogues .....	45
<b>CHAPTER 4: RESULTS AND ANALYSIS.....</b>	<b>47</b>
4.1 STRATIGRAPHIC ANALYSIS .....	47
4.1.1 Well Correlation .....	47
4.1.2 Overview of the Orange Basin.....	53
4.1.3 Stratigraphic Framework.....	57
4.1.3.1 Pre-Rift (Carboniferous to Mid Jurassic).....	57
i. Structural History Review.....	57
ii. Depositional Review .....	59
iii. Seismic Interpretation (own observations) .....	60
4.1.3.2 Syn-Rift.....	62
i. Structural History Review.....	62
ii. Depositional Review .....	63
iii. Seismic Interpretation (own observations) .....	63
4.1.3.3 <b>Early Drift</b> .....	65
i. Structural History Review.....	65
ii. Depositional Review .....	65
iii. Seismic Interpretation (own observations) .....	66
iv. Seismic facies (own observation) .....	66
4.1.3.4 <b>Late Drift</b> .....	69
i. Structural History Review.....	69
ii. Depositional Review .....	69
iii. Interpretation (own observations).....	70

iv. Seismic Facies (own observations).....	71
4.2. <i>Summary</i> .....	80
4.3 STRUCTURAL MAPPING.....	85
4.3.1 <i>Base Barremian</i> .....	85
4.3.2 <i>Mid-Aptian</i> .....	88
4.3.3 <i>Turonian Unconformity</i> .....	92
4.3.4 <i>Top Santonian Unconformity</i> .....	95
4.3.5 <i>Base Tertiary Unconformity</i> .....	99
4.3.6 <i>Summary</i> .....	104
4.4 PETROLEUM SYSTEMS.....	109
4.4.1 <i>Source Rock Intervals</i> .....	109
iii. Pre-rift source rock.....	109
ii. Syn-rift lacustrine source rock.....	110
iii. Barremian to Early Aptian.....	111
iv. Cenomanian-Turonian.....	115
4.4.2 <i>Reservoir Rock Intervals</i> .....	118
4.4.3 <i>Traps And Migration Paths</i> .....	120
4.4.4 <i>SEAL</i> .....	121
4.4.5 <i>SUMMARY</i> .....	122
<b>CHAPTER 5: ONSHORE ANALOGUE.....</b>	<b>124</b>
5.1 HUAB BASIN.....	124
5.1.1 <i>Background</i> .....	124
5.1.2 <i>Field Observation</i> .....	127
5.1.2.1 Geometries in 3D Exposures.....	127

i. KroneMamber .....	128
ii. Aeolian Twyfelfontein .....	131
iiv. Etendeka Volcanics.....	132
iv. Isolated barchans.....	134
5.1.2.1. Regional Scope.....	135
5.1.3 Summary.....	138
5.2 SOUTHERN NAMIBIA FIELDTRIP .....	141
5.2.1 Background.....	141
5.2.2 Ganigobis Shale Member.....	143
5.2.3 Whitehill Formation.....	144
5.2.4 Kalkrand Formation .....	146
5.2.5 Orange River System.....	147
5.2.6 Summary.....	153
<b>CHAPTER 6: CONCLUSIONS.....</b>	<b>155</b>
<b>RECOMMENDATIONS.....</b>	<b>158</b>
<b>REFERENCES.....</b>	<b>160</b>
<b>APPENDIX A: GLOSSARY .....</b>	<b>172</b>
<b>APPENDIX B: Kudu 2 &amp; 3 well Correlation after Wickens and Mclachlan (1990).....</b>	<b>178</b>
<b>APPENDIX C: Correlation of Orange Basin wells.....</b>	<b>179</b>
<b>APPENDIX D: Well panel correlation for the main kudu field wells (Kudu-1, Kudu-3 and Kudu-4).....</b>	<b>180</b>

## **LIST OF FIGURES**

Figure 1: Location of the Orange Basin; modified after <a href="http://www.namcor.com.na/kudu">www.namcor.com.na/kudu</a> ..	2
Figure 2: Bathymetry map of the study area showing the location of wells (coloured symbols with labels) in the Kudu Gas Field. ....	4
Figure 3: Hydrocarbon license map showing location of block 2815 in the Orange Basin east of Kudu Gas Field.....	12
Figure 4: Two-way travel time seismic section (Seismic line ECL 89-5) from within Block 2815 illustrating sedimentary drape over a hogback feature.....	13
Figure 5: Tectono-stratigraphic correlation across the four offshore sedimentary basins of Namibia (and the onshore Huab and Etjo area).....	16
Figure 6: Summary of seismic and sequence stratigraphy of the syn- and post-rift megasequences offshore Namibia (Bagguley, 1997).....	20
Figure 7: Seismic Base Map showing the Kudu field outline (red), location of wells and regional seismic grid used as the main database for this study. The grid is comprised of ECL-89 (bright green lines), VN03 (light blue lines) and SCOB12 (purple lines). ....	23
Figure 8: Gamma ray log for Kudu 3 used to identify sequence boundaries on W-E seismic line.....	27
Figure 9: Seismic to well tie for Kudu 2.....	29
Figure 10 A: Seismic to well tie on Kudu 6.....	30
Figure 10 B: Seismic to well tie on Kudu 6 displaying vertical shifting of Mid-Aptian unconformity from 3597.88m to 3581.55m and Base Barremian Shale	

unconformity from 4202.4m to 4618.42m in order to properly tie the well to seismic.....	31
Figure 11: Reflection termination patterns indicating upper and lower boundaries of depositional sequences (Mitchum et al, 1977).....	33
Figure 12: (A) Seismic reflection configurations, (B) Modified seismic reflection configurations, (C) Seismic reflection interpreted as prograding clinofolds, (D) Chaotic and reflection free reflection patterns (Mitchum et al., 1977).....	37
Figure 13: Diagram showing three different parasequence sets and their corresponding well log characteristics. ....	38
Figure 14: Trajectory of the shoreline associated with progradation and retrogradation, showing ascending and descending trends. After Allen and Allen (2013) referring to Catuneanu (2006). ....	39
Figure 15: Idealized sequence diagram outlining three types of system tracts and their respective boundaries resulting from one cycle of base level change (Brown & Fisher, 1977). ....	43
Figure 16A: Map showing the orientation of the well cross-section used for well correlation. ....	48
Figure 16B: Correlation of Orange Basin wells by identifying similar gamma ray signature corresponding to several geological formations.....	49
Figure 17: Well log analysis of wells in the Kudu main field. ....	51
Figure 18: Well panel correlation for the kudu main field wells (Kudu-1, Kudu-2 and Kudu-3). ....	52

Figure 19: Generalized stratigraphy offshore Namibia showing four tectonostratigraphic units separated by three major unconformities modified after Bray et al., (1998). .....	55
Figure 20: Simplified schematic geological section of the Orange Basin displaying its structural framework with the Pre-rift to Early drift sequences.....	56
Figure 21: Schematic outline of the sedimentary basins and their relative tectonic elements off the west coast Namibia and South Africa (after Nopec, 1991).....	58
Figure 22: Paleogeographic reconstruction showing the distribution of the Permian Whitehill Formation in Namibia and the Irati shale in Brazil. From Quad Consulting Ltd., 1996.....	60
Figure 23: W-E seismic line showing tectonostratigraphic units of the Orange Basin from the Pre-rift to Late drift. ....	61
Figure 24: Enlarged W-E line of the previous Figure 23 showing half graben fault structures within the Syn-rift sequences. ....	64
Figure 25: W-E seismic line showing onlapping of the Early-drift strata on the Mid Aptian unconformity. ....	67
Figure 26: W-E seismic line displaying onlapping of young strata and toplapping of old strata on Base Barremian unconformity in deep waters of approximately 3000m.....	68
Figure 27: W-E seismic line displaying extensional faults terminating just below Santonian unconformity (bright green line) which are down-lapping into the Turonian unconformity (purple line). Toe thrusts are numerous in the Late Cretaceous unit.....	70

Figure 28: A) Map showing the location of the submarine mountain in the southern part of the Orange Basin. B) W-E seismic line showing a single conspicuous flat-topped submarine mountain protruding above the sea bottom.....	71
Figure 29: W-E seismic line displaying Turonian-Santonian interval.....	72
Figure 30: Prograding wedge with steeply dipping truncated strata (red arrows) by Base Tertiary at the top, and downlaps (black arrows) on a sequence boundary at the bottom just above Santonian unconformity.....	73
Figure 31: Lowstand prograding wedge (highlighted in yellow) in which parasequences sets are bounded by sequence boundary at the bottom and a transgressive surface. ....	75
Figure 32: Base-Tertiary unconformity defined by underlying toplapping strata indicating erosional truncations (red arrows) and overlying onlapping strata (yellow arrows). ....	77
Figure 33: A. progradational sigmoidal clinoforms observed in Tertiary sequence which are downlapping (black arrows) on a maximum flooding surface and truncated (upper red arrows) by the overlying mid-tertiary unconformity. ....	79
Figure 33 B. Instantaneous phase attribute applied to enhance seismic geometries and improve the continuity of weak seismic events. Note that the sigmoidal clinoforms are pronounced in this image compared to image A. The zoomed in seismic image displays distinct truncation pattern.....	79
Figure 34: W-E seismic line displaying the interval between the Base Barremian Shale (Orange line) and the mid-Aptian unconformity (green line) thinning down dip.....	85

Figure 35A: Structural map of Base Barremian in time with minor closures identified in the northern part of the map.....	86
Figure 35 B: Structural depth map of Base Barremian displaying several major structural closures located in the middle of the Basin.....	87
Figure 36: W-E seismic line showing a volcanic feature protruding through the Early Cretaceous and cutting through the mid-Aptian as well as the Santonian unconformity. ....	88
Figure 37: A) 3D view of Mid Aptian map in time showing the location of the volcanic high. B) Volcanic high on 2D seismic line, note that it does not penetrate through the mid-Aptian unconformity but pushes against this horizon forming a dome with approximately 4 km width.....	89
Figure 38 A: Mid-Aptian map in time, a volcanic high was observed at this stratigraphic level to the west of the Basin. ....	90
Figure 38 B) Structural depth map of Mid Aptian Shale unconformity displaying several major structural features including a volcanic high and closed contours in the middle of the Basin. ....	91
Figure 39A: Turonian map in time displaying small structural closures to the southern part of the Basin. Note that the Turonian unconformity has been eroded to the eastern and also to the north-western part of the Basin.....	93
Figure 39B: Turonian map in depth displaying several structural closures in the middle of the Basin and to the southern part of the Basin. ....	94
Figure 40: W-E seismic line showing toe thrusts terminating onto the Turonian unconformity. Toe trusts become more prominent and better defined sea-ward. The Turonian unconformity is marked with a light purple .....	95

Figure 41: A) W-E seismic line showing Top Santonian unconformity (dark purple) located almost at the centre of study area. This section is heavily faulted to the east..... 96

Figure 41 B) 3D view of the Top Santonian unconformity. Note that major faults were picked on the shelf close to shore which extends from the Turonian sequence through the Santonian and terminates just below Mid-Tertiary unconformity. .... 96

Figure 42: W-E seismic line displaying chaotic seismic reflection patterns which makes it difficult to pick the Top Santonian unconformity. .... 97

Figure 43A: Top Santonian map in time, note that this horizon was eroded to the southern part of the study area. .... 98

Figure 43B: Top Santonian depth map showing no structural closures..... 99

Figure 44: W-E seismic line showing the Base Tertiary unconformity (green) sub-cropping into beach sands to the east of the Orange Basin..... 100

Figure 45: W-E seismic line showing channels in the Tertiary sequence..... 101

Figure 46A: N-S seismic line showing series of channel in the upper Tertiary section. .... 101

Figure 46B: N-S seismic line showing a conspicuous channel feature in the upper section of the Tertiary unit which attains a width of 6 km..... 102

Figure 47A: Base Tertiary Map in time displaying series of channels indicated by black arrows. .... 102

Figure 47B: Base Tertiary depth map displaying no significant closure ..... 103

Figure 48: Structural model displaying the geometry of the Basin. .... 105

Figure 49: Two structural highs identified both on the seismic profile and structural map for transitional Early Cretaceous sequence. ....	106
Figure 50: Map showing the location of leads identified in the study area. Base Barremian leads are indicated in purple, Aptian in Yellow and Turonian in green. ....	108
Figure 51: W-E seismic line showing graben structure with possible syn-rift source rock. ....	110
Figure 52: W-E line showing toplaps of Syn-rift strata towards the overlying unconformity indicated by red arrows. ....	111
Figure 53: W-E seismic line showing onlapping of the upper Aptian sequence onto the mid-Aptian unconformity. The Barremian (orange) to mid-Aptian (green) interval contains the proven source rock for the Kudu Gas Field. ....	112
Figure 54A: Thickness map of the Base Barremian to Sea Bed indicating the location of kitchen at the southern edge of the Namibian Orange Basin which attains a maximum thickness of about 5000m. ....	113
Figure 54B: Early drift thickness map showing the locations of the thick part of this unit to the southern part of the Basin reaching a maximum thickness of about 3000m. ....	114
Figure 55A: Turonian to Sea bed thickness map indicating the location of kitchen at the southern part of the Namibian Orange Basin attaining maximum thickness of about 3400m. ....	116
Figure 55B: Late drift thickness map indicating the thick part of this unit at the southern edge of the Namibian Orange Basin reaching a maximum thickness of 3300m. ....	117

Figure 56: N-S seismic line showing toe thrusts just above the Turonian unconformity, the amplitude is brighter at the top of the thrust and dims down dip due to change in seismic facies. ....	119
Figure 57: Petroleum system model showing reservoir intervals in yellow, source rock in black and seal in purple.....	122
Figure 58: Geological map showing the location of the Huab Basin modified after Mountney et al., 1998. The study area is circled in red. ....	126
Figure 59: Timestratigraphic offshore and tectonostratigraphy framework of the Karoo Supergroup and Etendeka Group in the Huab Basin showing a link between offshore and onshore units, modified after Mountney et al., 1998....	126
Figure 60: Lithological units across the Huab basin (Mountney et al., 1998). ....	127
Figure 61: Outcrop showing different types of deposits which were deposited in a different environments. ....	129
Figure 62: Inclined dolerite dyke cutting through Krone Formation sandstone (Syn-rift time equivalent). Eastern valley flank at 14°04.512'E, 20°37.568'S .....	130
Figure 63: Isolated barchans dune interbedded in basalt in the mid-section of the outcrop (Early drift time equivalent).....	131
Figure 64: Interlayering of basalt and aeolian sands. Note that the weathered basalt at the bottom of the outcrop has a light colour compared to the massive basalt with a dark colour (Early drift time equivalent). Hill at 14°09.377'E, 20°09.237'S	133
Figure 65: Red sandstone interbedded in weathered basalts.....	134
Figure 66: Series of barchanoid (multi-dunes) dunes preserved in volcanic unit in the lower part of the outcrop (Early cretaceous equivalent). View from 14°09.139'E; 20°39.978'S.....	135

Figure 67: Bypass section showing aeolian sand preserved in small cracks within the basalt (Early drift time equivalent). .....	136
Figure 68: Vertical cracks (fault) at the top of the basalt filled by aeolian sands (Early drift time equivalent). Outcrop close to exposure in Figure 67. ....	137
Figure 69: Depositional model for main aeolian unit in the Huab region, in which the orientation of aeolian bedforms indicates that the prevailing wind was blowing towards ENE (Mountney et al., 1998). ....	139
Figure 70: Depositional model for upper aeolian unit in the Huab region, in which the orientation of aeolian bedforms indicates that direction of prevailing wind changed to SE (Mountney et al., 1998). ....	140
Figure 71: Generalized Geological Map of Southern Namibia (modified after Geological Survey of Namibia). ....	142
Figure 72: Dark grey shales of the Ganigobis Shale Member capped by Kalahari sediments. ....	143
Figure 73: A) Cone shaped calcareous concretions observed in Ganigobis area. ...	144
B) Light coloured thin layer of volcanic ash in the Ganigobis shale outcrop. ....	144
Figure 74: A) Jointed weathered light grey shales of the Whitehill Formation . B) Mesosaurus fossil preserved in sandstone. ....	145
Figure 75: Planar laminated red sandstone interbedded with kalkrand flood basalts. .....	146
Figure 76: Thin layers of red sandstone interbedded with basalts dipping to the north east. ....	147
Figure 77: A map showing the location of the Orange River. ....	148
Figure 78: Picture showing the Orange River Mouth. ....	150

Figure 79: Schematic diagram of the Orange River system. .... 151

Figure 80: A. Heavy minerals sand deposits in Aeolian sand along bank of the Orange River, B. Heavy minerals deposited on the bank of the river in fluvial sand, C. mixture of fluvial and Aeolian sand at the bank of the Orange River, D. interbeds of high energy (coarse) and low energy (fine) material. .... 152

**LIST OF TABLES**

Table 1: Summary of seismic surveys used in the study. ....	22
Table 2: Summary of wells used in this study. ....	24
Table 3: Major horizon identified in Kudu wells.....	26
Table 4: Generalised Stratigraphy of the Orange Basin offshore Namibia. ....	84
Table 5: Outline of depositional environments and associated source and reservoir facies in the Orange Basin.....	156



## **CHAPTER 1: INTRODUCTION**

### **1.1 Background to the Research**

The hydrocarbon-bearing Orange Basin is located on the South-west African continental margin near the South Africa–Namibia international boarder (Figure 1) and is the study area of this research. The Basin formed during early Cretaceous Gondwana break-up that subsequently led to the opening of the South Atlantic Ocean. The Basin covers an area of approximately 150,000 km<sup>2</sup> and some of its depocentres attain a maximum thickness of 8 km (Roux et al., 2004). Two gas fields have been discovered within the Orange Basin: the Kudu Gas Field offshore Namibia and the Ibhubesi Gas Field offshore South Africa. The gas reserves of the Kudu field are estimated at 1.4 tcf (trillion cubic feet) and the reserves of the Ibhubesi field are 540 bcf (billion cubic feet) ( [www.namcor.com.na](http://www.namcor.com.na) and [www.sunbirdenergy.com.au](http://www.sunbirdenergy.com.au)). Despite the discovery of the gas fields, the offshore Namibia portion of the Orange Basin remains under-explored with only eleven wells drilled in the Basin to date. Eight out of the eleven wells in the Namibian part of the Basin were drilled in the Kudu Field. However, thirty-four wells have been drilled in the Basin offshore South Africa. So far, the petroleum systems are poorly understood and this research aims to achieve a comprehensive understanding of the operating petroleum systems through analysis of available data for the Orange Basin offshore Namibia.



Figure 1: Location of the Orange Basin; modified after [www.namcor.com.na/kudu](http://www.namcor.com.na/kudu).

## **1.2 Exploration History**

The Kudu Gas Field is the only hydrocarbon discovery in Namibia and it sits on the continental shelf at a water depth of about 170 m (Figure 2). Since its discovery in 1974, the Kudu Field has been owned by several different companies including SWAKOR, Royal Dutch Shell, Chevron Texaco, and Energy Africa and since 2004 until October 2014, by Tullow Oil in partnership with NAMCOR and Itochu. Tullow oil withdrew from the Kudu licence and NAMCOR became the operator of the block until today.

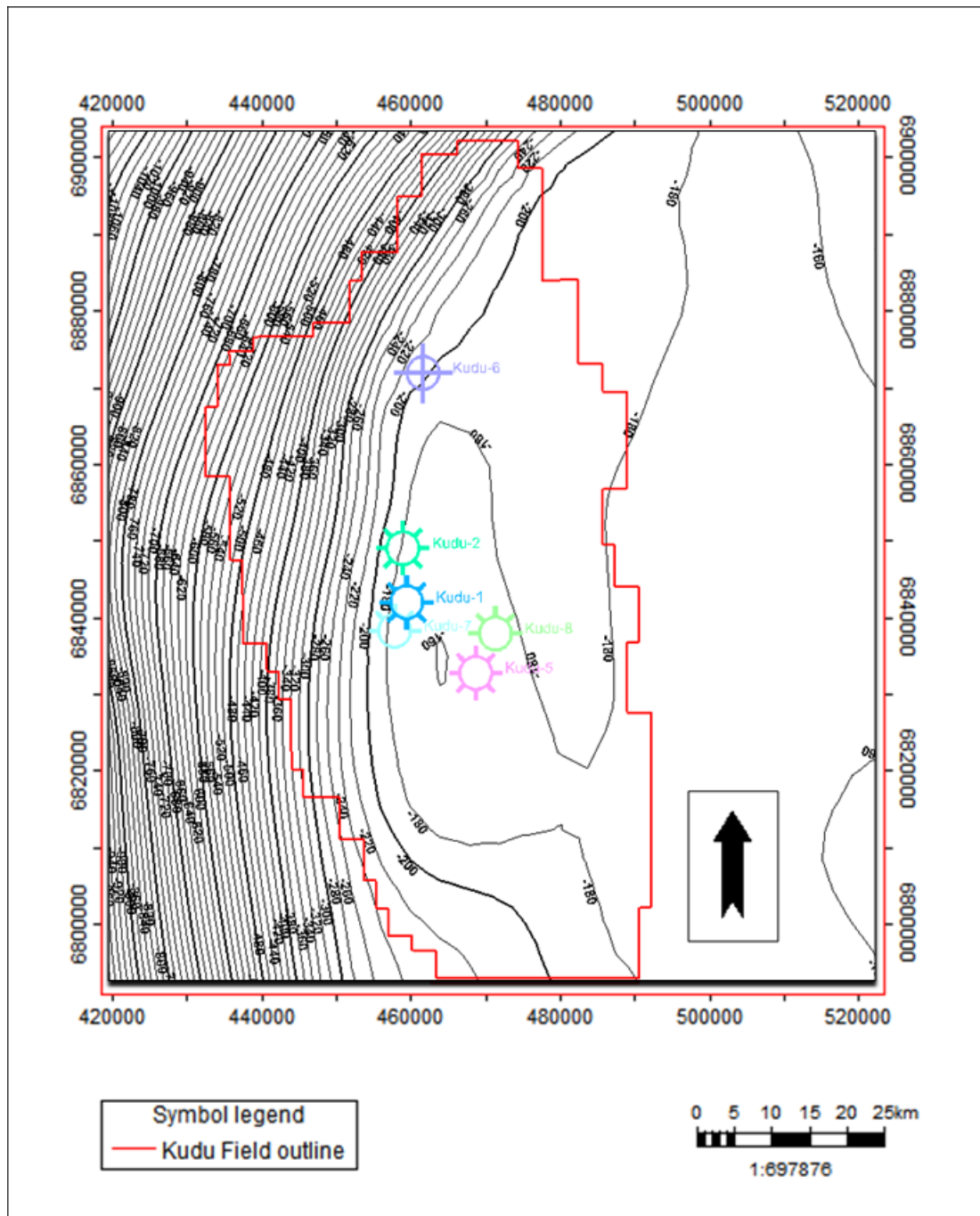


Figure 2: Bathymetry map of the study area showing the location of wells (coloured symbols with labels) in the Kudu Gas Field. Wells drilled in 170 m water depth. The map was derived from sea-bed mapping using Petrel software.

The Kudu field was discovered by Chevron Texaco in 1974 by drilling Kudu-1 well which was drilled 'blindly' with no accompanying exploration data such as seismic reflection. During drilling of Kudu-1, the reservoir rock was expected to be encountered at a depth of less than 3000m (sub-sea) with aid of South African geophysical data which was regionally extrapolated in order to develop the stratigraphy of the Namibian sedimentary basins (Chevron, 1974). The well revealed the occurrence of non-reservoir rock at that depth. Therefore, the well was drilled deeper and gas was encountered in the Lower Cretaceous, at depth below 4,400 m (sub-sea). A drill stem test (DST) was conducted and it was shown that the reservoir had a flow potential of 200 MMscf per day (Shell, 2002) which can be produced from five to six wells considering DST results from other Kudu wells.

Thereafter, further technical work such as seismic acquisition and interpretation was done by Chevron, leading to recommendations to drill more appraisal wells. Sanctions placed on Namibia (then a part of South Africa) by the United Nations prevented the drilling of additional wells, leading to the relinquishment of production rights by Chevron Texaco in 1977. In 1987, the Kudu licence was awarded to SWAKOR which was the National oil company of Namibia at that time. SWAKOR recommended the drilling of Kudu-2 north of Kudu-1 to appraise Kudu 1 discovery.

In 1987–88, SWAKOR drilled Kudu-2 and Kudu-3 as appraisal wells. Kudu-2 was not tested; Kudu-3 produced at a rate of 38 MMscf per day proving the presence of hydrocarbons in the field.

In 1993 the government of the Republic of Namibia, through its first bidding round for exploration licences, awarded the Kudu licence to Shell E&P Namibia (SEPN) with 75% shareholding interest and operatorship and Energy Africa a 25% interest. After conducting detailed geological and geophysical studies, in 1996 Shell and Energy Africa drilled Kudu-4 to investigate the potential of the field; tests produced at 40.5 MMscf per day. After Kudu-4 was drilled, Chevron Texaco acquired 60% of Energy Africa's interest. This consortium drilled Kudu-5 in 1998 which tested at 20.8 MMscf per day. In 2002, Kudu-6 and Kudu-7 were drilled to appraise the field outside the already investigated area. These two new wells encountered tight sands and no production tests were performed due to the absence of moveable hydrocarbons. Subsequently, Shell withdrew from the licence due to poor production rates from the new appraisal wells (Kudu-6 and 7); Chevron Texaco became the operator of the block.

In 2003 Chevron relinquished the license and Energy Africa took over operatorship with 90% shareholding and NAMCOR holding 10%.

In 2004 Tullow Oil became the operator of the Kudu Gas Field by buying out Energy Africa. Then Tullow drilled Kudu-8 in 2007 which did not find any additional reserves but proved the main gas bearing reservoir. In 2009 the initial licence for Tullow expired and was renewed the same year with new shareholding contracts: 31% Tullow, 15% Itochu, and 54% NAMCOR. Despite these changes Tullow remains the operator of the Kudu Gas Field. In October 2014, Tullow announced its withdrawal from the Kudu licence and transferred operatorship to NAMCOR. As a result, NAMCOR became a shareholder of 85% and Itochu 15% up to today.

Apart from the Kudu wells and 2815/15-1, two more wells were recently drilled in the Orange Basin which are Kabelijou-1 and Moosehead-1. Kabelijou-1 (2714/6-1) was drilled in July 2012 by a consortium consisting of Chariot Oil & Gas 25% and Petrobras (operator) 30% and BP 45% in water depth of about 377 m. This well drilled the Nimrod prospect north east of the Kudu field and reached a total depth of 3150 m. It encountered good Turonian source rock and hydrocarbon shows, but no commercial hydrocarbons were found in the target Albian reservoir ([www.chariotoilandgas.com](http://www.chariotoilandgas.com), September 2012).

Moosehead-1 well was drilled in water depth of about 1727 m by HRT Africa in partnership with GALP Energy (14%) in 2013. The well was drilled to a total depth 4170 m to test Barremian Carbonates to the west of the Kudu field. The well encountered nearly 100 m thick Cretaceous carbonates but their porosity were less developed than expected and no hydrocarbons were found. However, wet gas shows were encountered and at least two potential source rocks were penetrated which are the Turonian and Aptian (<http://www.galpenergia.com>, September 2013).

### **1.3 Statement of the Problem**

Little is known about regional petroleum systems in the Orange Basin. In particular, the depositional architecture of reservoir and seal rocks, and the tectonic structures controlling their geometry remain largely unresolved. This is partly because sedimentary reservoir rocks interfinger with lava flows; a petroleum geological assemblage that is unusual and not well-studied anywhere in the world.

Due to this lack of fundamental information, the following ‘big picture’ issues require investigation:

- What are the tectonostratigraphic sequences produced during evolution of a volcanic passive margin such as the one that is found in the Orange Basin?
- What are the depositional events during the rift and drift phase?
- Which structural development took place during the drift phase?

### **1.4 Objectives of the Study**

The aim of this research is to characterize and describe the regional petroleum systems of the Orange Basin and bring these results to bear upon the ‘big picture’ questions stated in Section 1.3. above.

In order to fully understand the petroleum systems, a stratigraphic and structural analysis is required to identify the sequence and relative timing of depositional and

structural events that generated the petroleum systems in the Orange Basin. In particular, a structural analysis will show the distribution of traps, basement ridges and fault zones, all of which may impact migration of basinal fluids from source to reservoir. In addition, a structural study will give insight into the timing of faulting and associated structures, and thus it will aid recognition of the sequence of structural events related to passive margin evolution.

Once the petroleum systems are understood, a foundation for predicting hydrocarbon sources, migration paths, seal and reservoir distribution will be created. This will refine predictions regarding depositional setting, lithology and texture for sections where data-log or core samples are not available. This research will incorporate new 2D seismic data acquired by Spectrum in 2012 and is therefore the first regional study of the Orange Basin to describe the deeper offshore geology of the Basin using modern data.

## **CHAPTER 2: LITERATURE REVIEW**

The Namibian margin formed during the break-up of the supercontinent Gondwana with subsequent rifting and drifting tectonics which led to the opening of the South Atlantic Ocean during the Late Jurassic to Early Cretaceous. The Namibian margin formed tectonically; therefore, it is classified as a passive margin. The Formation of the South Atlantic began at ~130 Ma offshore South Africa and continued northward (Gladchenko et al., 1998). The deposition of a thick wedge of Cretaceous to Tertiary sediments over the margin resulted in the formation of a major basin system extending over the entire offshore Namibia (Bray et al., 1998). There are four sedimentary basins that are defined offshore Namibia, namely the Namibe, Walvis, Luderitz, and Orange Basins (in order from north to south; as shown in Figure 1).

The basement of the four offshore basins comprises of metasediments derived from the Kaoko, Damara and Gariiep orogenic belts, and they are envisaged by Frimel et al, 2010 to be Neoproterozoic sediments similar to the Dom Feliciano Belt of South America. Synrift, sedimentary basin rocks sit unconformably on the pre-rift basement of Precambrian or Paleozoic age (Soekor Ltd, 1989), and the basins are predominantly filled with Early Cretaceous sediments.

Cartwright et al. (2002 & 2005) investigated the conjugate margins of the South Atlantic and provide a geological overview of the study area for this current research. They concluded that the Namibian margin is a volcanic passive margin consisting of a post-rift progradational-aggradational wedge with a thickness of 3 to 5 km of mainly

clastic post-rift sediment overlying a rifted continental basement. They proposed that the Namibian continental margin is in fact the 'mirror image', a conjugate margin, of the margin along northern Argentina and southern Brazil. These authors believe that the gas-bearing sands of the Kudu Gas Field are equivalent to the fluvial sands that host the Ibhubesi Gas Field in the southern Orange Basin of South Africa. Despite such interpretations the authors concede that, in fact, the crustal structure of the Namibian continental margin is poorly constrained in comparison to other more intensively studied margins such as those of the north-eastern Atlantic.

Petroleum Agency SA, 2003 stated that the Syn-rift half graben play in the Orange Basin South Africa consists of oil which was proven by the A-J1 well. This is the only oil system confirmed in the entire Orange Basin to date. It was sourced from the lacustrine shales interbedded with lacustrine sandstone the reservoir rock contained in half graben structures. A-J1 well reached a maximum flow rate during testing of approximately 200 barrels of oil per day.

Houghton (1993) identified play potential in license area 2815 (Figure 3), offshore Namibia which is part of the Orange Basin. Houghton's (1993) geological model revealed primary reservoir targets within the Early Cretaceous. This target includes matured source rocks in transitional intervals adjacent to the reservoir section, and potential trap structures. The proposed reservoir is located in Neocomian lacustrine deltaic and fluvial sandstones, which are interbedded with shales, where structural plays related to sedimentary drape overlying hogbacks and horsts were identified (Figure 4). The author also identified fault block plays, in which faulting extends from underlying pre-Karoo basement structures into the Early Cretaceous interval. The

eastward extension of the gas-bearing aeolian sandstones within the Aptian-Barremian section in the Kudu Gas Field also provides an important reservoir target over this license area. Therefore much attention will be dedicated to this interval in this current study.

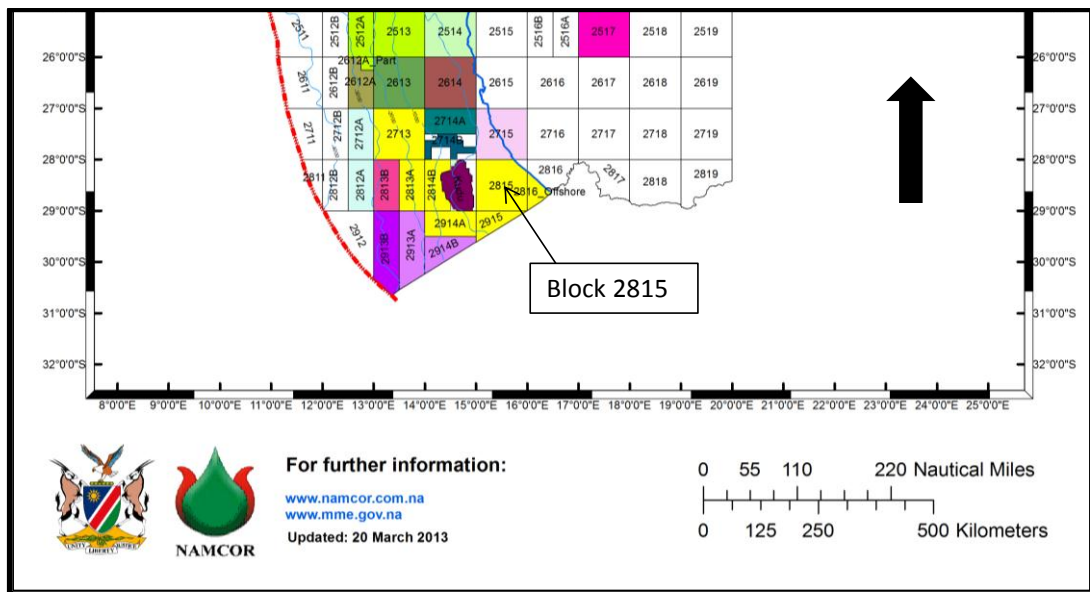


Figure 3: Hydrocarbon license map showing location of block 2815 in the Orange Basin east of Kudu Gas Field obtained from Ministry of Mines and Energy, Energy Division. All the blocks high-lighted in yellow surrounding the Kudu field were licensed by HRT Africa Petroleo when this map was produced in March 2013.

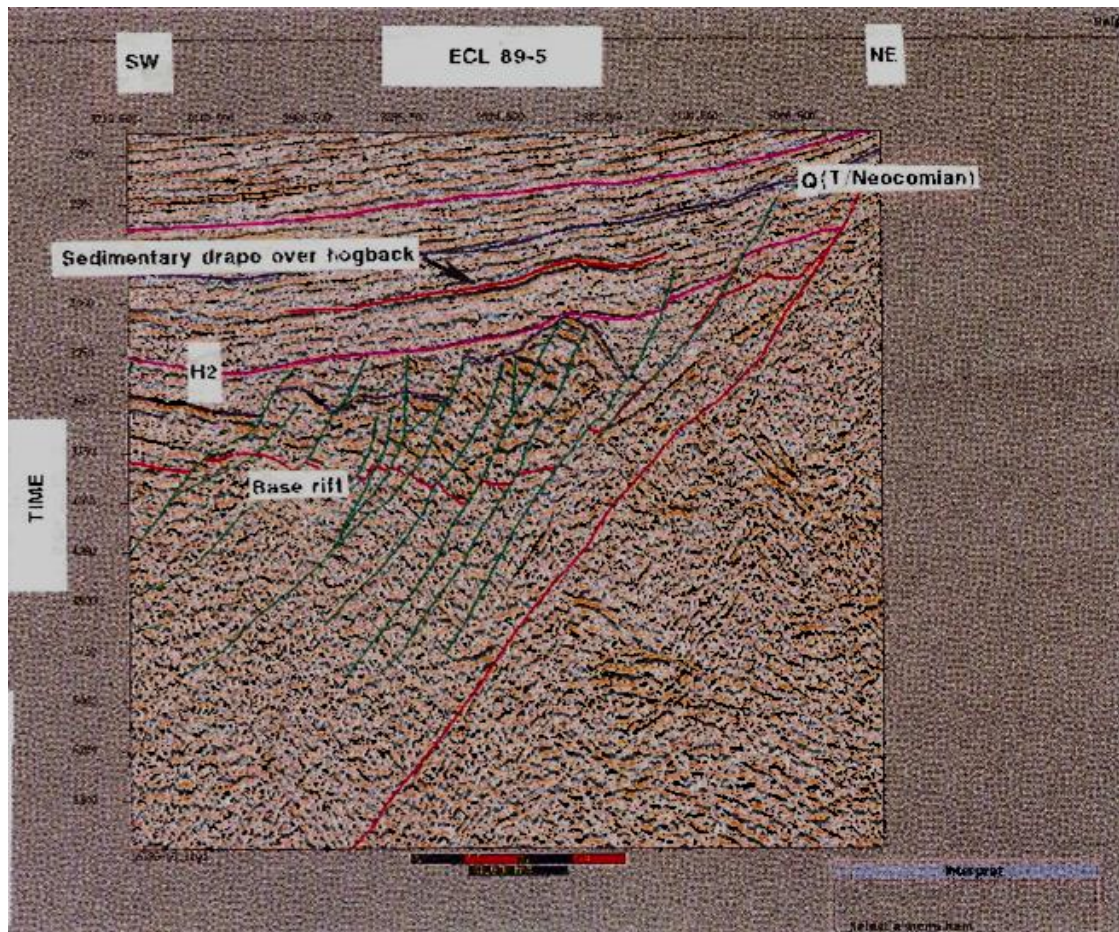


Figure 4: Two-way travel time seismic section (Seismic line ECL 89-5) from within Block 2815 illustrating sedimentary drape over a hogback feature. Note that some of the faults extend from the basement into Early Cretaceous strata which could serve as a migration path for hydrocarbons. Abbreviations: Q – Neocomian, H2 – Hauterivian (Houghton, 1993).

Stanistreet & Stollhofen (1999) studied onshore equivalents of the reservoir rock within the Kudu Field. They correlated the Kudu Sandstone Reservoir with evaporitic-aolian deposits interbedded with the Early Jurassic Kalkrand flood basalts (Kalkrand interlayers) of southern Namibia. The Kalkrand sedimentary interlayers are situated

northeast of the Kudu Gas Field in the southern part of onshore Namibia. This correlation improved the recognition of the main Kudu reservoir geometries and associated lithologies, as well as clarifying the tectonic setting and volcanic controls. Radiometric dating Potassium-Argon (k-Ar) and biostratigraphy of the Kalkrand sedimentary interlayers by Duncan et al. (1997) showed that the Kudu reservoir fits perfectly into a southern Gondwana tectonic context because the age of the Kalkrand basalts is almost equivalent to that of the Kudu Field. However, the time constraints do not support previous assumptions that the Kalkrand interlayers and the Etjo Sandstone located further north are time-stratigraphic onshore equivalents to the Kudu reservoir.

Jerram et al. (1999) report on the facies architecture of the Etjo Sandstone and its interaction with the Etendeka Flood Basalt in the onshore area of northwest Namibia. They observed that the stratigraphic relations of the major exploration production reservoir of the Kudu Gas Field are essentially similar to those characterizing the Etjo sandstone. The similarity was particularly observed in the aeolian-lava interactions, which occur in both, the Etjo sandstone and the Kudu reservoir rock. However, the sedimentary horizons associated with the Kudu basalts are not entirely characterized by fluvio-aeolian facies and also have a variety of lacustrine lithologies and evaporites. Therefore, the main facies assemblage of the Kudu gas reservoir is suggested to be transitional in its palaeo-environmental setting between the aeolian interbeds of the Etendeka Flood Basalt in the northwest and the fluvio-lacustrine interbeds of the Kalkrand Basalt Formation in southern Namibia (Figure 5). Observations by Jerram et al. (1999) indicate that the findings of Stanisstreet & Stollhofen (1999) cannot be

directly applied to the Kudu Gas Field and further refinements of the depositional model are required.

The biostratigraphic study of the Etjo formation by Holzförster et al. (1999) and recent dating of the overlying units in Waterberg area by Marsh et al. (2003) clearly confirm that the Etjo Formation is a Lower Jurassic unit as already stated in SACS (1980). Despite this, some authors are still referring to the underlying aeolian units interfingering with the Etendeka lavas as “Cretaceous Etjo Formation” which is not correct. Therefore, Stranistreet & Stollhofen (1999) and Stollhofen (1999) introduced the term “Twyfelfontein Formation” for the aeolinites underlying the Etendeka Volcanic in North Namibia (Huab area) and this terminology has now been adopted by Miller (2008) and all other recent publications. This reveals that the Barremian Kudu reservoir is probably time equivalent to the Lower Cretaceous Twyfelfontein Formation in Huab area but not the Lower Jurassic Etjo Formation in Waterberg area.

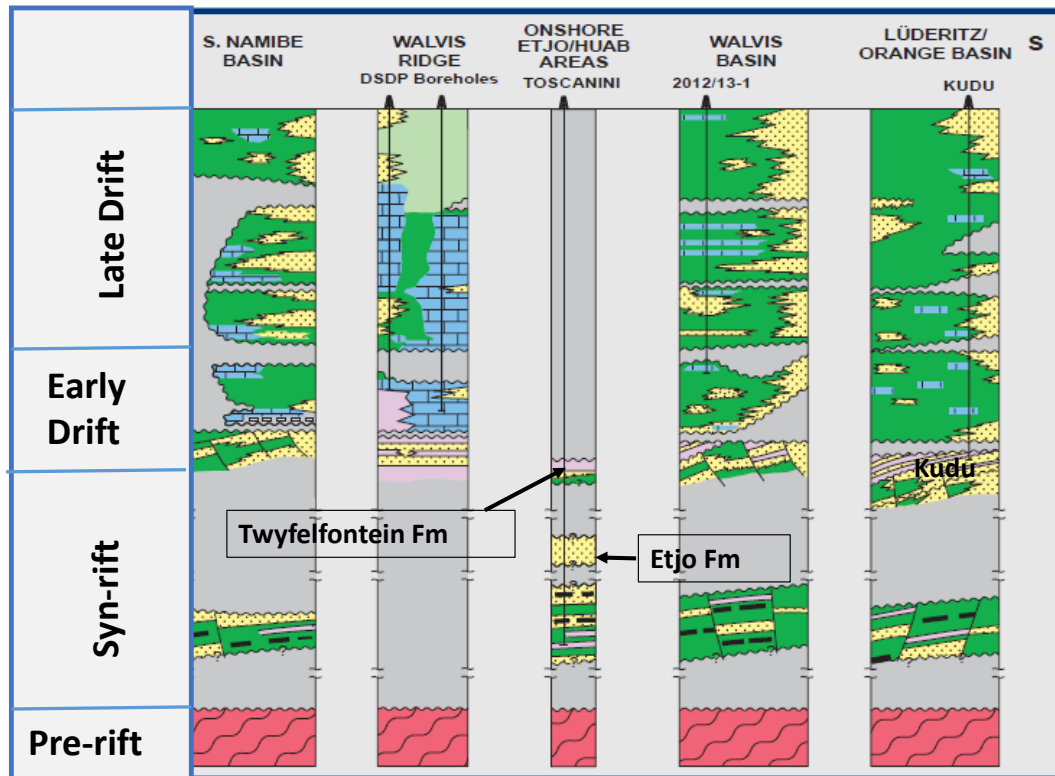


Figure 5: Tectono-stratigraphic correlation across the four offshore sedimentary basins of Namibia (and the onshore Huab and Etjo area). Modified after Norsk Hydro's report for the third licensing round (1998) prepared for NAMCOR. Note that the chronostratigraphic level of the Kudu reservoir rock is almost time equivalent to the Twyfelfontein Sandstone.

Schmidt (2004) studied the hydrocarbon potential of the conjugate continental margins of southwest Africa and Argentina. This was in part a complement to an earlier work by Schumann (2002) which evaluated the hydrocarbon potential of the Argentinean continental margin. Schmidt (2004) states that the thermal maturity of rocks at the Argentinean margin is lower than that of the African continental margin, due the fact that the Argentinean margin has a lower heat flow. This is consistent with Schmidt's

(2004) interpretation that the Kudu Gas Field hosts mainly dry gas with minor quantities of condensate. The Kudu reservoir is located at the upper edge of a basaltic seaward dipping reflector sequence and is found in predominantly aeolian sandstones inter-fingering with basalts. This reservoir rock is overlain by Aptian shales which act as both, seal and source rock.

Wickens and Mclachlan (1990) analysed the stratigraphy and sedimentology of the Kudu gas reservoir interval in Kudu 2 and Kudu 3 wells. The main aim of this study was to define the extent of the Barremian gas bearing sandstones by correlating these two wells. It was deduced that the Kudu reservoir constituents of two major parts, which are the Lower Non-marine and the Upper Marine units (Appendix B).

The Lower Non-marine consists of Lower Gas sand in Kudu 3 and probably part of the Lower Gas Sand in Kudu 2. The lithology of this section includes basalt, anhydritic aeolian sandstone and volcanoclastic sandstone.

The Upper Marine unit consists of upper Gas Sands which occurs both in Kudu 3 and Kudu 2. This unit is also envisaged to probably being part of the Lower Gas Sand in Kudu 2 and it constituents of fine to medium grained shallow marine sandstones with minor limestone and volcanoclastic sandstones.

The change in depositional environment from non-marine to marine is marked by a distinctive unconformity. The lateral extent of the kudu reservoir was difficult to determine due to lack of data.

Paton et al. (2007) studied the petroleum systems evolution of the southern Orange Basin using Petromod Vs.8 and 9 software (IES GmbH, Germany). Their 2D

petroleum system modelling revealed that the source rocks of Jurassic and Cretaceous age reached a high level of kerogen conversion. The peak source rock maturity was reached during maximum burial, at the end of the Cretaceous. This was followed by an erosional event which cooled the source rocks resulting in a discontinuity of hydrocarbon generation. The models of Schmidt, 2004 and Paton et al. 2007, suggest that the maturity of the source rocks and the actual presence of petroleum systems in the basin, indicate that a variety of petroleum systems operates within the Basin and not just one.

Bagguley (1997) investigated the application of seismic and sequence stratigraphy to the post-rift megasequence offshore Namibia. This study has resulted in the identification of five megasequences based on the large scale regional framework in this area. A summary of findings from that study is outlined in Figure 6, where megasequences MS10 to MS30 represent three periods of regional rifting. MS10 represents the first event of rifting during the Permian-Jurassic when Africa was still part of the supercontinent Gondwana. Megasequence MS20 and MS30 represent the Late Jurassic - Early Cretaceous rifting events which led to the separation of Africa from South America and the opening of the South Atlantic. This megasequence has already been recognized by Hubbard (1988). MS40 is characterized by submarine canyons and represents the earliest stage of evolution of a post-rift clastic wedge. During this interval the structural development of the margin was mainly due to tectonic subsidence. The succeeding MS50a post-rift unit is dominated by a river-dominated delta system, which was active during the Turonian until the Base Tertiary Unconformity. A remarkable high sedimentation rate, related to the progradational

nature and the development of listric growth faults in the Orange Basin, characterize this time interval (Bagguley, 1997). MS50b represents a period with decreasing sedimentation due to aridification of the Namibian landmass and the consequent increased ephemeral nature of many onshore river systems from the late Oligocene onwards.

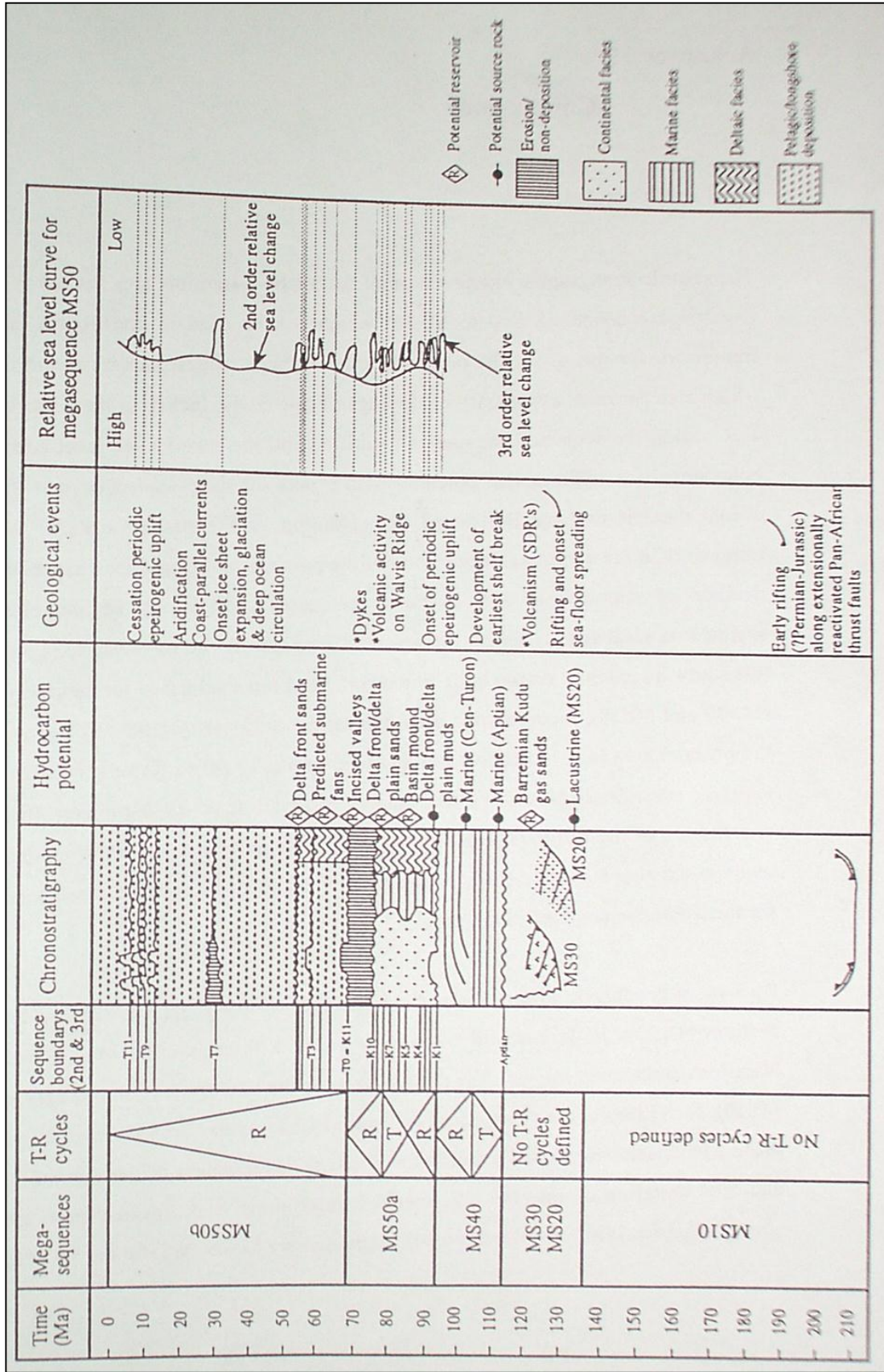


Figure 6: Summary of seismic and sequence stratigraphy of the syn- and post-rift megasequences offshore Namibia (Bagguley, 1997). Note that the initial rifting of the continental crust occurred during Permian and the Kudu main reservoir was deposited during the Barremian.

Aizawa et al. (2000) correlated offshore and onshore major stratigraphic events with the aid of depth converted and interpreted seismic profiles coupled with well data. This was carried out to determine the link between offshore and onshore geology. The study revealed that there is limited evidence to support this hypothesis. Therefore the offshore subsidence cannot be related in any simple way to the structural developments onshore. The hinge zone a region of pronounced bending of the continental lithosphere forming a critical boundary which separates the offshore from the onshore morphological elements. However, this study also revealed that there is a significant difference between the geodynamic and topographic evolution of the northern and southern part of continental margin.

Apart from technical reports produced for hydrocarbon exploration purposes, most of the offshore studies conducted in Namibia cover the entire continental margin and only few have been done for individual sedimentary basins including the Orange Basin. Subsequently, little is known about the depositional history and the regional petroleum systems in the Orange Basin which will be covered in this study.

## CHAPTER 3: MATERIAL AND METHODOLOGY

### 3.1 Available data

The data required for this study has been acquired during hydrocarbon exploration activities in the Orange Basin offshore Namibia by different seismic acquisition companies. This research is mainly based on interpretation of the existing data.

Approximately 15,500 line kilometres of regional 2D seismic data have been interpreted for this study. Apart from the 2D seismic, other available offshore Namibia data used in this study include well data and onshore field observations. Hence, all of the data used for the study were obtained from the Petroleum Corporation of Namibia (NAMCOR). The details of the seismic database used for the study are summarized in Table 1. The seismic grid and well locations in the study area are outlined in Figure 7.

Table 1: Summary of seismic surveys used in the study.

<b>Survey ID</b>	<b>Year</b>	<b>Company</b>	<b>General comment</b>
ECL89	1989	WesternGeco	Regional Survey
VN03	2003	Veritas	Regional Survey
SCOB12	2012	Spectrum	Regional Survey

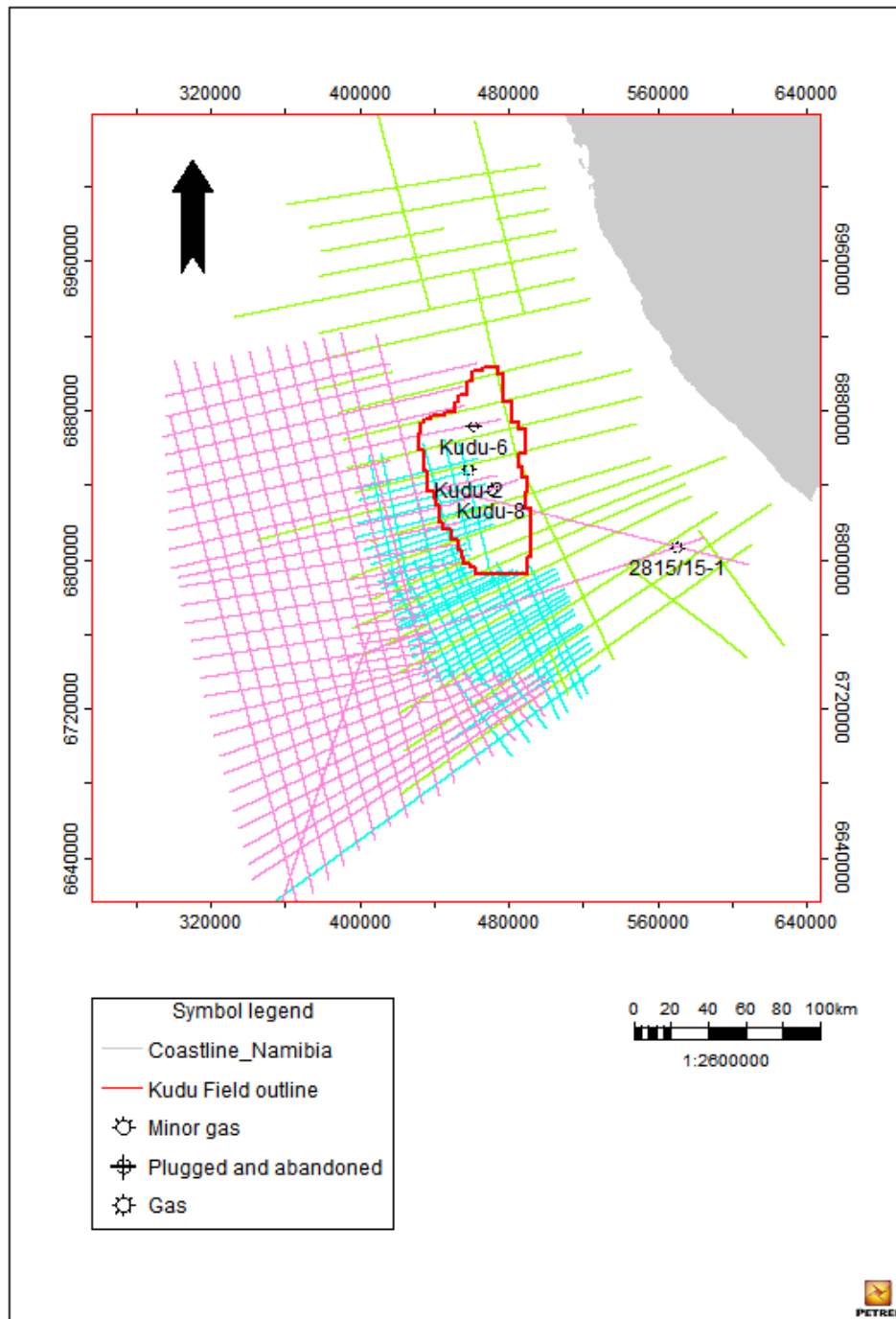


Figure 7: Seismic Base Map showing the Kudu field outline (red), location of wells and regional seismic grid used as the main database for this study. The grid is comprised of ECL-89 (bright green lines), VN03 (light blue lines) and SCOB12 (purple lines).

The well data were obtained from eight non-proprietary wells drilled in the Orange Basin by various companies, which include gamma ray wire-line, sonic, density, resistivity as well as check-shots data. Except for well 2815/15-1, almost all the exploration wells used in this study are localized in the Kudu Gas Field on the edge of the continental shelf. HRT drilled Moosehead-1 well in the Orange Basin which is currently the only well drilled to the west of the Kudu field in water depth of approximately 1727 m. Mousehead-1 and Kabelijou-1 could not be included in this study since they are still proprietary wells. Formation tops obtained from Kudu and 2815/5-1 well reports were made available for this project by the National Petroleum Corporation of Namibia (NAMCOR) Pty, Ltd. Details of all wells used for this study are summarized in Table 2.

Table 2: Summary of wells used in this study.

<b>Well ID</b>	<b>Year</b>	<b>Company</b>	<b>Total Depth (meters)</b>	<b>Results</b>
Kudu-1	1973	Chevron	4452	Gas
Kudu-2	1987	Swakor	4539	Gas
Kudu-3	1988	Swakor	4522	Gas
Kudu-4	1996	Shell	4705	Gas
Kudu-5 (2814/11-4)	1999	Shell	4887	Gas
Kudu-6 (2814/7-2)	2002	Shell	5275	Gas show
Kudu-7 (2814/11-5)	2002	Shell	4732	Gas
2815/15-1	1996	Chevron	4750	Gas show

## **3.2 Interpretation Approach**

### **3.2.1 Data analysis**

The data analysis involves a stratigraphic and structural analysis approach. A subsequent synthesis of both enables recognition of the petroleum systems at work and reveals the tectonostratigraphic sequences, depositional events and structural development that took place in the Orange Basin.

This analysis mainly involves seismic interpretation which was carried out using Petrel software. The software was donated to the Geological Department of the University of Namibia by Schlumberger in 2012.

Well log correlation was carried out with the aid of well picks which were correlated across the well section identifying similar gamma ray signature corresponding to a specific geological Formation. This revealed the distribution of the reservoir rock and also provided a better understanding of the geology of the study area. The stratigraphic framework developed from well log correlation was matched against seismic reflection events, and with this six major horizons were identified (table 3). The age of the seismic picks has also been identified with the aid of Kudu well reports and published results of the Kudu 9A-1, Kudu 9A-2 & Kudu 9A-3 boreholes such as Communications of the Geological Survey of Namibia (Volume 6, 1990). Well panels were also generated using AutoCad software which provided an insight of the distribution of the Kudu reservoir rock.

Table 3: Major horizon identified in Kudu wells.

<b>Formation tops</b>	<b>Pick Colour</b>
Sea Bed	Blue
Base Tertiary	Bright green
Santonian	Purple
Turonian	Pink
Mid-Aptian	Green
Base Barremian	Orange

The initial framework for seismic sequence stratigraphic interpretation was generated by inspecting all seismic lines and identifying sequence boundaries that were correlated over the study area. Hence, wells data were converted from depth to time with the aid of checkshots data and posted on seismic section to ease the identification of sequence boundaries (Figure 8). Major faults were mapped to depict displacements of strata. Successively, the identified sequence boundaries were picked in time.

A chronostratigraphic diagram which outlines the Orange Basin evolution was generated from resultant information after picking of seismic surfaces, with subsequent analysis of seismic facies and delineation of major seismic sequence boundaries.

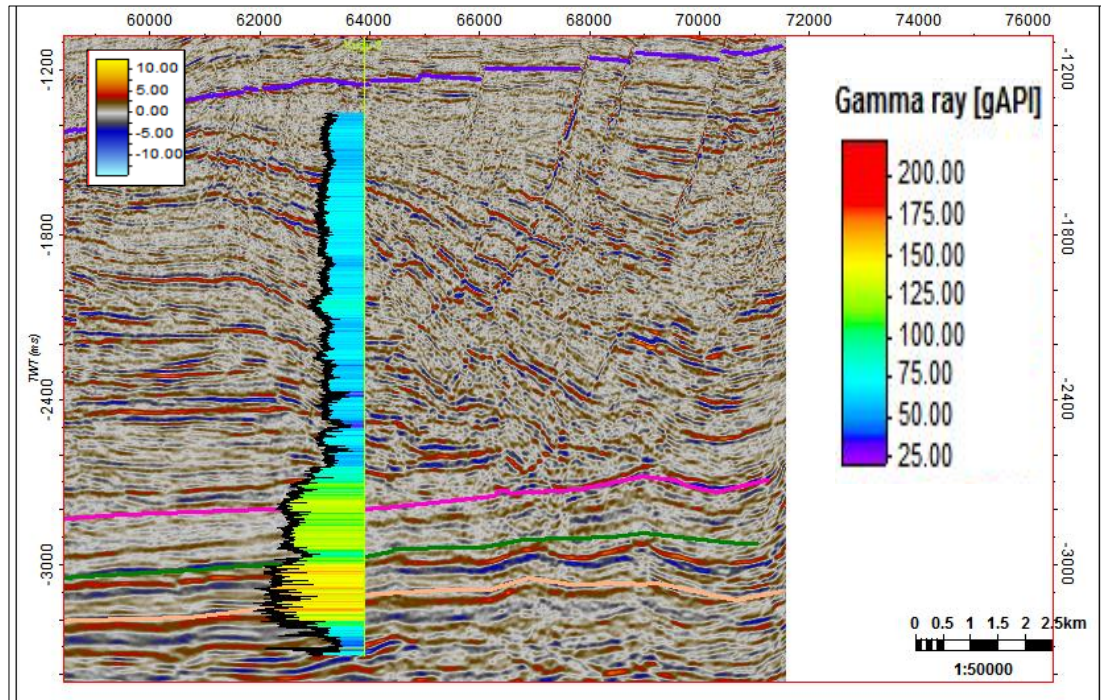


Figure 8: Gamma ray log for Kudu 3 used to identify sequence boundaries on W-E seismic line. Identified sequence boundaries shown in this section are Santonian (purple), Turonian (pink), Mid-Aptian (Green) and Base Barremian (Orange).

### 3.2.2 Seismic to well tie

Two wells were tied to the seismic sections; these wells include Kudu 6 and 2. The rest of the wells were not tied to seismic, because apart from Kudu 6 almost all of the kudu wells in the Orange Basin are located very close to each other. Kudu 6 and 2 were tied to seismic using checkshot data to obtain a time-depth relationship of well data. Subsequently, sonic and density logs were used to generate a synthetic seismogram for each well which was then matched to seismic reflection creating a relationship between well logs (measured in depth) and the seismic (measured in time). The synthetic seismogram was generated to bridge the gap between the seismic trace and the well data which provided means to tie wells to seismic data. The Turonian unconformity, Mid Aptian and Base Barremian shale tied fairly well to seismic in Kudu 2 (Figure 9). There were 'misties' observed in Kudu 6 which required vertical shifting of Mid-Aptian unconformity from 3597.88m to 3581.55m and Base Barremian Shale unconformity from 4202.4m to 4618.42m in order to properly tie the well to seismic (Figure 10 A & B).

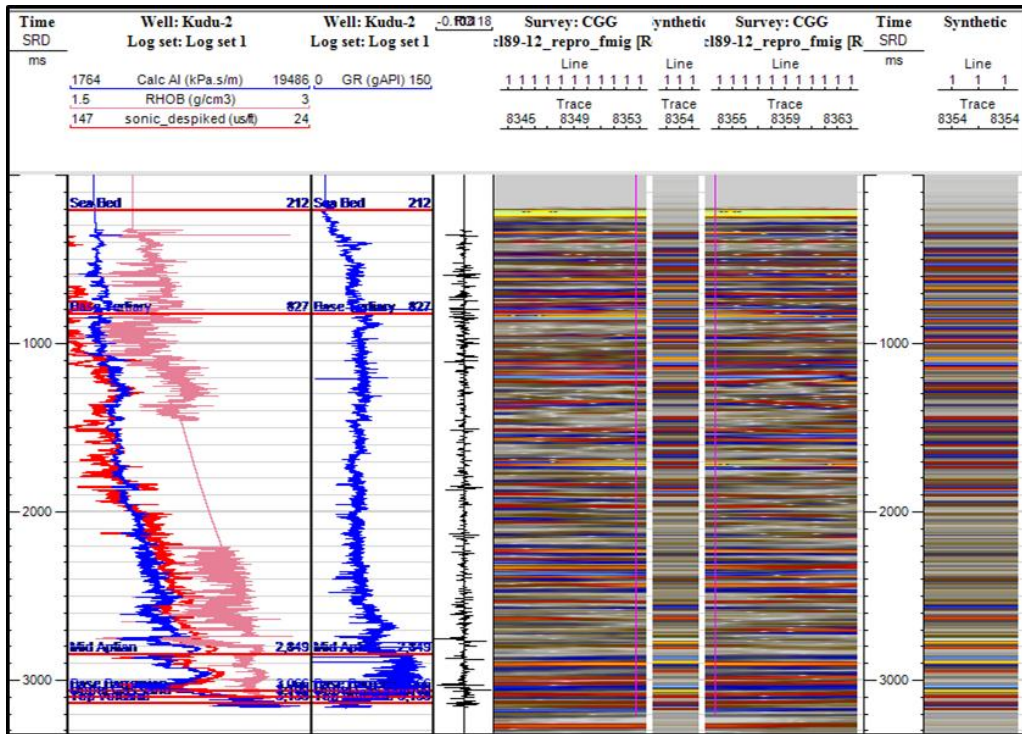


Figure 9: Seismic to well tie for Kudu 2. The seismic reflectors tying to the well tops were identified as major horizons on seismic sections with the aid of a synthetic seismogram. Note that major horizons tie fairly well with the well tops.

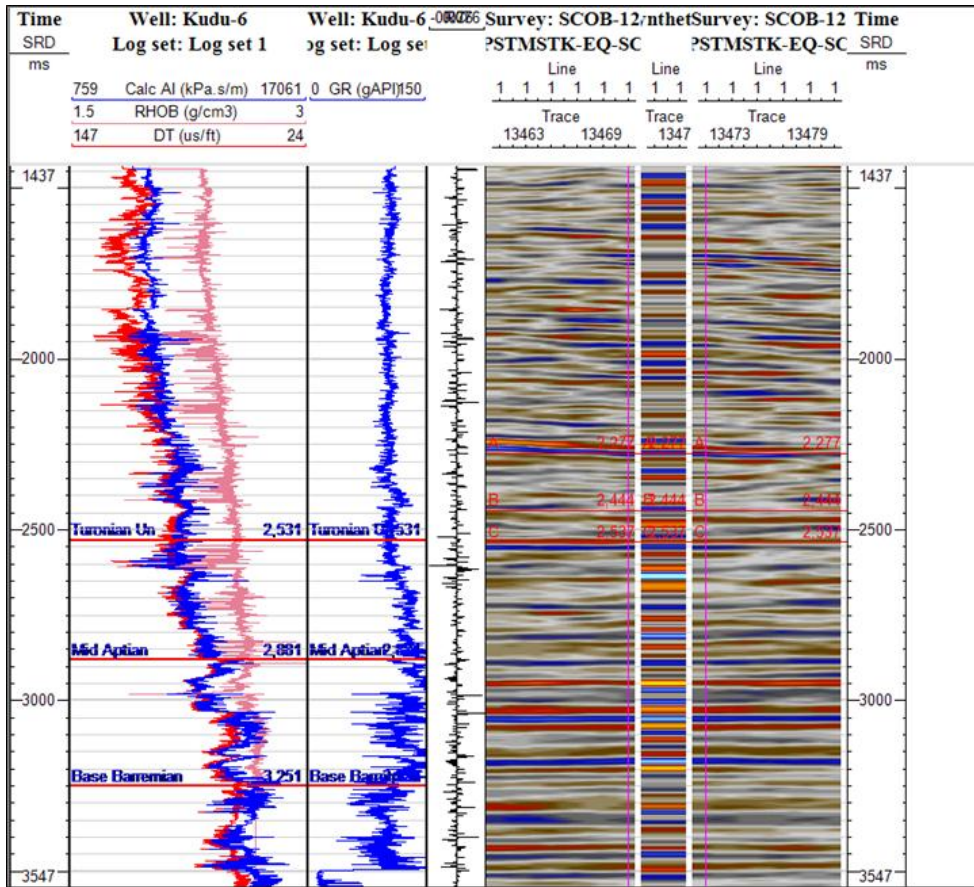


Figure 10 A: Seismic to well tie on Kudu 6. The seismic reflectors corresponding to well tops were identified as major horizons on seismic sections with the aid of a synthetic seismogram which did not tie well.

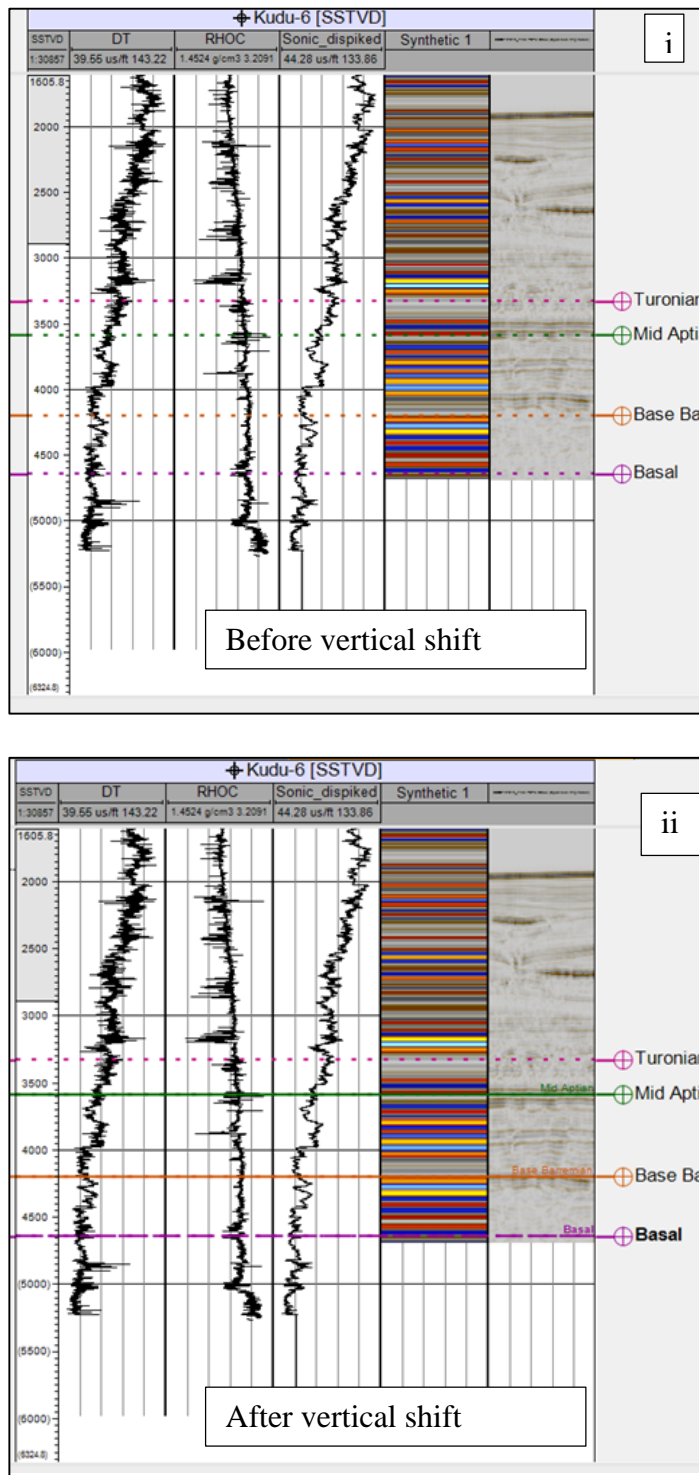


Figure 10 B: Seismic to well tie on Kudu 6 displaying vertical shifting of Mid-Aptian unconformity from 3597.88m to 3581.55m and Base Barremian Shale unconformity from 4202.4m to 4618.42m in order to properly tie the well to seismic.

### 3.2.3 Stratigraphic analysis

Seismic stratigraphy is a geological approach to the interpretation of stratigraphic information from seismic data which can provide an insight on the depositional processes, lithological predictions and stratigraphic relations of different seismic reflection packages (Mitchum et al., 1977). Stratigraphic units consist of relatively conformable succession of genetically correlated strata, and they are bounded by top and base unconformities or their correlative conformities. The stratigraphic units can be deduced from the identification of seismic surfaces which are represented by seismic reflections that follow bedding planes on seismic images. The seismic surfaces are recognized through the identification of different reflection terminations patterns.

The identification of the lower and upper boundaries on a seismic section leads to the subdivision of the seismic section into stratigraphic units called Megasequences. These megasequences are seen as chronostratigraphic intervals with continuous seismic reflections and their sequence boundaries are considered as quasi-isochronous surfaces. Megasequences epitomize sedimentary responses to major phases of Basin evolution and their development is mainly controlled by tectonics episodes. Typical subdivisions of megasequences in most of the passive margin sedimentary basins world-wide would be post-rift, syn-rift and pre-rift, which has also been used in this study with further subdivision of the post-rift section into early and late drift subsections.

Within a Megasequence, seismic sequences were identified as correlative strata bounded by smaller scale seismic surfaces. The upper and lower boundaries of these

sequences are characterized by different termination patterns, which represent characteristic periods of deposition (Mitchum et al, 1977) (Figure 11). Sequence boundaries were picked as seismic surface at which reflections terminate.

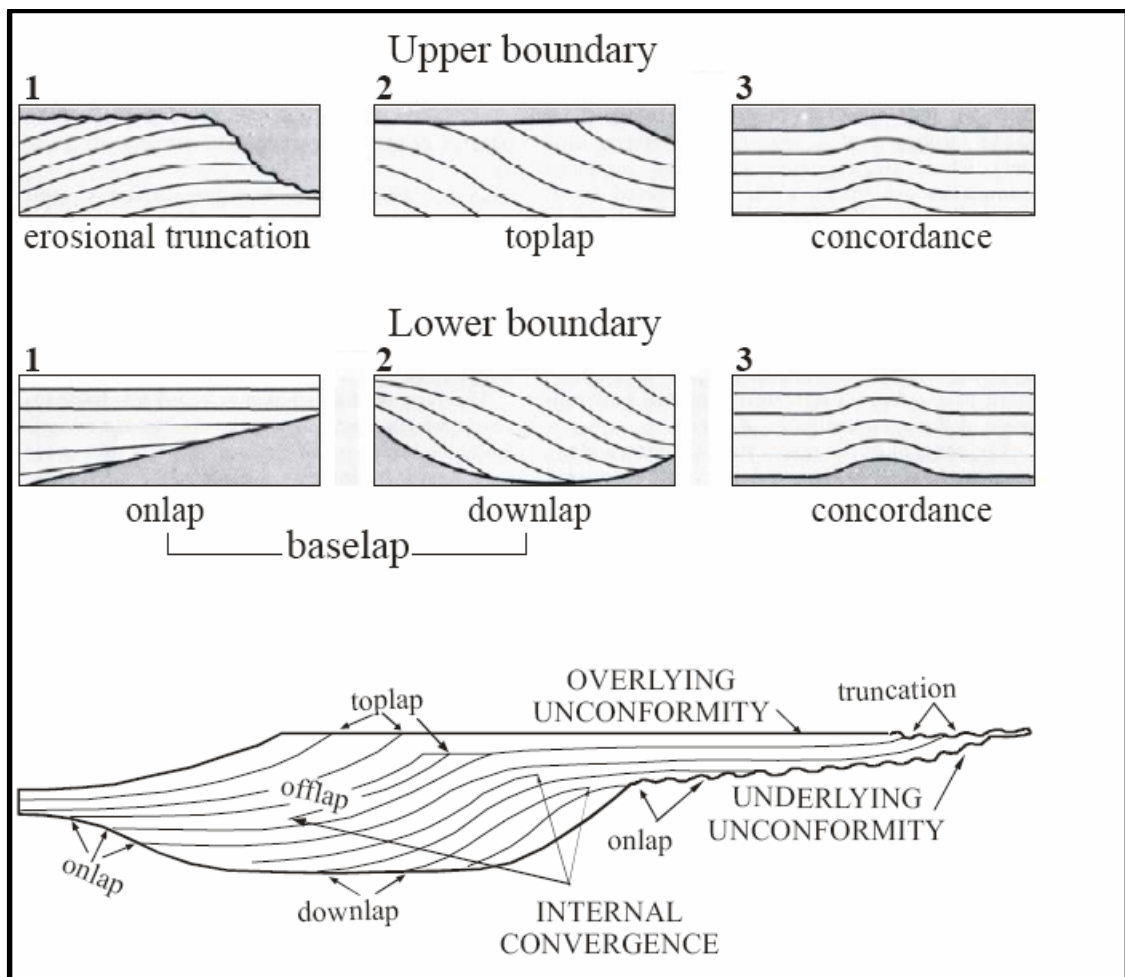


Figure 11: Reflection termination patterns indicating upper and lower boundaries of depositional sequences (Mitchum et al, 1977).

The upper boundaries are characterised by toplap or erosional truncation termination patterns, while onlap and downlap usually defining lower boundaries. Occasionally

the upper and lower boundaries may also be characterized by concordant reflection patterns and thus do not terminate against a boundary, but they tend to be parallel to the overlying and underlying boundaries. The sediment deposition for each sequence occurred during a single sea level change cycle. The main characteristics of reflector termination are the following:

- Toplap is characterized by inclined seismic reflections that terminate against a low-angle upper boundary. It represents a proximal deposition limit due to non-deposition along the underlying basin-wards prograding strata.
- Erosional truncation is defined by tilted seismic reflections terminating on an erosional surface which signifies a period of uplift followed by erosion. An erosional surface can act as oil and gas trap because the sedimentary layer of different lithology above it can act as a seal (Hyne, 2001).
- Onlap is characterized by seismic reflections that terminate progressively against an inclined surface due to basin fill caused by rise in sea level.
- Downlap occurs when inclined seismic reflection terminates against the lower boundary. This type of termination results from constant deposition of sediments over a smooth surface during a certain period. The term baselap can be used in instances where it is difficult to distinguish whether seismic reflectors are onlapping or downlapping.
- Offlap is not a true termination pattern. Offlap is rather a pattern of stratal packages that build upwards and outwards into the Basin.

Concordant seismic reflections do not terminate, but are parallel seismic reflections to the sequence boundary. This type of seismic reflection patterns occur as result of low energy, slow and uniform deposition of sediments over period of time.

Upon identification of unconformities, terminations were marked using arrows to indicate the orientation of the strata. The reflection boundaries between seismic sequences were mapped thorough-out the study area to establish lateral continuity of the seismic sequences.

Thereafter the depositional history of the Orange Basin was deduced from the identification of isochronous seismic surfaces and depositional sequences. The depositional sequences were used to construct a tectonostratigraphic framework for the pre and post-rift evolution of the Basin including the investigation of sediment supply to the Orange Basin.

i. Seismic Facies Analysis

Once seismic sequence boundaries are defined, further information about the depositional history of individual reflection packages within a depositional sequence can be deduced through seismic facies analysis. This process involves the investigation of seismic reflector characteristics such as configuration, reflection continuity, amplitude, frequency, and attributes (Mitchum et al., 1977b). Hence, the identification of seismic facies can reveal types of lithologies associated with an individual depositional sequence which can aid the prediction of the depositional environment and the energy of the depositing medium.

The interpretation was carried out by identifying types of reflection patterns which include parallel, subparallel, divergent, prograding, chaotic and free patterns (Figure 12A to 12D). The configurations of prograding patterns can be subdivided into clinoforms such as sigmoid, oblique, complex sigmoidal-oblique, shingled and hummocky stratifications (Figure 12 C).

Moreover gamma-ray logs from Kudu wells were used during facies analysis to delineate the depositional system tracts and identify Gamma-ray facies associated with sequence stratigraphic units.

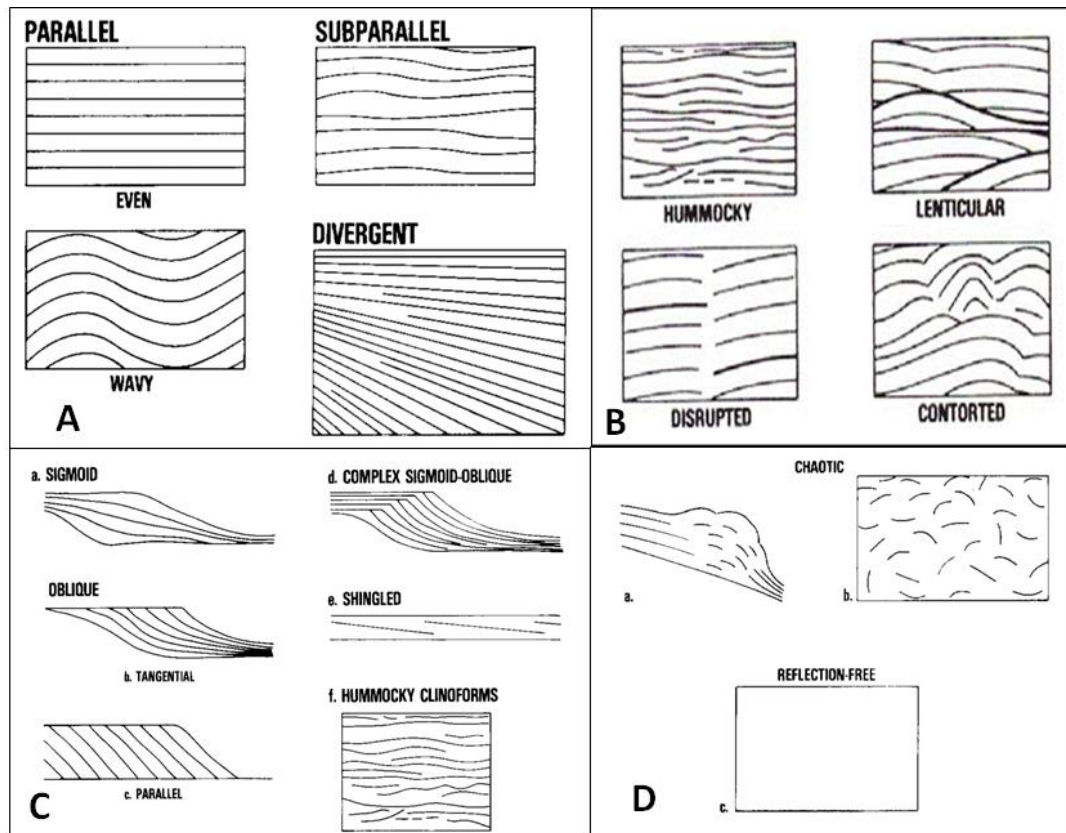


Figure 12: (A) Seismic reflection configurations, (B) Modified seismic reflection configurations, (C) Seismic reflection interpreted as prograding clinoforms, (D) Chaotic and reflection free reflection patterns (Mitchum et al., 1977).

Parasequence sets consist of stacked parasequences. The latter are the building blocks of sequences of relatively conformable successions of genetically related beds, typically bounded by a marine flooding surface and their correlative surfaces. Marine flooding surfaces bounding parasequences are usually laterally extensive and separate older from younger strata. A rapid increase in water depth is implied.

Progradation, Aggradation and Retrogradation parasequences were defined by analyzing sigmoidal reflection patterns (Figure 13) and shoreline trajectories *c.f.* Catuneanu (2006) (Figure 14). These reflection configurations result from changes in accommodation space in relation to the rate of sediment supply to the Basin over a certain period. Thus, they are a response to relative sea level change (Figures 13 and 14).

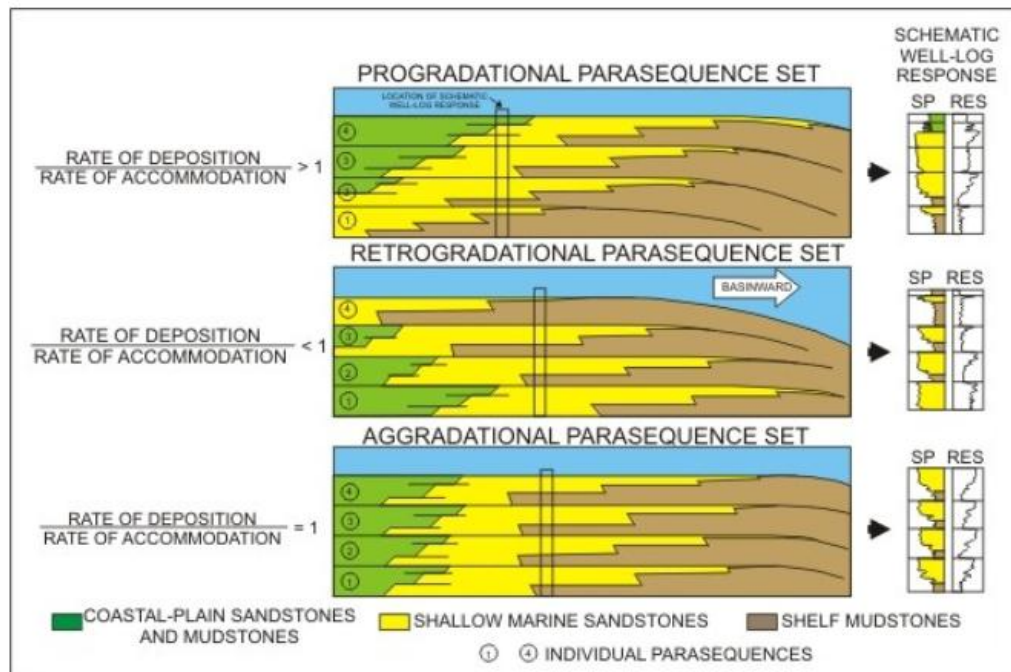


Figure 13: Diagram showing three different parasequence sets and their corresponding well log characteristics. Note that Progradational Parasequence set associate with coarsening-upward well log pattern, Retrogradational Parasequence sets associate with fining-upward well log pattern, and Aggradational Parasequence sets show uniform well log pattern. After Van Wagoner et al. (1990).

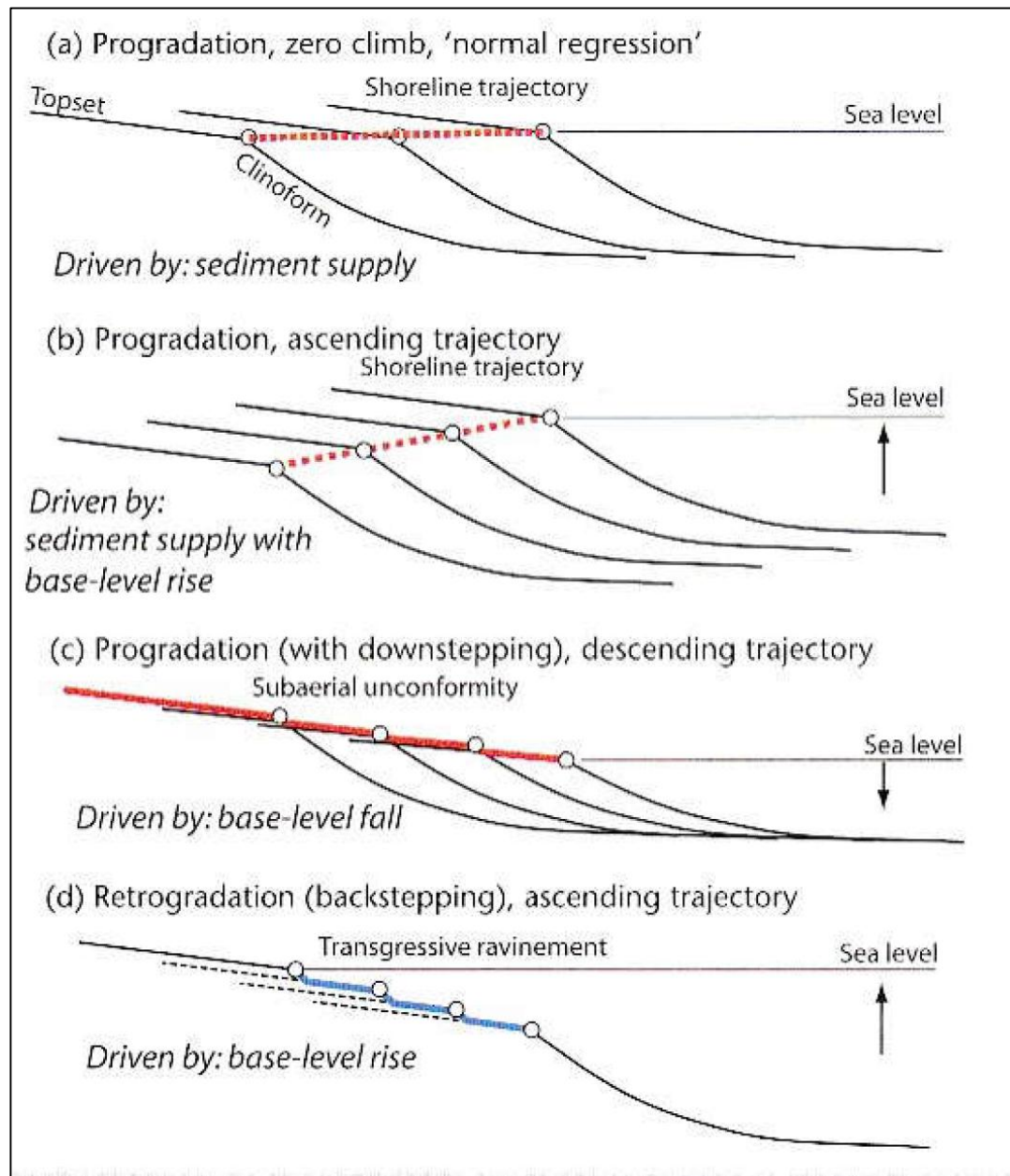


Figure 14: Trajectory of the shoreline associated with progradation and retrogradation, showing ascending and descending trends. After Allen and Allen (2013) referring to Catuneanu (2006).

**Progradational Parasequences** are characterized by sediments deposited more basinward during stable or slowly rising relative sea level due to insufficient accommodation space to accommodate all of the sediment supply without a steady basin-ward migration of facies. Younger parasequence sets are deposited further basinwards resulting in sea-wards expanding strata.

**Retrogradational Parasequences** are defined by sediments deposited more landward during rapidly rising relative sea level. The overall rate of sediment supply is less than the rate of accommodation space created resulting in onlapping strata. Younger parasequence sets are deposited land-wards and therefore define a transgression.

**Aggradational parasequences** defined by younger sequences deposited above one another, it occurs between retro and progradation periods, thus the rate of accommodation space creation is in balance to the rate of sediment supply and no significant lateral shifts in facies belt occurs (Howell & Fitzsimmons, 1997). Younger parasequence sets are deposited on top of older parasequences resulting in vertical build-up of sedimentary layers.

The identification of seismic facies units led to the generation of seismic facies maps. Based on all this information deductions about the depositional environment, associated lithologies and increments in basin evolution were made.

## ii. Identification of System Tracts

System tracts are three-dimensional units of deposition within a sequence consisting of stacked parasequences. They define various phases of sequence development within a relative sea level cycle from which palaeogeographic reconstruction of Basin geometry and facies distribution can be deduced. System tracts were identified on seismic by the nature of its bounding surfaces, parasequences stacking patterns coupled with the aid of gamma-ray logs. The boundary between system tracts developed as result of sea level change, subsidence, sediment supply and change rate of accommodation space. Three types of system tracts were identified: lowstand, transgressive and highstand system tracts (Figure 15).

**Lowstand System Tract (LST)** develops when both relative sea-level fall is rapid and accommodation space is limited, or when the rate of sediment deposition exceeds the rate of sea level rise during the early stage of sea level increase. Typically progradational parasequences sets built a lowstand wedge, a slope fan and a basin floor which are bounded by a sequence boundary at the base and a transgressive surface at the top (Van Wagoner et al., 1990). The transgressive surface is recognized on seismic as a surface that marks the end of lowstand progradation and beginning of transgression. It does not necessarily need to be associated with reflection terminations, but it marks the boundary between lowstand and transgression systems tracts.

**Transgressive System Tract (TST)** is formed when the rate of sedimentation is surpassed by the rate of sea level rise leading to development of retrogradational parasequences stacking in which facies belt move land-wards. In seismic this

transgressive retrogradation is expressed with strong onlap in land-ward direction. TST are characterised by thin shelfal sediment deposits which becomes even thinner in the outer continental shelf. This is caused by reduced sediment influx to the Basin since a large amount of sediments are usually trapped in the alluvial and coastal plain environments.

A transgressive systems tract is bounded by a transgressive surface at the base and a maximum flooding surface at the top. The transgressive surface may form a ravinement surface when it is of erosional character. A maximum flooding surface is recognized on seismic as a downlap boundary on which the overlying highstand system tract propagates.

**Highstand System Tract (HST)** develops during the late stage sea-level rise but sediment deposition rate exceeds the rate at which accommodation space is being created. Consequently, the rate of sea-level rise decreases through time resulting in development of a HST. As relative sea-level decreases high energy channelized fluvial and shallow marine successions invades low energy lagoonal and over-bank deposits. HST are bounded by maximum flooding surface at the base and a sequence boundary on top marking the inception of the next sequence. HST consists of progressively progradational parasequences sets with depositional characteristics similar to that of TST such as alluvial, coastal and shallow marine.

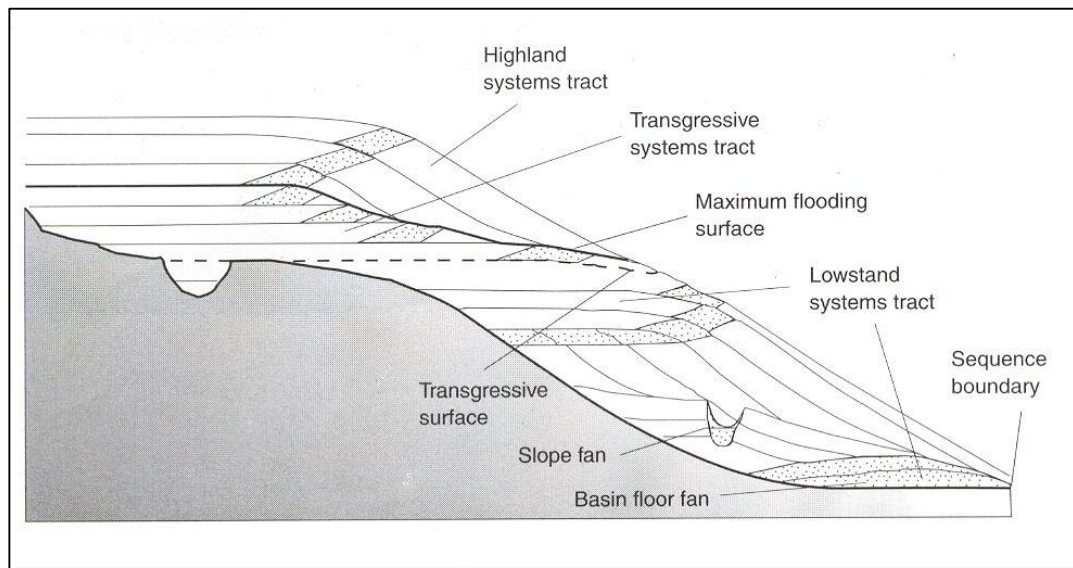


Figure 15: Idealized sequence diagram outlining three types of system tracts and their respective boundaries resulting from one cycle of base level change (Brown & Fisher, 1977).

### **3.2.4 Structural Analysis**

The stratigraphic analysis complements the seismic structural analysis, since major horizons mapped to represent first order unconformities which delineate Megasequences were used as horizon markers for structural investigations. Early mapped regional faults depicts displacements of strata and more complex structures such as toe-thrusts during stratigraphic analysis. Time structural contour maps were generated using six seismic horizons that were identified through seismic sequence analysis. Subsequently, depth contour maps were generated from time contour maps using interval velocities obtained from vertical seismic profile (VSP) data from wells. Structural contour maps were used to visualize topographic surfaces related to depositional systems within the Basin. Structural traps were identified as closed contours both in time and depth. Isopach maps were generated from structural maps to determine the thickness of stratigraphic units, which can be used for hydrocarbon reserve estimates.

### **3.2.5 Petroleum System**

The petroleum system investigation involved the describing of the genetic relationship between the identified source rocks, reservoir, trap and seal identified during the stratigraphic and structural analysis of the data. This led to determination of probable migration path of hydrocarbons. The generation of thickness maps reveals possible location of hydrocarbon kitchens at different stratigraphic level in areas which attains maximum thickness.

### **3.2.6 Onshore Analogues**

The field excursion to study analogues of petroleum play elements was conducted from 20<sup>th</sup> to 25<sup>th</sup> March 2010. Areas visited during the field excursion which include Kalkrand Formation in the vicinity of Hardap Dam, exposures of the Ganigobes Shale member near Tses, the Whitehill Formation on farm Spitzkoppe and the deltaic-fluvial deposits at the Orange River Mouth in Oranjemund.

In July 2013 a fieldtrip to Huab Basin was undertaken within the hyper arid Namib Desert. The outcrops visited stretches across the Kunene area in the North-Western part of Namibia covering an area of approximately 5,000 Km<sup>2</sup> (Duncan et al., 1998). The Neoproterozoic outcrops, Phanerozoic to Mesozoic Karoo rocks units, Cretaceous

igneous complexes, volcanics and the Tertiary alluvial gravels of the Huab Basin are well exposed with little to no vegetation cover in most sites.

The Kudu reservoir onshore analogues provided additional information on the geometric and depositional architecture of offshore rock units which improves the understanding of petroleum system.

## **CHAPTER 4: RESULTS AND ANALYSIS**

### **4.1 Stratigraphic Analysis**

#### **4.1.1 Well Correlation**

The gamma ray signatures appeared to be the most powerful logs in well log analysis and subsequent well correlation. Gamma ray signatures were related to corresponding geological Formations and thus allowed to reveal the regional distribution of stratigraphic units in the Orange Basin (Figure 16A and 16B). In most of the wells the gamma ray was recorded below the Base Tertiary unconformity, with the exception of 2815/15-1 and Kudu 2 where the gamma ray was recorded just below sea bed to total depth (TD). The interval between Base Tertiary unconformity to Sea Bed appears to occur almost at the same level in all wells except for 2815/15-1 where the Base Tertiary unconformity is outcropping. The Turonian to Base Tertiary interval appears to be the thickest succession in most of the wells except for 2815/15-1 where the thicker interval is Aptian to Turonian. The thick succession is an indication of high sedimentation rates at those intervals.

The Turonian unconformity marks the beginning of slight increase in gamma ray in most wells which increases more below the Aptian unconformity. The highest gamma ray values in the wells were recorded in the interval between the Base Barremian Shale and the Aptian unconformity which was proven to be the Kudu source rock. The high gamma likely relate to the shaleness and OM content of the source rocks in this

interval. The Base Barremian Shale unconformity coincides with the base of the high gamma interval.

The succession below the Base Barremian Shale unconformity show gradual decrease in gamma ray. This interval has been proved to be the reservoir rock for the Kudu Field and consists of two gas-bearing sandstone intervals interbedded with volcanics (Shell, 2002).

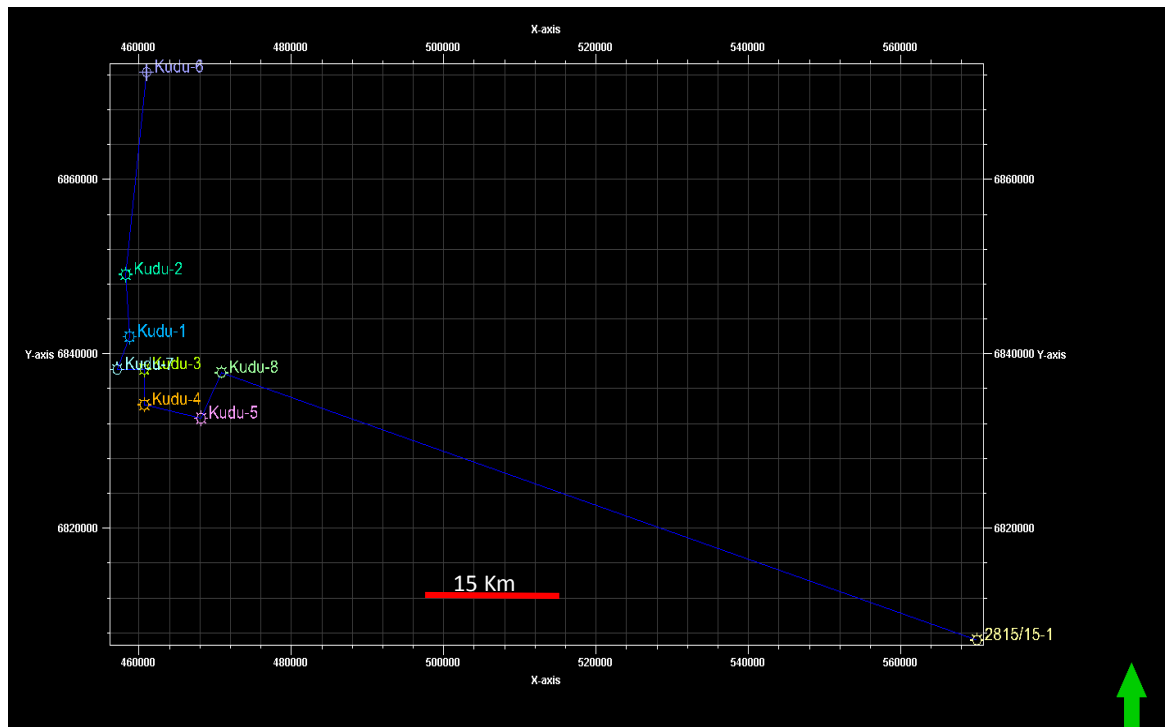


Figure16A: Map showing the orientation of the well cross-section used for well correlation.

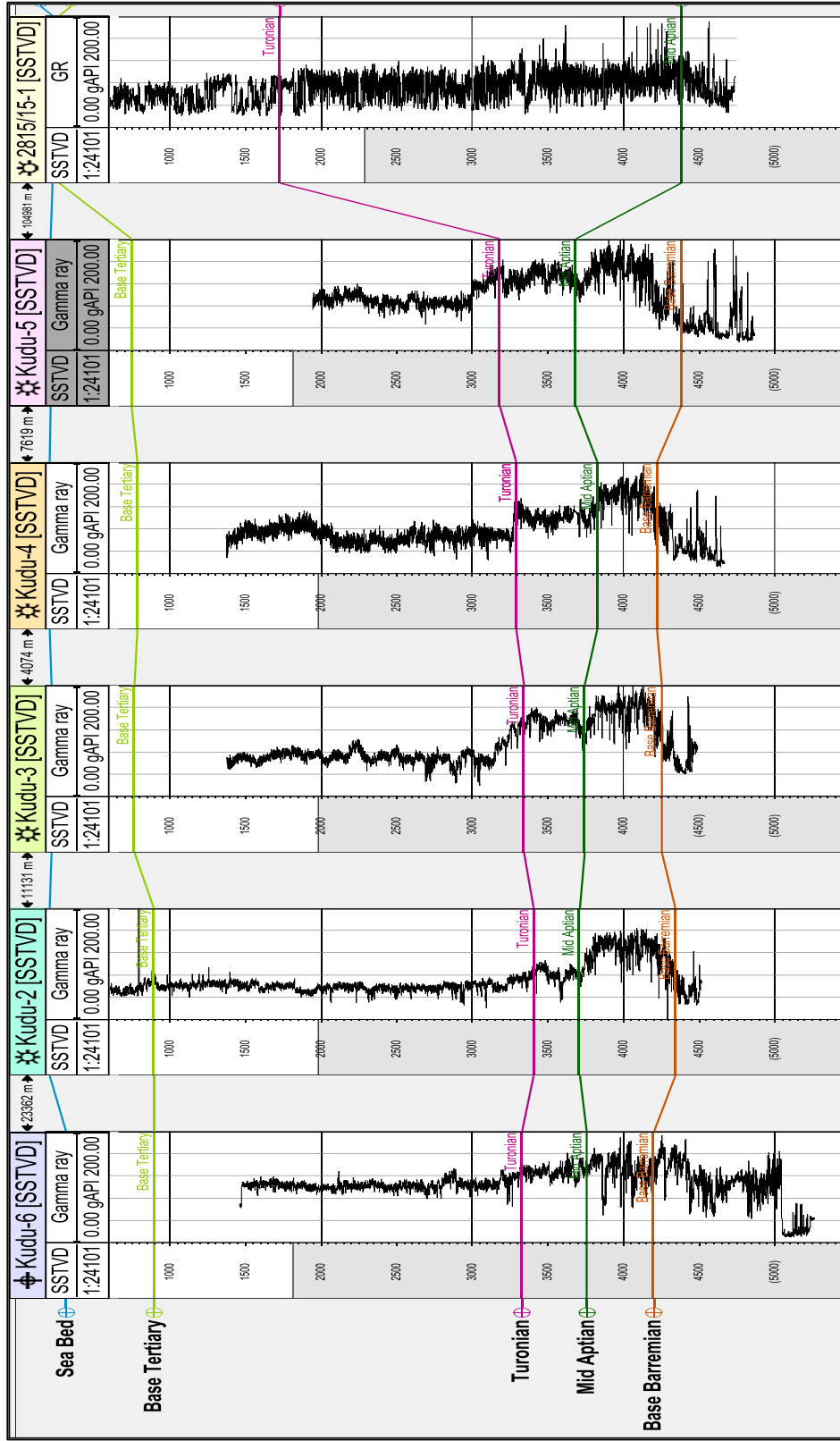


Figure 16B: Correlation of Orange Basin wells by identifying similar gamma ray signature corresponding to several geological formations. Note that the Base Tertiary unconformity outcrops in 2815/15-1. In this well the interval between Turonian (purple line) and Aptian (dark green line) is thick compared to all other wells. Enlarged diagram in Appendix C.

In order to understand the distribution of the reservoir rock in the Kudu area a well log analysis was carried out for the wells (Kudu-1, Kudu-3 and Kudu-4) located in the Kudu main field (Figure 17). The intervals were identified as described in the Subsurface Evaluation of the Kudu Licence report for Block 2814A, Offshore Namibia by Shell. Two main sandstone intervals were observed in all three wells.

The first reservoir interval which is the Kudu main reservoir occurs between the Upper Gas sand and Volcanic 1 markers. The second reservoir occurs at interval between Lower Gas Sand and Volcanic 2 markers and exhibit low gamma ray signature compared to that of the first reservoir interval. Kudu 3 recorded a third reservoir interval which occurs at 4474 to 4480 meters. The interval between the Top test and Bottom test markers (black markers) is the main Kudu reservoir target.

Well picks from several well reports were used to generate well panels with the aid of AutoCad software which refines the distribution of kudu reservoir rock (Figure 18). Kudu 3 attains thick reservoir interval compared to Kudu-1 and Kudu-4. Lower Cretaceous shale (green interval) is also thicker in Kudu 3 compared to Kudu-1 and Kudu-4.

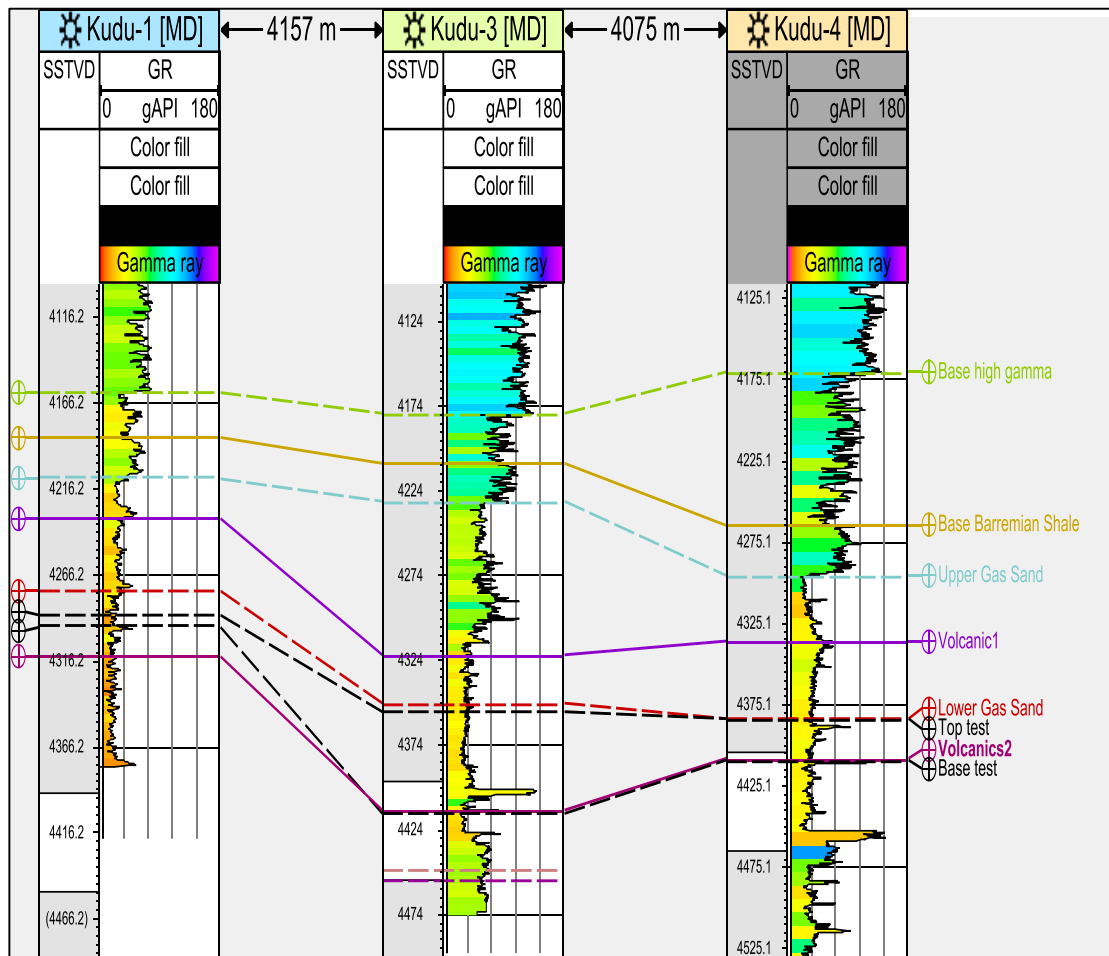


Figure 17: Well log analysis of wells in the Kudu main field. Note that Kudu 3 has three sandstone intervals, unlike Kudu-1 and Kudu-4 with only two sandstone intervals. Note that the youngest sandstone interval is between top Upper Gas Sand (light blue) and Volcanic 1 (purple) markers. The main gas reservoir spans from top of the Lower Gas Sand (red) to Volcanic 2 (light purple) markers. The stem drill test was performed in this interval. The third and oldest sandstone interval is between the orange and the lower purple line which only occurs in Kudu-3.

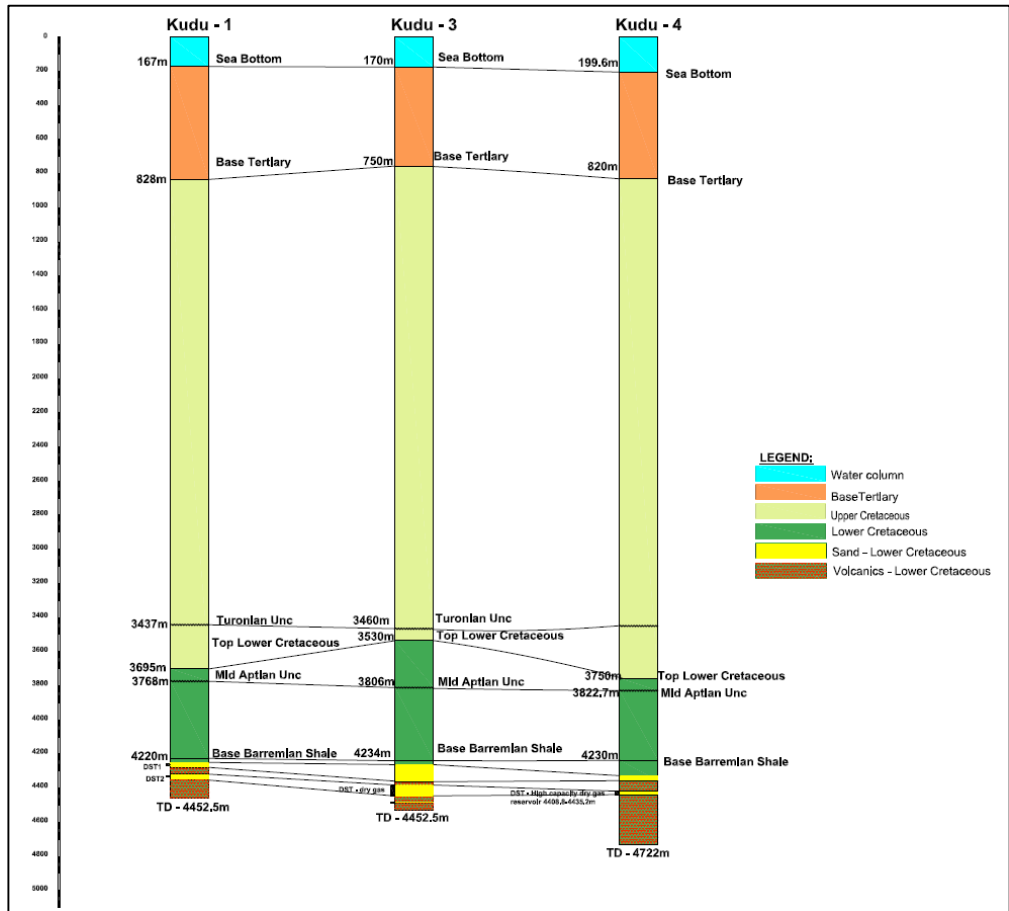


Figure 18: Well panel correlation for the kudu main field wells (Kudu-1, Kudu-3 and Kudu-4). Note that there are three reservoir intervals (yellow) in Kudu-3 as earlier indicated in the previous diagram. Enlarged diagram in Appendix D.

#### **4.1.2 Overview of the Orange Basin**

The Orange Basin is the largest and deepest Mesozoic Basin along the rifted Namibian continental margin. Four tectonostratigraphic units (mega sequences) have been identified in the Orange Basin, namely Pre-Rift, Syn-Rift, Early Drift and Late Drift (Figure 19). These units are separated by three major unconformities which were identified with the aid of wellpicks obtained from Kudu well reports. Each megasequence corresponds to a major tectonic event.

Rifting commenced along the area of the southwestern Africa margin during the late Jurassic and progressed until the Hauterivian. This resulted in a divergent passive margin with underlying grabens and half grabens (Van der Spuy et al., 2000). The Orange Basin was formed in the Early Drift of the African and South American continents which occurred between Hauterivian (130 Ma) to mid Aptian (100Ma). This succession is classified as the intermediate succession (Van der Spuy et al., 2000). The transition phase is envisaged to be Barremian in age comprised of aeolian sandstone interbedded with lava in the lower part of this succession (Nopec, 1991).

The drifting phase is characterized by a thick sedimentary wedge which contains large growth faults and slump structures forming toe thrusts along the shelf edge. The late drift section (Turonian to recent) volumetrically forms the main part of the basin fill. The Base Tertiary unconformity divides the late drift section into a lower and upper division (Bray et al, 1998).

A major structural feature of the Namibian margin is a hinge line marking the landwards wedging out of the syn-rift sequence. Generally the hinge line defines the

boundary between areas of thin sediment overlying shallow basement and the zone of rapid sediment thickening in sea-wards direction (Figure 20). An inner half graben east of this hinge accommodates parts of the syn-rift sequence, whereas a central graben occurring west of the hinge accommodates thick wedges of all sequence, possibly also including a Pre-rift sequence.

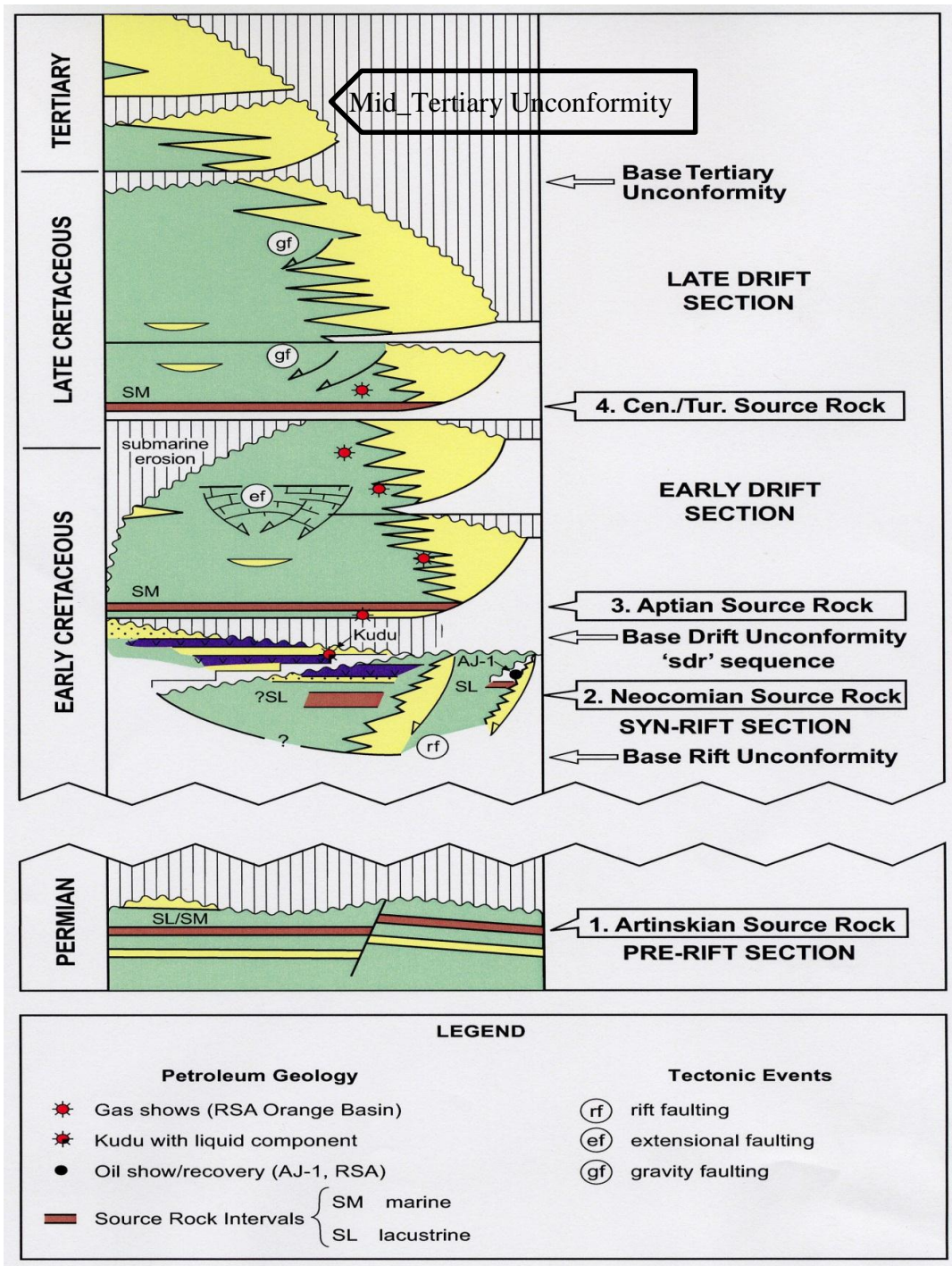


Figure 19: Generalized stratigraphy offshore Namibia showing four tectonostratigraphic units separated by three major unconformities modified after Bray et al., (1998). Note that tectonostratigraphic units are delineated by sequence boundaries defined by erosional surfaces.

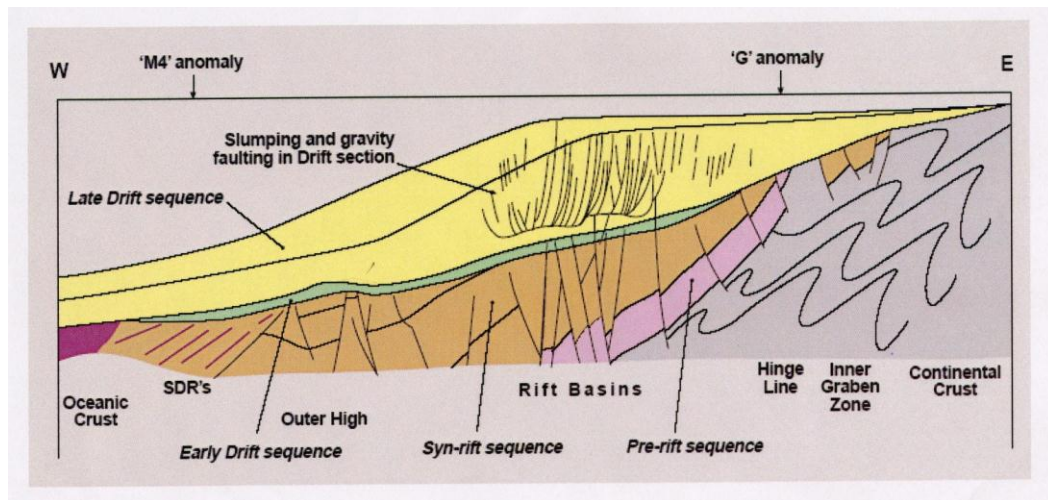


Figure 20: Simplified schematic geological section of the Orange Basin displaying its structural framework with the Pre-rift to Early drift sequences. A shallow inner half-graben occurs east of the hinge, whereas central deeper graben structures occur west of the hinge. Note that the central grabens are covered with a particular thick wedge of the lower part of the Late drift succession. Adopted from Veritas DGC Limited, 2004.

### 4.1.3 Stratigraphic Framework

#### 4.1.3.1 Pre-Rift (Carboniferous to Mid Jurassic)

##### i. Structural History Review

The Pre-rift overlies basement and is the oldest tectonostratigraphic unit associated with the initial rifting. The Pre-rift period spans from the Late Carboniferous to the Mid-Jurassic and it resulted in the development of the Proto-Antlantic rift (Gladczenko *et al*, 1998). The basement is predicted to consist of Precambrian high grade metamorphic rocks and Cambrian greenschist to amphibolite grade metasediments similar to the Damara Sequence that outcrops along the southern coast of Namibia (Baker Hughes INTEQ, 1996).

The Pre-rift structures are envisaged to be located east of the Orange Basin (Nopec, 1991) where initial rifting started. This area is intersected by the Damara Fault (Figure 21) which acted as a thrust during the Gariiep orogeny. Later this basement anisotropy acted as a zone of weakness for the initiation of the extensional Pre-rift grabens.

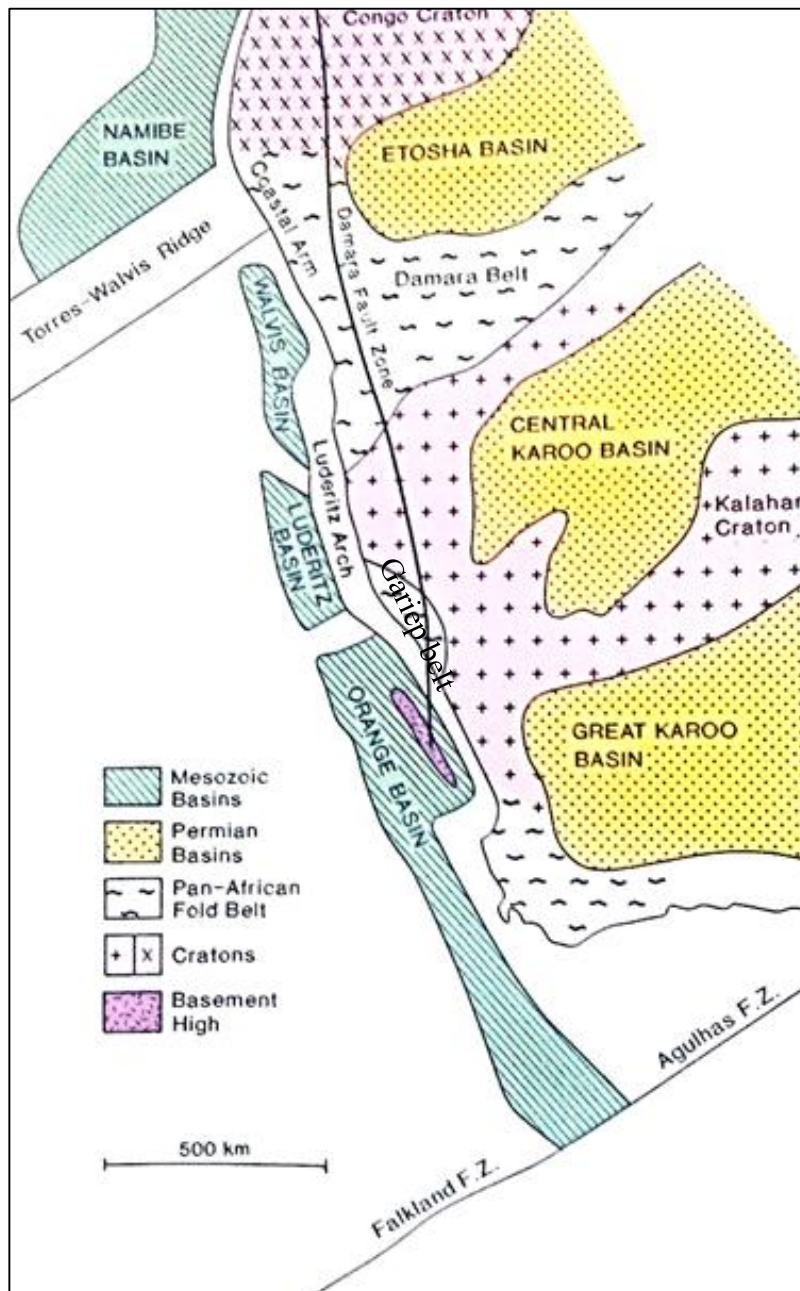


Figure 21: Schematic outline of the sedimentary basins and their relative tectonic elements off the west coast Namibia and South Africa (after Nopec, 1991). Note the extension of the Damara Fault Zone into the Orange Basin.

## ii. Depositional Review

The pre-rift succession includes sequences that were deposited in the basin before the more pronounced rifting onset. It consists of Jurassic and possibly Paleozoic sedimentary rocks (HRT Petroleum, 2008). The pre-rift Karoo sediments were deposited in NNW-SSE trending fault confined graben structures (Stewart et al, 1999). It is envisaged that the pre-rift Karoo section and possibly the late Proterozoic basement contains oil-prone source rocks. The presumed late Paleozoic Karoo source rocks are considered to be equivalent to the Whitehill Formation onshore Namibia and the Irati shales in Brazil (Bray et al. 1998) (Figure 22). These two onshore shale members are considered to be the only oil-prone sources in the whole Karoo Supergroup with average TOC 4.3% to 10%, and maximum values of 12% to 14% TOC. The Neoproterozoic in the Nama Basin may also contain source rocks. An oil seep has been identified on farm Heigums 105 east of Aus in fault breccia of the basal Nama Group quartzite below the Whitehill Formation. Black oil inclusions in clear quartz crystals have been observed on a rock unit above the Whitehill Formation on farm Aussenkjer 147. Another hydrocarbon show was observed in the Fish River sandstone SE of Berseba as a vertical, bituminous brecciated vein occurring beneath Karoo rocks (Walter et al., 1996).

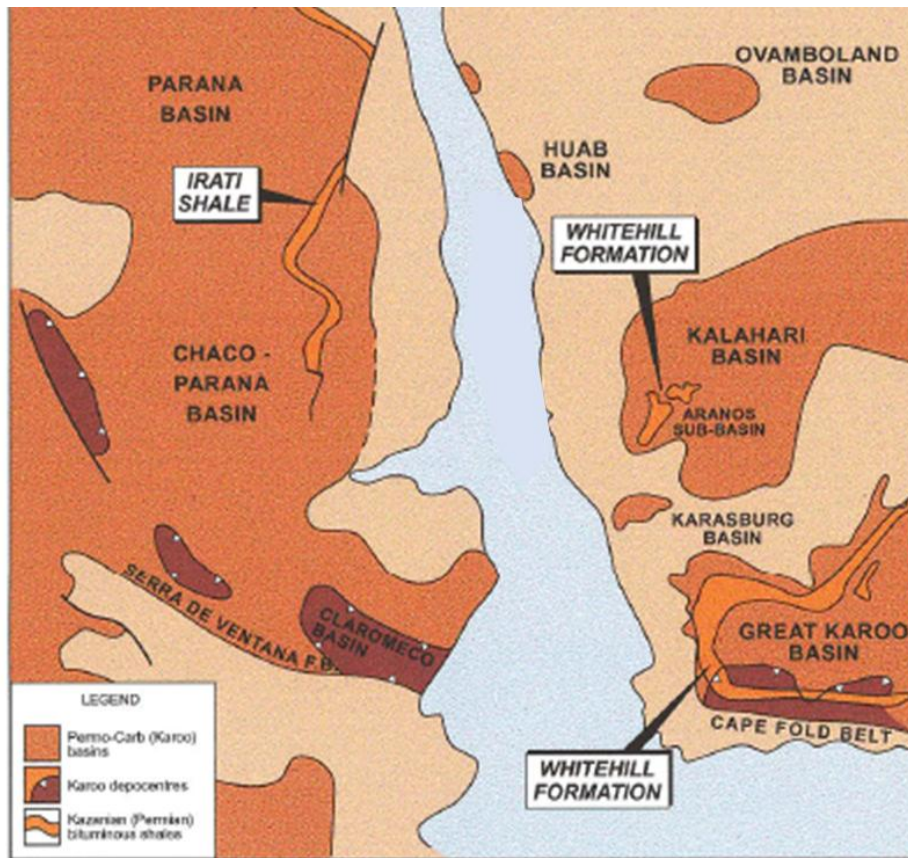


Figure 22: Paleogeographic reconstruction showing the distribution of the Permian Whitehill Formation in Namibia and the Irati shale in Brazil. From Quad Consulting Ltd., 1996.

### iii. Seismic Interpretation (own observations)

The pre-rift is separated from the syn-rift unit by the base rift unconformity. The seismic reflectors within this section are not distinctive enough and very difficult to interpret. Interpretation is hampered by the fact that none of the wells drilled in the Orange Basin and the entire offshore Namibia has intersected the pre-rift section. As a result, the lithology description of this unit is based on analogues exposed in

onshore outcrops. The main geometries observed in the pre-rift seismic sections are triangular-shaped rotated blocks constrained in mid amplitude seismic reflectors (Figure 23).

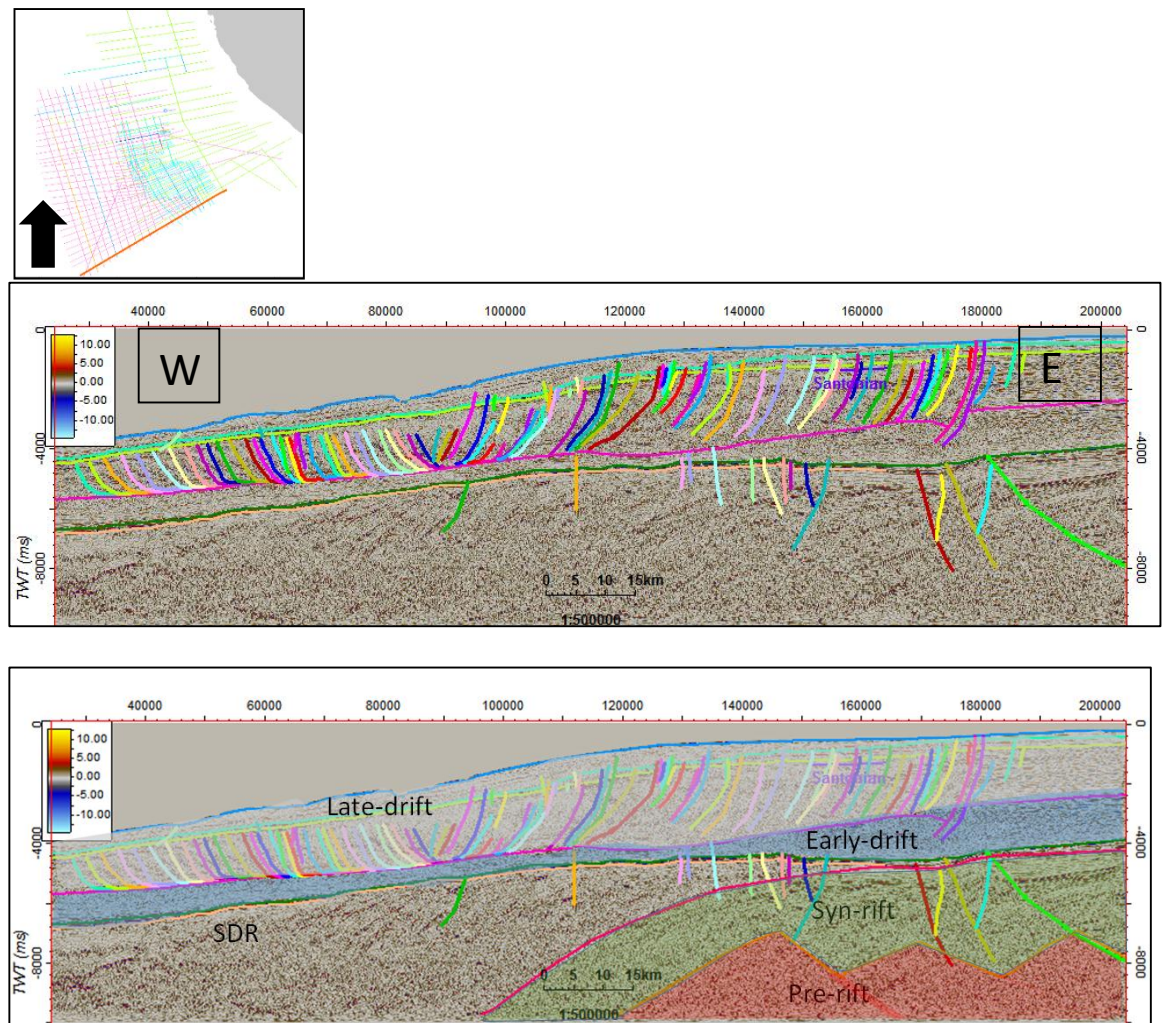


Figure 23: W-E seismic line showing tectonostratigraphic units of the Orange Basin from the Pre-rift to Late drift. Note that the Pre-rift is demarcated by rectangular shaped synthetically rotated blocks.

#### 4.1.3.2 Syn-Rift

##### i. Structural History Review

The top Syn-rift unconformity is late Hauterivian and Early Barremian of age (Van der Spuy, 2005). The lavas in the Orange Basin erupted in the Early Cretaceous period (Gladczenko et al., 1998).

The extensional stress caused by the imminent break-up of the African and South American plates initiated rifting between the two continental margins in Late Jurassic (Muntingh & Brown, 1993). This was accommodated by dextral motion on the Agulhas Falkland Fracture zone approximately 170 to 150Ma. Even though the magnetic anomalies that symbolize the onset of sea-floor spreading evidently indicate the end of extension, the timing of initial rifting is unclear due to insufficient wells that have penetrated this section, as well as lack of evidence onshore Namibia (Stewart et al., 1999). However, the age of the Syn-rift section can be deduced from seismic structures offshore Namibia as they appear to be equivalent to Late Jurassic rock units found both onshore and offshore the Argentinian-Brazilian conjugate margin (Uliana et al., 1989). Additionally, The A-J1 well offshore the Orange Basin South Africa revealed that the syn-rift is late Hauterivian and possibly late Jurassic to Neocomian in age (Van der Suy, 2005). This is the only well that intersected the Syn-rift in the entire Basin. The initial rifting resulted in the development of several grabens and half grabens structures sub-parallel to the present-day coastline (Muntingh & Brown, 1993).

## ii. Depositional Review

The Syn-rift refers to the period of active rifting including the formation of rift valleys and rift shoulders. The Syn-rift sequence comprised of late Jurassic to Hautveterivian units succeeded by terrestrial-coastal-shallow marine deposits (Petroleum Agency SA, 2007). The later act as both source rock and reservoir, and structural closures have been observed. The Syn-rift succession is characterized by continental clastic “red-bed”, volcanic rocks and occasional lacustrine shales. Syn-rift half graben red-beds include fluvial claystones, sandstones and pebble beds (Hirsch, 2008). The A-J1 well revealed that the sediments that filled the syn-rift inner graben are mainly oil prone lacustrine claystones interbedded with sandstones (Van der Suy, 2005).

The top volcanic rocks of the syn-rift have been dated to be 132Ma (Seranne & Anka, 2005). Seawards rift structures of the oceanic crust formed with sea floor spreading that commenced some 127Ma (Seranne & Anka, 2005) and herewith initiated the succeeding drift-phase.

## iii. Seismic Interpretation (own observations)

In Figure 23 the mid-Syn-rift unconformity is marked with a bright pink horizon representing a continuous moderate amplitude seismic reflector. The Syn-rift sequence overlying the Pre-rift is represented by medium to high amplitude seismic reflectors on seismic images which dips west-wards and becomes chaotic in this direction (Figure 24). The upper section of the Syn-rift is comprised of several faults forming horst and graben structures. The end of the Syn-rift can be mapped on seismic as a break-up unconformity where some of the extensional faults terminate with on-lapping

sub-parallel seismic reflectors. The seismic reflectors bulge over faults that cut through the Syn-rift horizons and penetrate the overlying Early-drift section. Strong seismic reflectors of the Syn-rift section represents volcanics and weak seismic reflections are likely volcanoclastics.

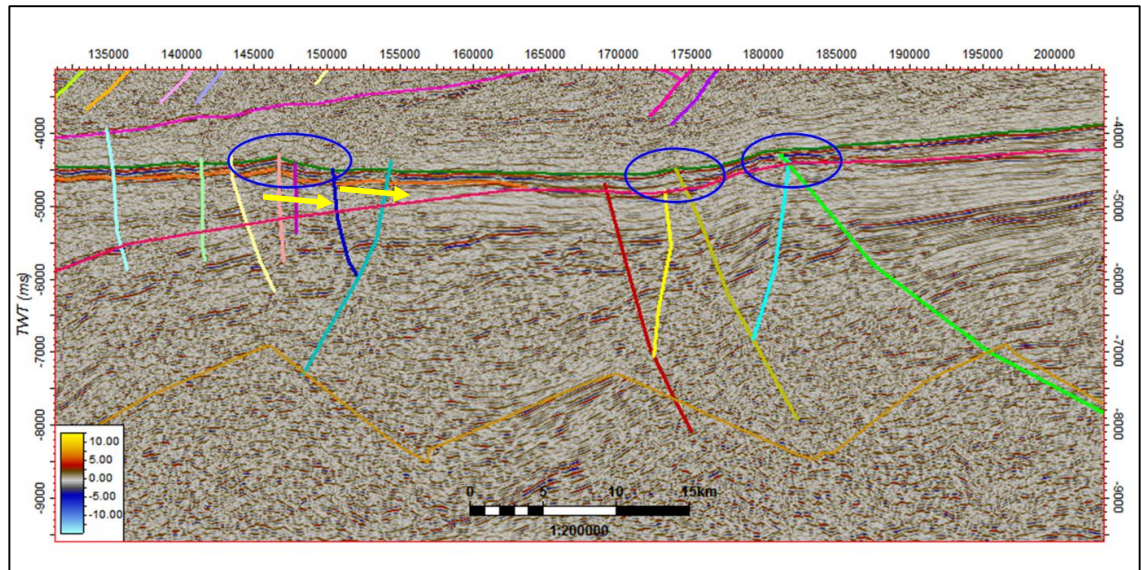


Figure 24: Enlarged W-E line of the previous Figure 23 showing half graben fault structures within the Syn-rift sequences. Blue circles highlight the bulging of seismic reflectors over faults that cut through the Syn-rift unconformity. The on-lapping strata are marked with yellow arrows.

#### 4.1.3.3 Early Drift

##### i. Structural History Review

The separation of South America from the African Plate and emplacement of oceanic crustal rocks singled the early Cretaceous onset of the South Atlantic drifting phase. The Early drift section overlies the Syn-rift which is comprised of a Barremian to Cenomanian marine claystone- dominated sequence containing organic rich intervals (Bray et al, 1998). The Hauterivian/Barremian base drift unconformity marks the transition from marine to non-marine depositional environment (Bray et al, 1998).

##### ii. Depositional Review

This succession was deposited immediately after rifting and it follows the Syn-rift topography, especially in areas consisting of the earliest part of the sequence. The Early drift section has been intersected by almost all Kudu wells. Well data shows that sediments deposited during the Early Cretaceous are mainly aeolian sands interfingering with basaltic lava (Nopec, 1991). A rapid marine transgression occurred at the upper part of this succession. The resulting deposition of Aptian organic rich shales indicates deposition under poorly oxygenated conditions (Quad Consulting Ltd, 1996). The organic rich shale have been proven as the source rock that has charged the Barremian aeolian reservoir sandstones in the Kudu wells as well as the Barremian fluvial sandstones of the Ihubesi gas field (van der Spuy, 2005). The Mid Aptian unconformity marks the transition to more oxygenated conditions.

### iii. Seismic Interpretation (own observations)

The transitional phase from rifting to drifting is represented by a section between Base Barremian shale unconformity and Mid Aptian unconformity. Two Palaeo-highs were observed at this interval, one in mid-waters and another one down-dip (Figure 26). Thin sedimentary fill compared to all other three mega-sequences characterizes this interval. The economic importance and available data of this interval allowed for a closer investigation of internal reflectors and a seismic facies analysis (next section).

### iv. Seismic facies (own observation)

The Early drift section shows parallel and continuous well-imaged seismic reflectors. A palaeo high was observed in Mid-waters where Seawards Dipping Reflectors (SDR) top lap on a major unconformity just below the Base Barremian unconformity. This unconformity marks the top of the Syn rift sequence (Figure 25), which is composed of parasequence sets prograding without aggradation. Local pinch-outs are observed in the top Syn-rift sequence which marks the end of the rift phase just below the Base Barremian Shale unconformity west of the palaeo high. The age of this major unconformity is envisaged to be Early Barremian to Jurassic age.

The upper strata of the Early Drift sequence can be seen onlapping on the Mid Aptian unconformity on the western flank of the palaeo high. This onlapping implies a drowning of the topography during a transgressive system tract. The Mid-Aptian is the major flooding surface in the Basin, and highest gamma ray values are recorded in the Aptian-Barremian interval (see previous chapter). These high gamma values relate to the presence of radioactive elements such as uranium found in organic rich successions. Shales deposited during later stages of transgressive system tracts and

early stages of high stand system tracts tend to be higher in TOC as they are less diluted by sandy material and deposited in water depths with restricted oxygenation (Craeney and Passey, 1995).

Further seawards, in areas close to the Economic Exclusive Zone (EEZ), the onlapping of young strata on the Base Barremian Shale unconformity was observed (Figure 26). Moreover, the Syn-rift strata is directly toplapping on the Base Barremian unconformity unlike in mid-water where it is toplapping on the unconformity below the Base Barremian. This area also displays similar patterns of seismic reflection termination patterns observed in mid-waters, which is the onlapping of younger strata on the Mid-Aptian unconformity.

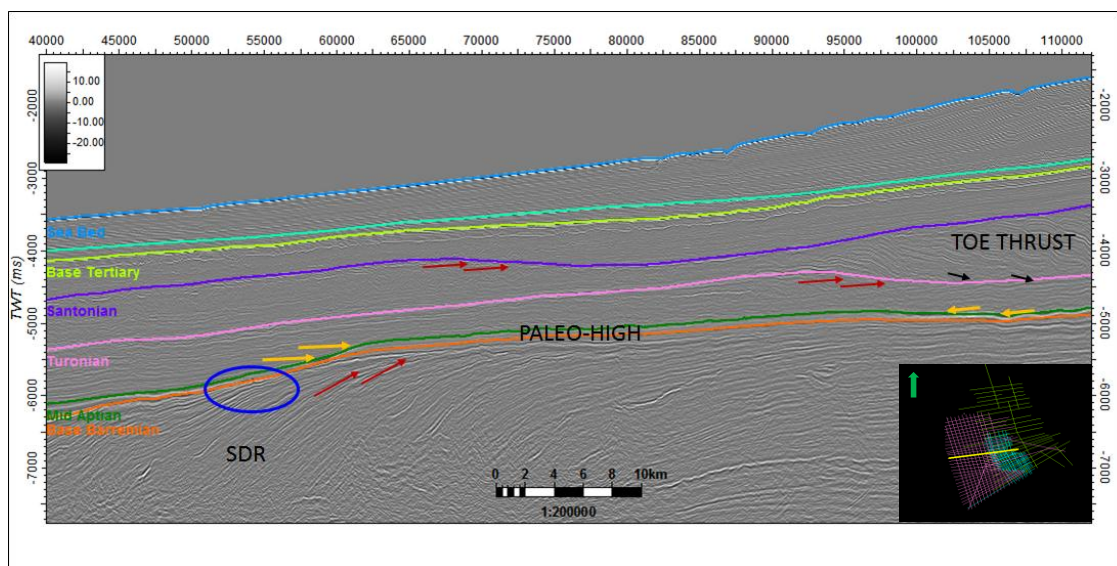


Figure 25: W-E seismic line showing onlapping of the Early-drift strata on the Mid Aptian unconformity. SDR reflectors are toplapping towards a major unconformity just below the Base Barremian Shale unconformity. The pinch out of the Syn-rift is indicated in a blue circle just below the Base Barremian shale in the western half of the seismic line.

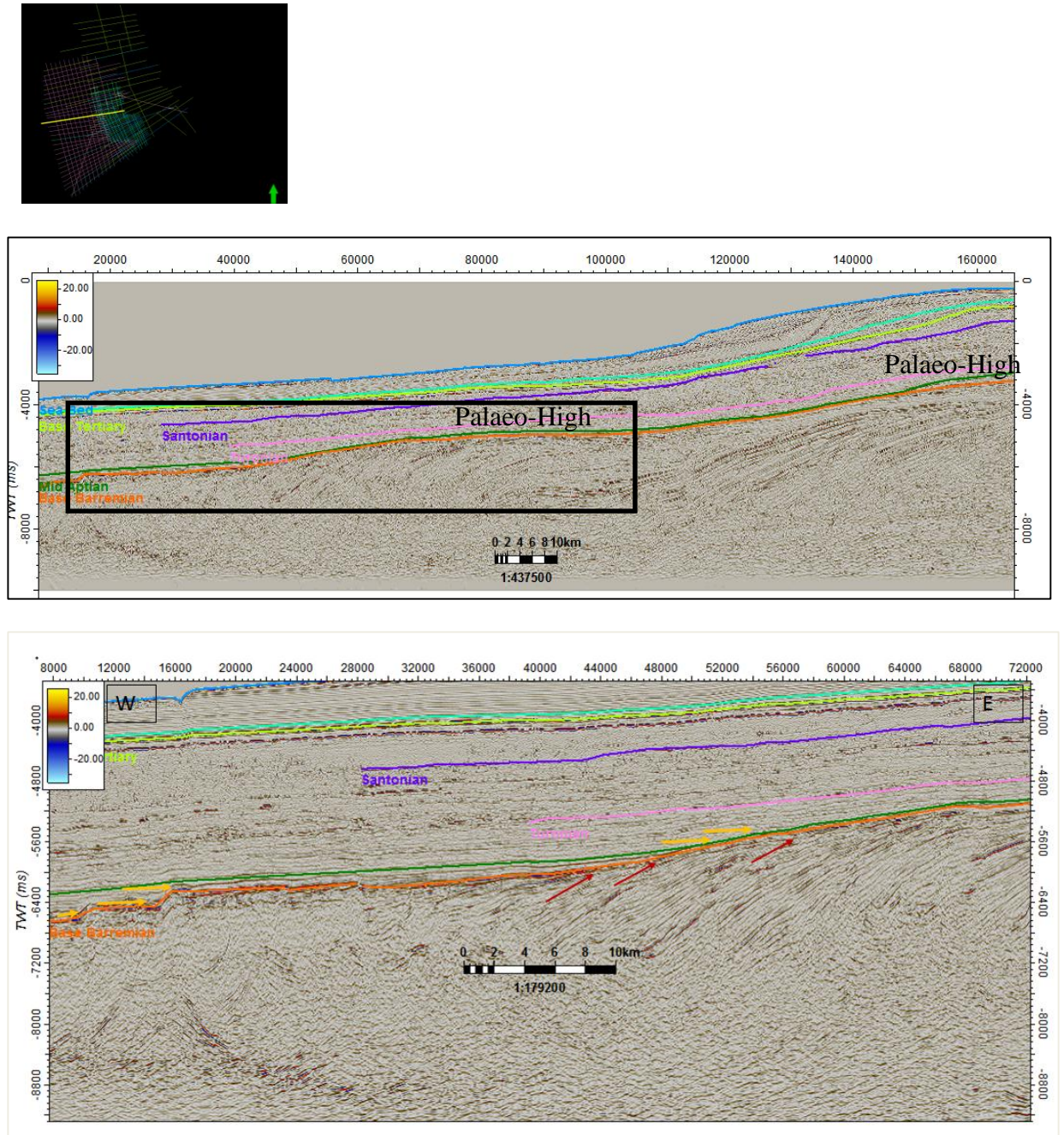


Figure 26: W-E seismic line displaying onlapping of young strata and toplapping of old strata on Base Barremian unconformity in deep waters of approximately 3000m.

#### 4.1.3.4 Late Drift

##### i. Structural History Review

This sequence comprises of Turonian to recent units and it forms volumetrically the main part of the basin fill. The Base Tertiary Unconformity divides the Late Drift sequence into lower (Turonian-Campanian/Maastrichtian) and upper (Tertiary) sections. The thin late drift sediments are separated from the region of rapid sediment thickening by a distinct hinge -line (Bray et al, 1998; Figure 20). A Basin margin uplift that occurred during Late drift resulted in rapid sedimentation, collapse of a Cretaceous delta and mass transportation of sediments downslope, with a detachment above the base Turonian unconformity. It is envisaged that associated listric faults, roll overs and toe thrusts may act as structural traps for hydrocarbons generated by the Turonian source rock.

##### ii. Depositional Review

The rock unit in the Cretaceous consists of continental siliciclastics sediments in the east to deep marine sediments in the west (Muntingh & Brown., 1993). In Kudu wells the Albian-Turonian interval consists of massive dark grey to black shales suggesting a deep marine deposition environment with restricted circulation. Rapid sediment loading and slope instability in the Late Cretaceous resulted in deformation of the palaeo-shelf edges and palaeo-slopes sediments.

### iii. Interpretation (own observations)

The interval above the Turonian contains extensive normal faults around the shelf zone which terminates just below the mid-Tertiary unconformity. The Turonian unconformity forms a detachment surface where toe thrusts downlap and older strata beneath the Turonian gently toplap characterizing an erosive surface. The succeeding Santonian unconformity can be interpreted as an erosional surface as it truncates the underlying toe thrust section removing the upper part of the rotated fault blocks (Figure 27). A volcanic submarine mountain was identified in the southern part of the Orange basin protruding above sea bed (Figure 28). Series of channels are displayed in the Late Tertiary sequence mostly in the southern part of the study area.

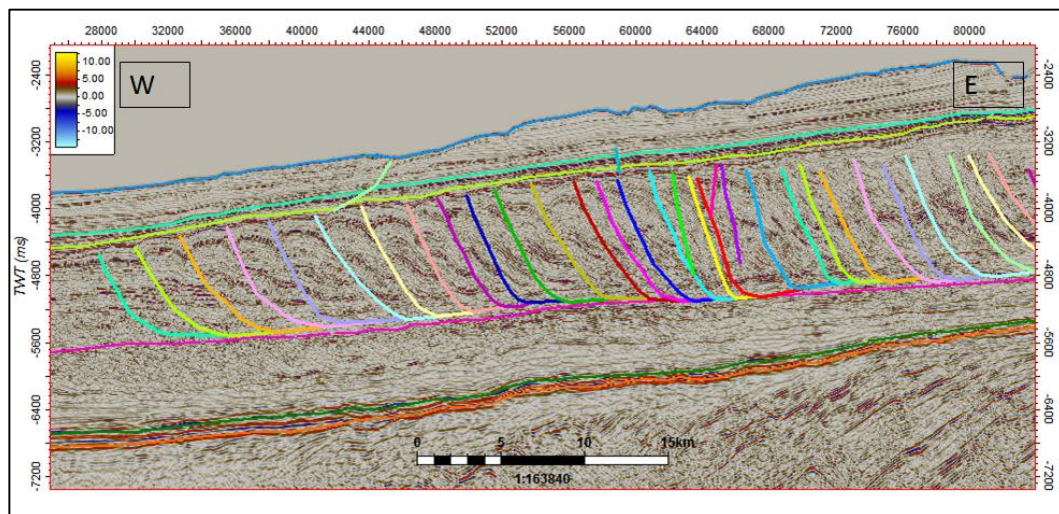


Figure 27: W-E seismic line displaying extensional faults terminating just below Santonian unconformity (bright green line) which are down-lapping into the Turonian unconformity (purple line). Toe thrusts are numerous in the Late Cretaceous unit.

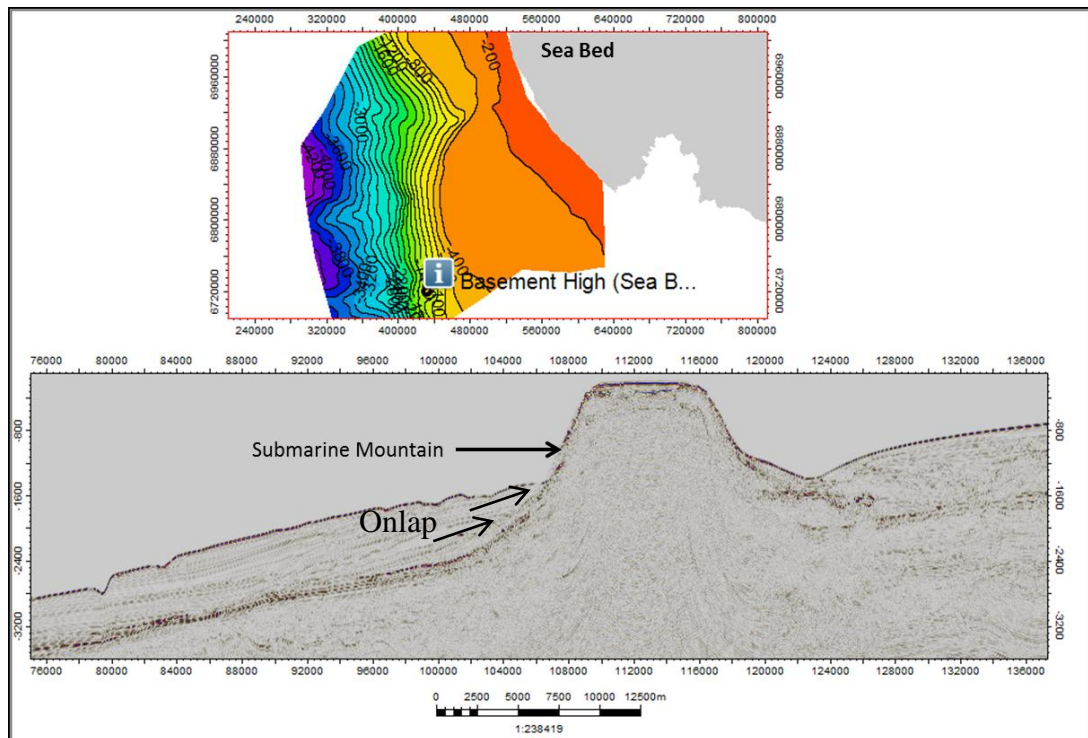


Figure 28: A) Map showing the location of the submarine mountain in the southern part of the Orange Basin. B) W-E seismic line showing a single conspicuous flat-topped submarine mountain protruding above the sea bottom.

#### iv. Seismic Facies (own observations)

Apart from the toe thrusts proximal to the basin margin, the Cenomanian-Turonian interval is characterized by parallel continuous seismic reflection with no internal reflection termination observed in sea-wards direction.

The Santonian to Base Tertiary interval displays a series of progradational wedges with steeply dipping clinoforms. These clinoforms are toplapping towards the Base Tertiary unconformity at the basin slope. Furthermore, these prograding clinoforms tend to downlap on a sequence boundary that has been recognized just above the

Santonian unconformity. The seawards seismic facies displays continuous seismic reflections with no internal termination patterns observed (Figure 29). The seismic facies within the prograding wedge displays sigmoidal reflector patterns typical for high stand system tracts when sediment supply exceeds the rate of accommodation space is created during stable or slowly rising relative sea level (Figure 30).

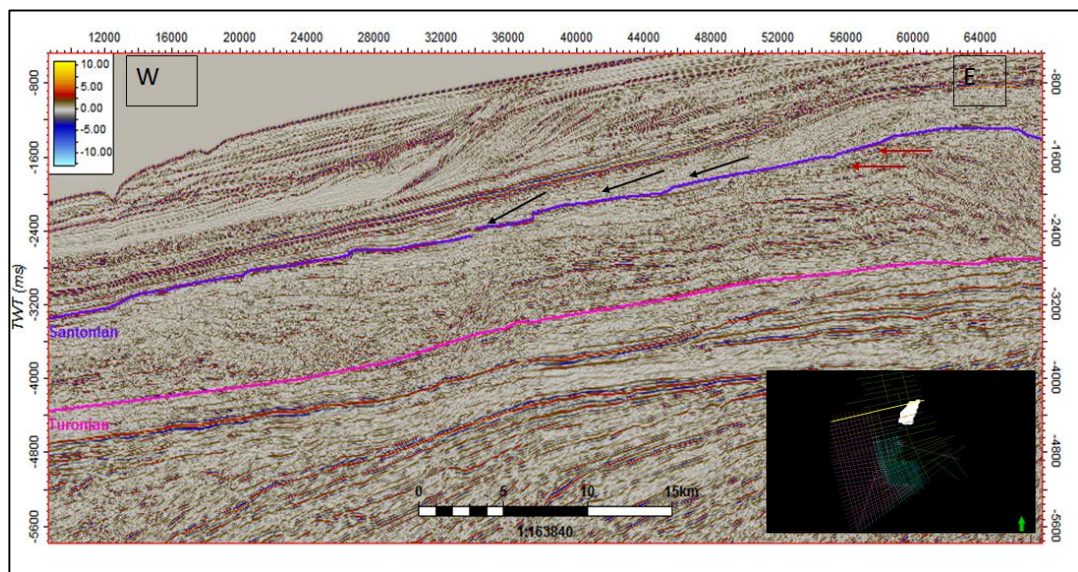


Figure 29: W-E seismic line displaying Turonian-Santonian interval. Well-noticeable toplap patterns (red arrows) occur in the eastern section, while reflection patterns become chaotic sea-wards. Downlaps on the Santonian unconformity relate to minor prograding patterns above the Turonian-Santonian interval.

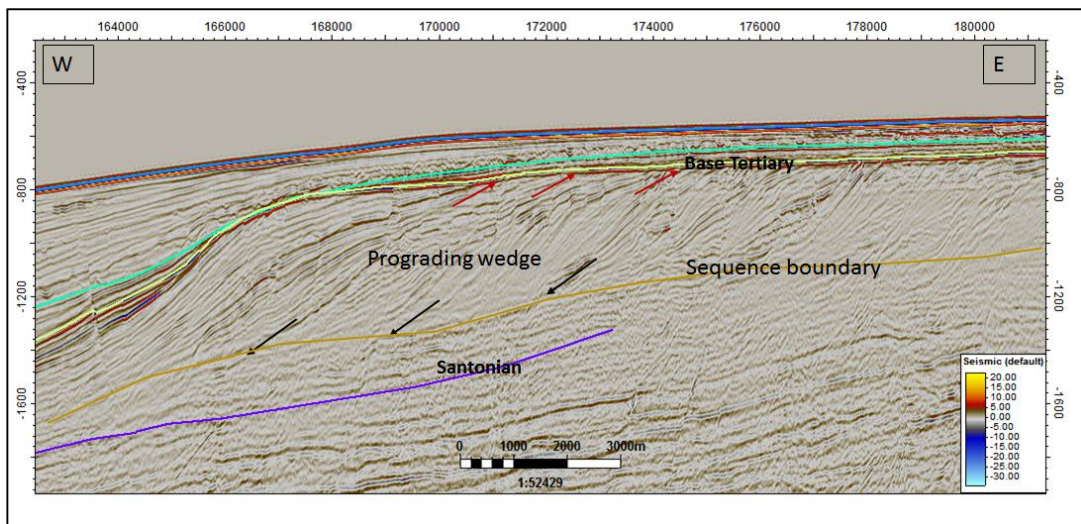
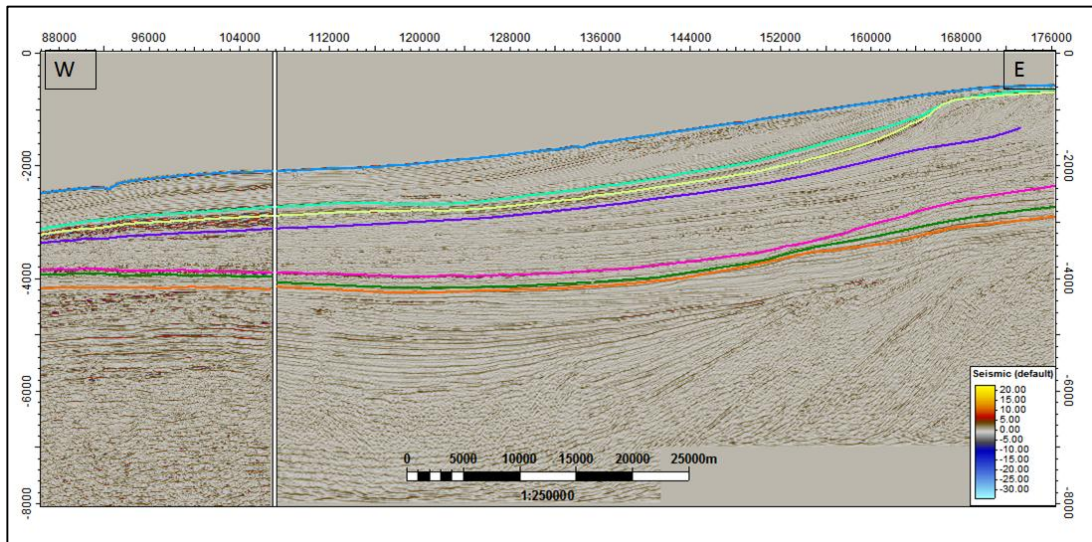
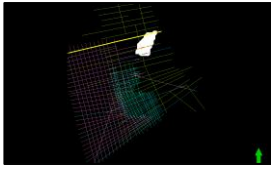


Figure 30: Prograding wedge with steeply dipping truncated strata (red arrows) by Base Tertiary at the top, and downlaps (black arrows) on a sequence boundary at the bottom just above Santonian unconformity.

The progradational parasquences along the shelf slope are sub-divided by sequence boundaries according their stratal geometries (Figure 31). A younger Lowstand progradational wedge was deposited further sea-ward (high-lighted in yellow).

The Lowstand prograding wedge is bounded by a sequence boundary at the bottom where young strata downlaps (black arrows). The top of the wedge is delineated by a transgressive surface where younger strata onlaps (yellow arrows). The transgressive surface marks the boundary between progradational Lowstand and retrogradational deposits layered down during the following transgression.

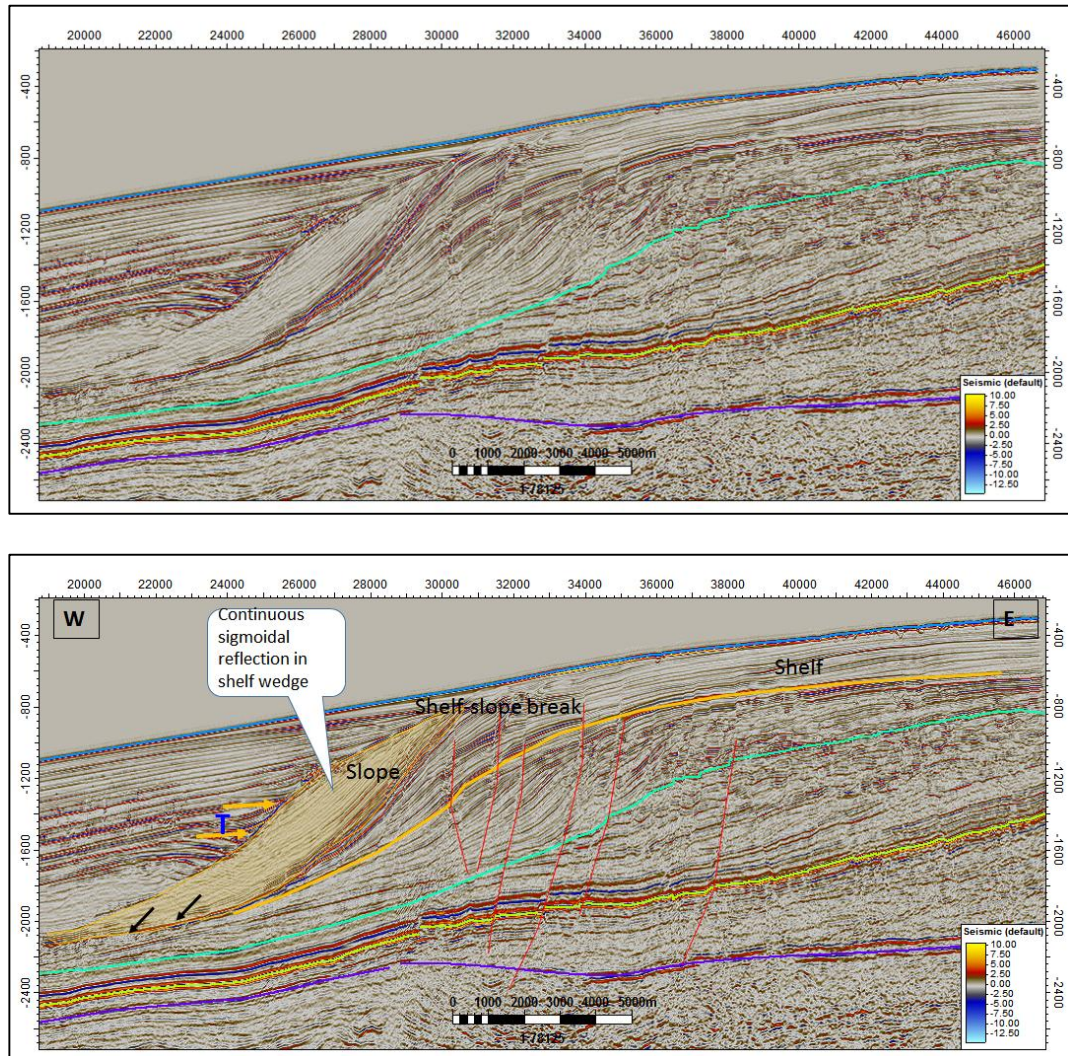


Figure 31: Lowstand prograding wedge (highlighted in yellow) in which parasequences sets are bounded by sequence boundary at the bottom and a transgressive surface. Younger strata onlap (marked with yellow arrows) the transgressive surface. Clinoforms geometries are divided by sequence boundaries picked with dark yellow lines. Transgressive deposits are indicated with the blue T.

Base Tertiary to Mid-Tertiary interval shows little or no internal reflection terminations. However, reflection terminations were observed along the Base Tertiary unconformity, where the overlying strata onlaps (yellow arrows) just before the shelf break. The onlapping strata coincide with facies deposited during sea level rise (Figure 32).

The underlying strata near the shore gently shows a gentle erosional truncation while toplaps (red arrows) develop closer to the shelf break at the Base Tertiary unconformity. The toplap geometry formed as sediment bypassed proximal to the shore line along an erosional surface and deposited further west forming a prograding wedge expressed as clinoform reflectors.

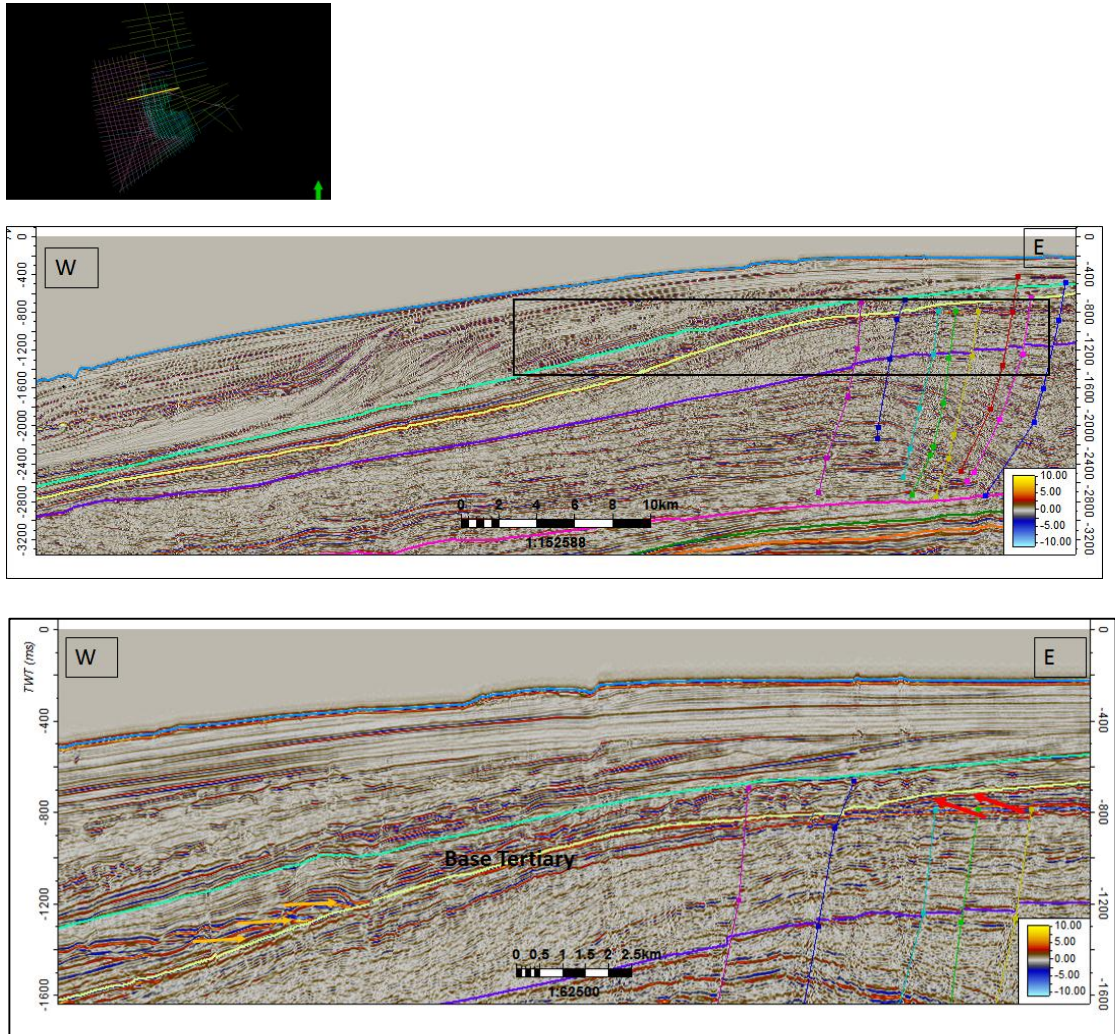


Figure 32: Base-Tertiary unconformity defined by underlying toplapping strata indicating erosional truncations (red arrows) and overlying onlapping strata (yellow arrows).

The Tertiary succession consists of progradational clinoforms building from east to west in the northern part of the study area proximal to coastline (Figure 33A). The progradational geometries of these clinoforms vary from oblique to sigmoidal towards the coastline. These clinoforms downlap on a horizontal reflector which defines a maximum flooding surfaces that coincides with the Mid-Tertiary unconformity. The latter truncates the underlying strata locally giving evidence of a minor forced regression.

Instantaneous Phase was used as seismic attribute to substantiate sequence seismic reflection geometries and their corresponding sequence boundaries (Figure 33B) by enhancing seismic events. This type of seismic attribute is commonly used to increase the continuity of weak events and enhance the reflectivity of dipping seismic features. It removes amplitude information from seismic which improves the visibility of seismic reflectors (Barnes, 2007).

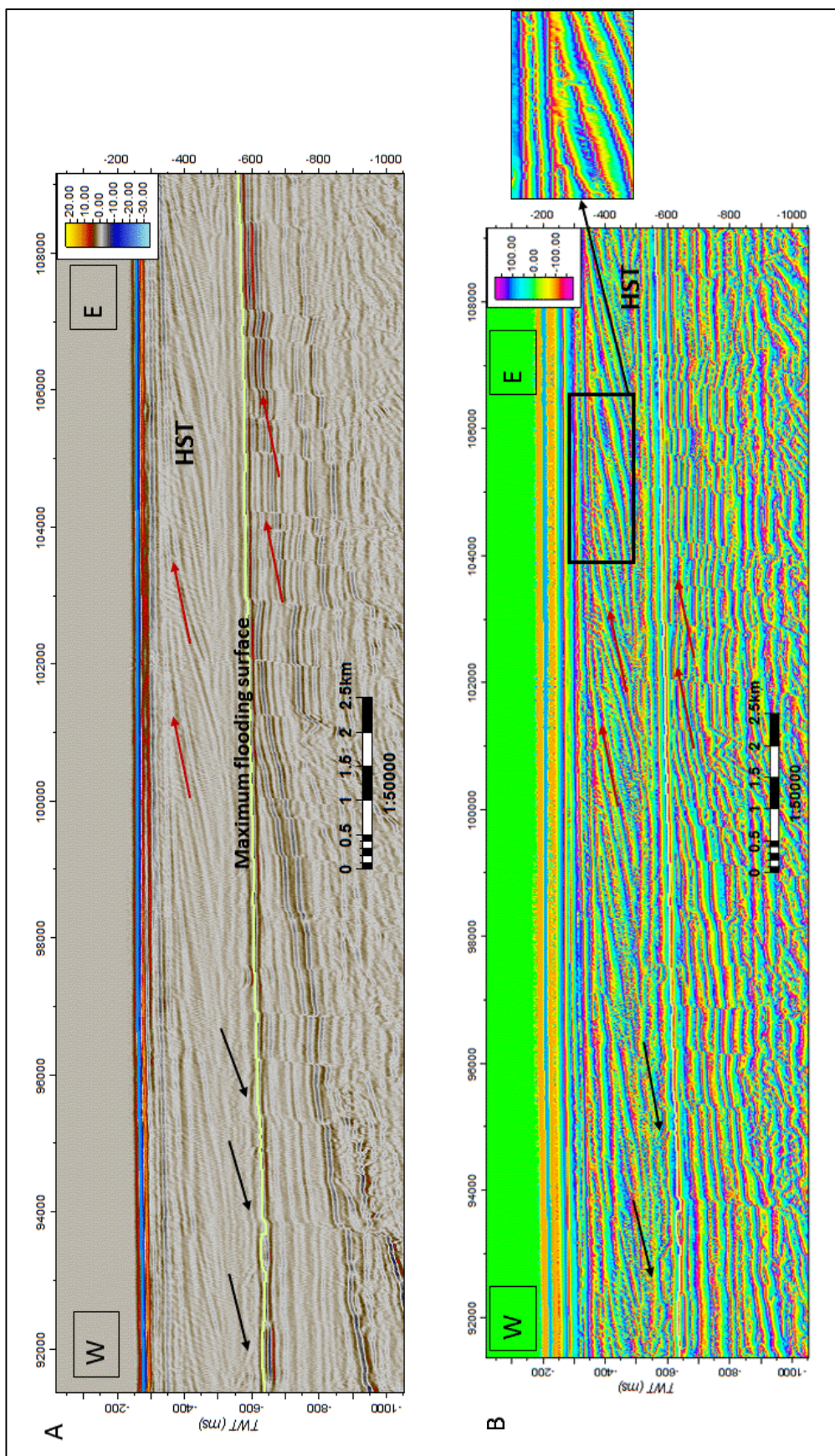


Figure 33: A. progradational sigmoidal clinoforms observed in Tertiary sequence which are downlapping (black arrows) on a maximum flooding surface and truncated (upper red arrows) by the overlying mid-tertiary unconformity. Note that the Mid-Tertiary sequence boundary is marked with a light green horizontal line. The lower red arrows show underlying strata truncated by Mid-Tertiary unconformity.

Figure 33 B. Instantaneous phase attribute applied to enhance seismic geometries and improve the continuity of weak seismic events. Note that the sigmoidal clinoforms are pronounced in this image compared to image A. The zoomed in seismic image displays distinct truncation pattern.

## 4.2. Summary

The well correlation analysis displays a clear distinction between rates of sedimentation deposited near shore and in deep water deposits. A shallow water well (2815/15-1) shows a thick sediment succession during the Aptian to Turonian compared to deep water wells (Kudu wells). The opposite was observed in the Turonian to Base Tertiary interval where Kudu wells display thick sediment deposits as, for example, seen in well 2815/15-1.

The well correlation for the Kudu main reservoir confirmed the geometry of the Kudu main reservoir as an interlayering of sandstones and volcanic rock.

The deepest section intersected by Orange Basin wells is located at a depth just below 4500 m where the Barremian Kudu reservoir was encountered. Therefore, the lithology for deeper sections such as the Pre-rift can only be deduced from onshore analogues. In addition, the seismic reflection patterns of the Pre-rift could not be determined due to poor seismic resolution at that depth. The chaotic seismic reflection in both, the Pre-rift and western part of the Syn-rift represents rock bodies with no well-ordered bedding.

Even though, seismic reflection in the Syn-rift is almost chaotic, the section proximal to shore displays clear basinwards progradational seismic patterns. These patterns have been interpreted as continental deposits (Petroleum Agency SA, 2007). The seaward dipping reflectors (SDRs) to the west, which top lap at the Base Barremian Shale unconformity, are construed as sub-aerial flood basalts. SDRs in South Atlantic

developed during the early crustal stretching phase which was dominated by oblique movements and shearing. The width of the SDRs in the Orange Basin decreases towards the north (Koopman et al. 2013). These basalts were rapidly discharged on attenuated continental crust just before onset of drifting. The Syn-rift constitutes of graben structures which formed during the rifting event which led to ultimately to the separation of Africa from South America with the opening of the South Atlantic. The half graben structures contain fluvial to lacustrine deposits interbedded with volcanics.

The Early drift represents a transition from continental to marine environments, until fully marine conditions were established. This was proven by most Kudu wells which revealed that the lower part of the Barremian consists of aeolian sandstones interbedded with basaltic lavas. These continental deposits are clearly capped by marine shales. The toplap geometry against the Base Barremian shale indicates limited accommodation space for the deposition of the underlying continental deposits during that time. The geometry of the underlying strata support this conclusion, as it pinches out in the landward direction, while the Base Barremian unconformity dips sea-ward. The pinch-out below the Base Barremian shale unconformity provides a possible stratigraphic trap for hydrocarbons.

Further west, down the continental slope in ultra-deep waters, onlap patterns refer to a marine transgression over the Base Barremian Shale unconformity. A transgressive system tract is recognized.

The Mid-Aptian unconformity displays deep water land-ward onlaps of overlying strata. This situation mirrors a continuation of relative sea level rise causing a

landwards retrogradational sediment fill. Correspondingly, successively finer grained sediments have been deposited including the Kudu source rocks encountered in the Kudu wells. The bulk of the Early drift sequence describes a sedimentary wedge with significant variations in thickness. A broad palaeo high just above the Mid-Aptian unconformity in the southern part of the study area was observed on seismic profile. The palaeo high might have formed due to relative sea level rise during a transgressive cycle coupled with gradual flooding of the shelf resulting in formation of carbonate build-ups. Alternatively, it could have formed during relatively sea level fall exposing the shelf coupled with the sea ward shift of a dune complex during Lowstand (Bagguley, 1996). Palaeo highs are considered as possible reservoirs for hydrocarbons.

The sequence between Mid-Aptian and Turonian comprises prograding strata without internal termination patterns. Toplap geometries occur land-wards onto the Turonian unconformity followed by down-lapping of overlying strata. The toplapping of the underlying strata signifies limited deposition below the Turonian unconformity corresponding to sea level standstill and no increase in vertical accommodation space.

The down-lapping overlying strata derives from deposition of mudstone units.

During Mid-Aptian to Turonian sequence sediments were deposited near shore, this is attested by thick sediment section at this interval in 2815/15-1 located close to the coastline compared to that of Kudu well positioned in mid-waters.

The Turonian-Cenomanian interval displays gravity driven thrust faults to the East but further sea-ward parallel prograding strata with little internal termination. The Cenomanian unconformity truncates the underlying strata which coincide with characteristics of an erosional surface.

The Santonian to Base Tertiary unconformity consist of series of progradational Highstand wedges near shore and parallel strata dipping sea-ward. This results in deposition of fine grained sediments, possible source rock for hydrocarbons. The wedges are supposed to be separated by Transgressive System Tracts but they are not visible on current seismic profiles.

The Base Tertiary to Sea bed sequence display series of Highstand and Lowstand sediment wedges which reflects cycles of relative sea level fall and rise during this period. Fine grained sediments are deposited during Hightstand, while coarse grained sediments are deposited during Lowstand. The fine and coarse sediments are possible source and reservoir units, respectively. The Base Tertiary truncates the underlying strata indicating the occurrence of erosional processes during this period. The overlying strata onlaps the Base Tertiary corresponding to drowning of the topography at that time. The upper part of this sequence displays series of channels which indicates the subaerial exposure and erosion of marine sediments and subsequent channel deposition.

The upper part of the Tertiary sequence displays prograding clinoforms which change from sigmoidal near shore to oblique sea ward. The angle of clinoforms on seismic profiles does not reflect the original deposition geometries which might have been rather caused by compaction of sediments. Upon deposition sands have a lower porosity compared with mud and thus muds compact to greater degrees on burial than sands. Therefore, clinoforms may develop as a result of differential compaction from sandstone units laterally grading into shales.

MEGASEQUENCES	G-C 0.00 gAPI 200.00	SSTVD 1:19860	SEQUENCES BOUNDARIES	SYSTEM TRACTS	REFLECTION PATTERNS	DEPOSITIONAL PATTERNS	REMARKS
Late Drift		-5.5 800 1500 1800 2000 2500 3000 3800 4200 4800 (HEFLB)	Mid- Tertiary	HST, LST, TST	Erosional Truncation below (Toplap), onlap and Concordance, and downlap above	Progradational, and Retrogradational	sequence boundaries and internal seismic reflection patterns can be easily identified in this interval.
			Base Tertiary	HST, LST	Erosional Truncation below (Toplap), onlap and Concordance, downlap above	Progradational and Retrogradational	Highly faulted proximal to coast line and not easy to identify internal seismic reflection patterns
			Santonian	HST	Erosional Truncation below (Toplap) and downlap above	Aggradational and Progradational	Prograding clinoforms can be easily indentified in the northern part of the area close to shore. The southern part consists of toe thrust structures which diminishes Northward where it becomes chaotic.
Early Drift		-5.5 800 1500 1800 2000 2500 3000 3800 4200 4800 (HEFLB)	Turonian	HST	Erosional Truncation below (Toplap) and downlap above.	Aggradational and Progradational and Retrogradational	mild chaotic internal seismic reflections
			Mid Aptian	LST, HST	Erosional Truncation below (Toplap), onlap and Concordance, onlap above	Progradational, and Retrogradational	Continuous prograding internal seismic reflections
Syn-Rift		-5.5 800 1500 1800 2000 2500 3000 3800 4200 4800 (HEFLB)	Base Barremmian Shale	LST	Erosional Truncation below (Toplap) and onlap above	Aggradational, Retrogradational and Progradational	Diminishing seismic imaging, but internal seismic patterns can still be identified.
			Syn-Rift	N/A	Onlaps and chaotic sea-ward	Progradation proximal to coast line and chaotic sea-ward	Prograding internal seismic reflection near shore, chaotic sea-ward
Pre-Rift		-5.5 800 1500 1800 2000 2500 3000 3800 4200 4800 (HEFLB)	Pre-Rift	N/A	Chaotic	Chaotic	Chaotic, no internal reflection patterns observed.

Table 4: Generalised Stratigraphy of the Orange Basin offshore Namibia.

## 4.3 STRUCTURAL MAPPING

### 4.3.1 Base Barremian

The Base Barremian unconformity is characterized by a high amplitude reflection which was picked throughout the study area except in the areas near shore. The unit between the Base Barremian Shale and Mid-Aptian unconformity tends to be thicker around the shelf break and gradually dipping basin-ward where it also thins down dip (Figure 34). This section consists of faults extending from the Syn-rift (previous section). Minor closures were observed on time maps, while the depth map revealed several structural closures at this stratigraphic level (Figure 35 A & B).

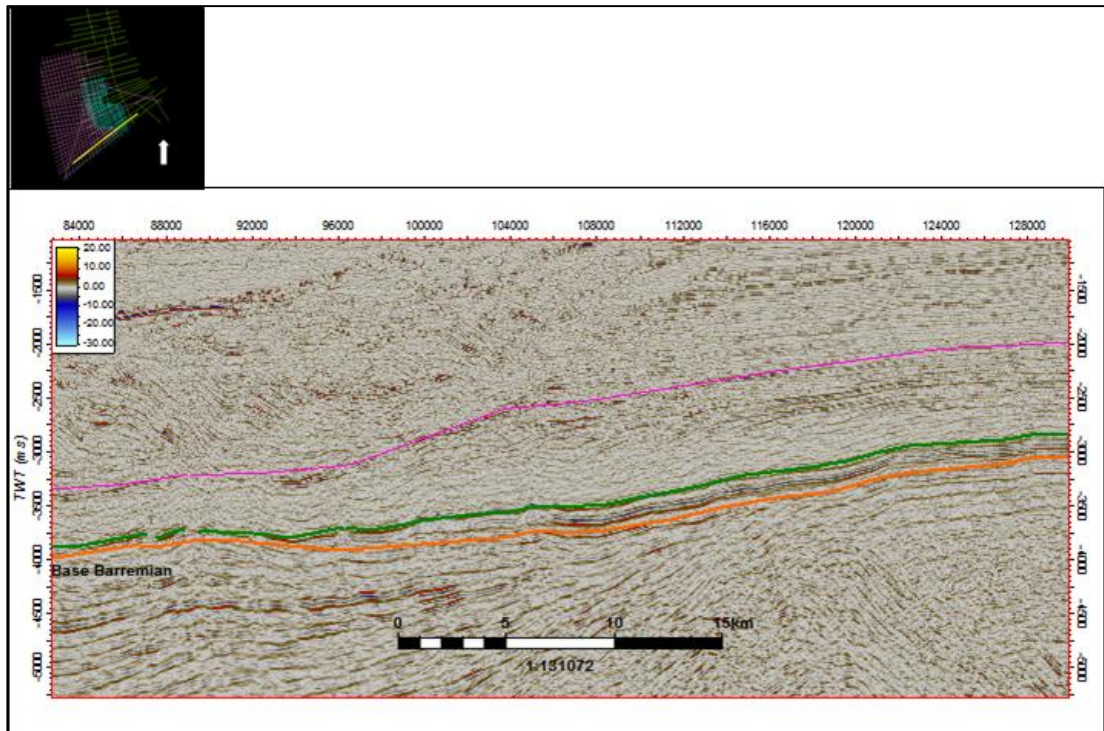


Figure 34: W-E seismic line displaying the interval between the Base Barremian Shale (Orange line) and the mid-Aptian unconformity (green line) thinning down dip.

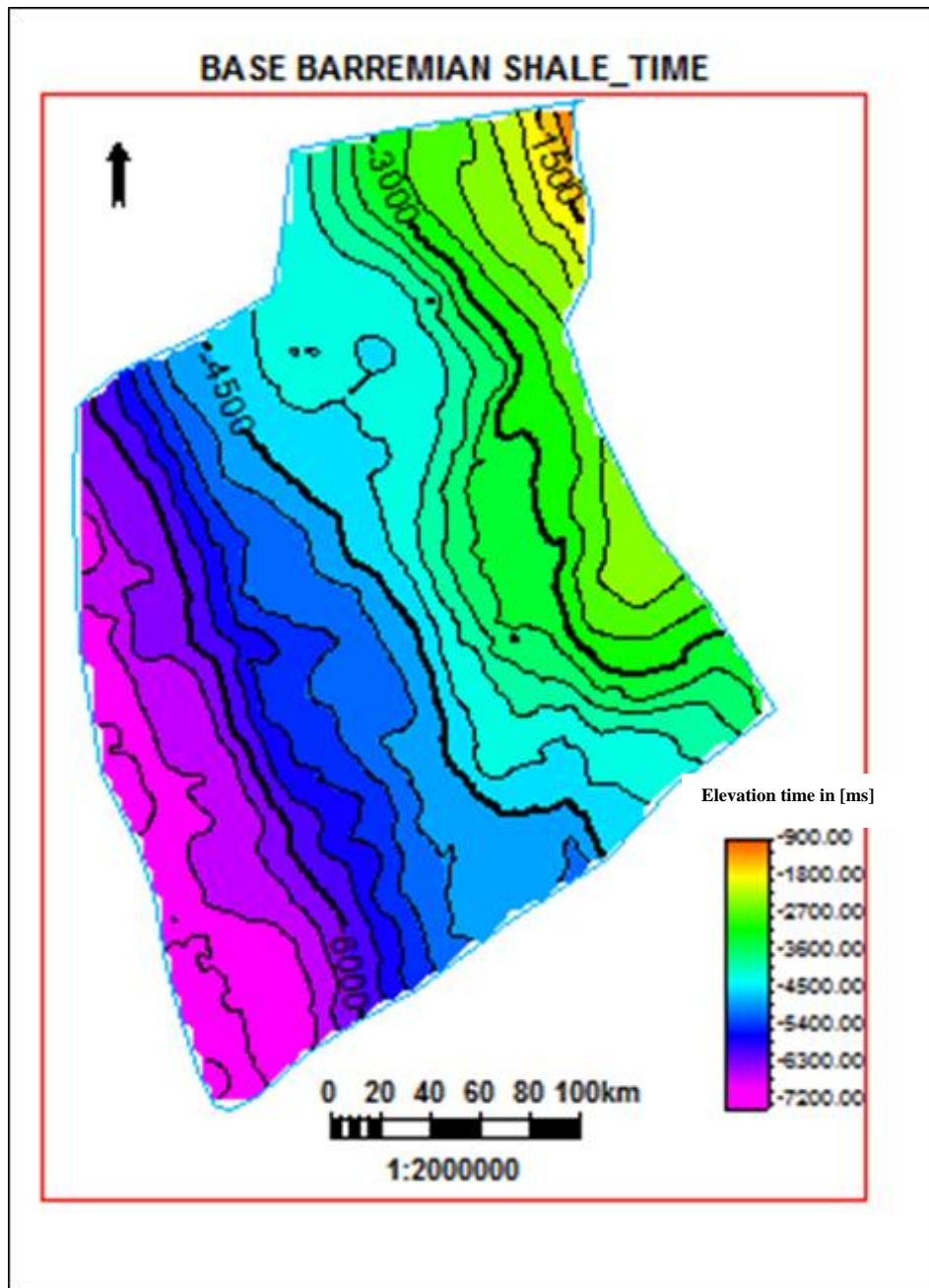


Figure 35A: Structural map of Base Barremian in time with minor closures identified in the northern part of the map.

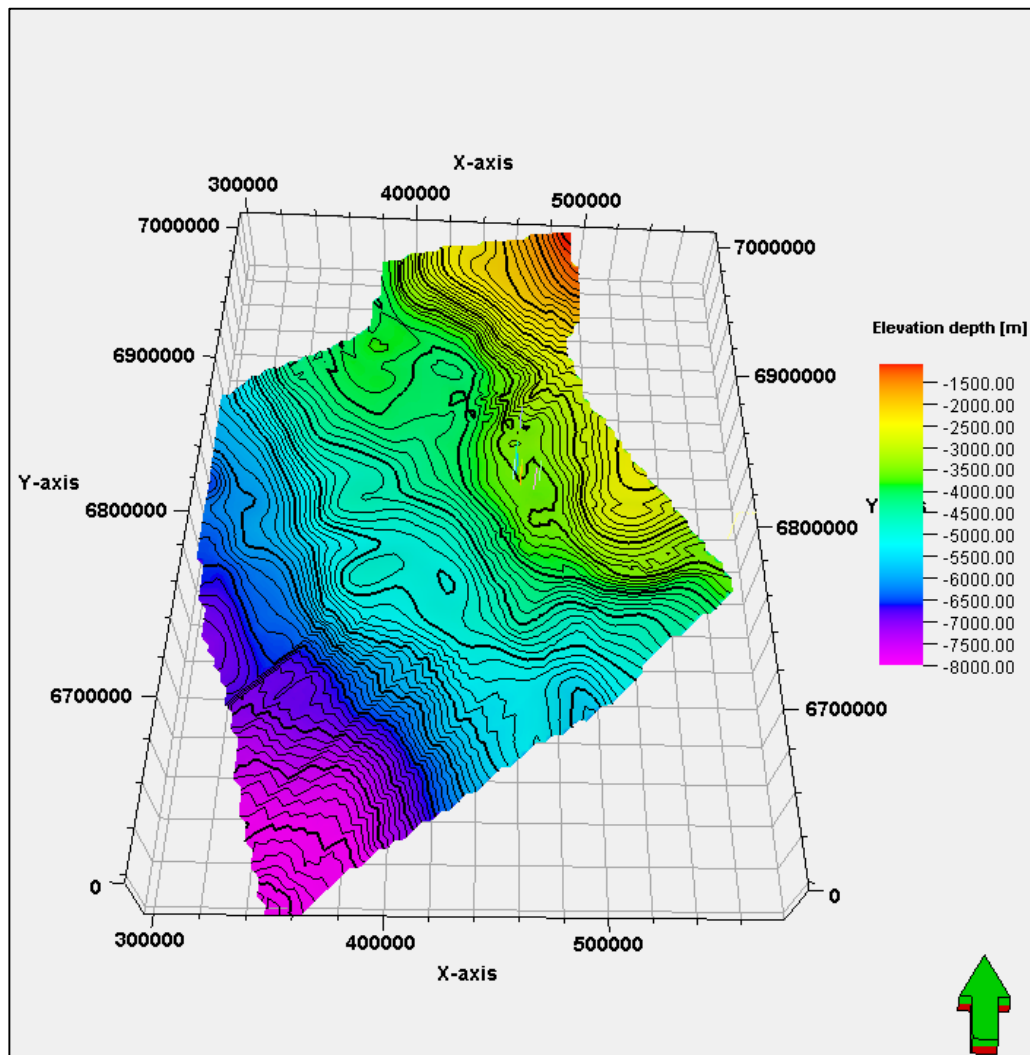


Figure 35 B: Structural depth map of Base Barremian displaying several major structural closures located in the middle of the Basin.

### 4.3.2 Mid-Aptian

The mid-Aptian unconformity has a high reflection which was easily mapped over the entire study area except for the extreme east where it onlaps the break-up unconformity. Some volcanic features protruding and rising above the mid-Aptian are clearly visible on seismic profiles (Figure 36 & 37). Some of the volcanic features do not penetrate through the Mid-Aptian unconformity; rather terminate at the unconformity resulting in dome structure. Those are mapped as a volcanic high (Figure 37). No major closures were observed on the time map (Figure 38A). The depth map revealed several major structural closures in the middle of the basin which are possible hydrocarbon traps (Figure 38 B).

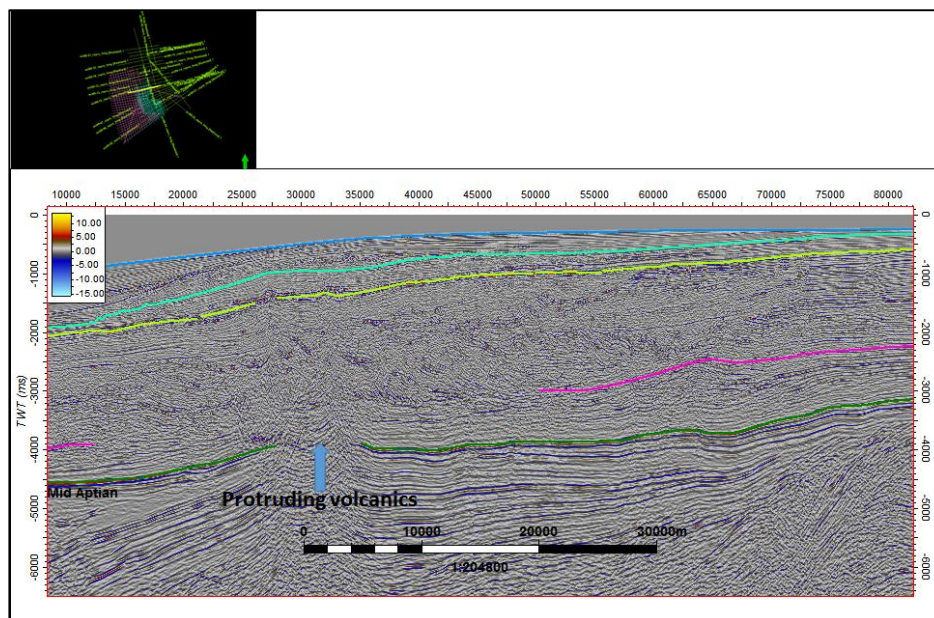


Figure 36: W-E seismic line showing a volcanic feature protruding through the Early Cretaceous and cutting through the mid-Aptian as well as the Santonian unconformity. The result is a dome like shape of the overlying Base Tertiary unconformity.

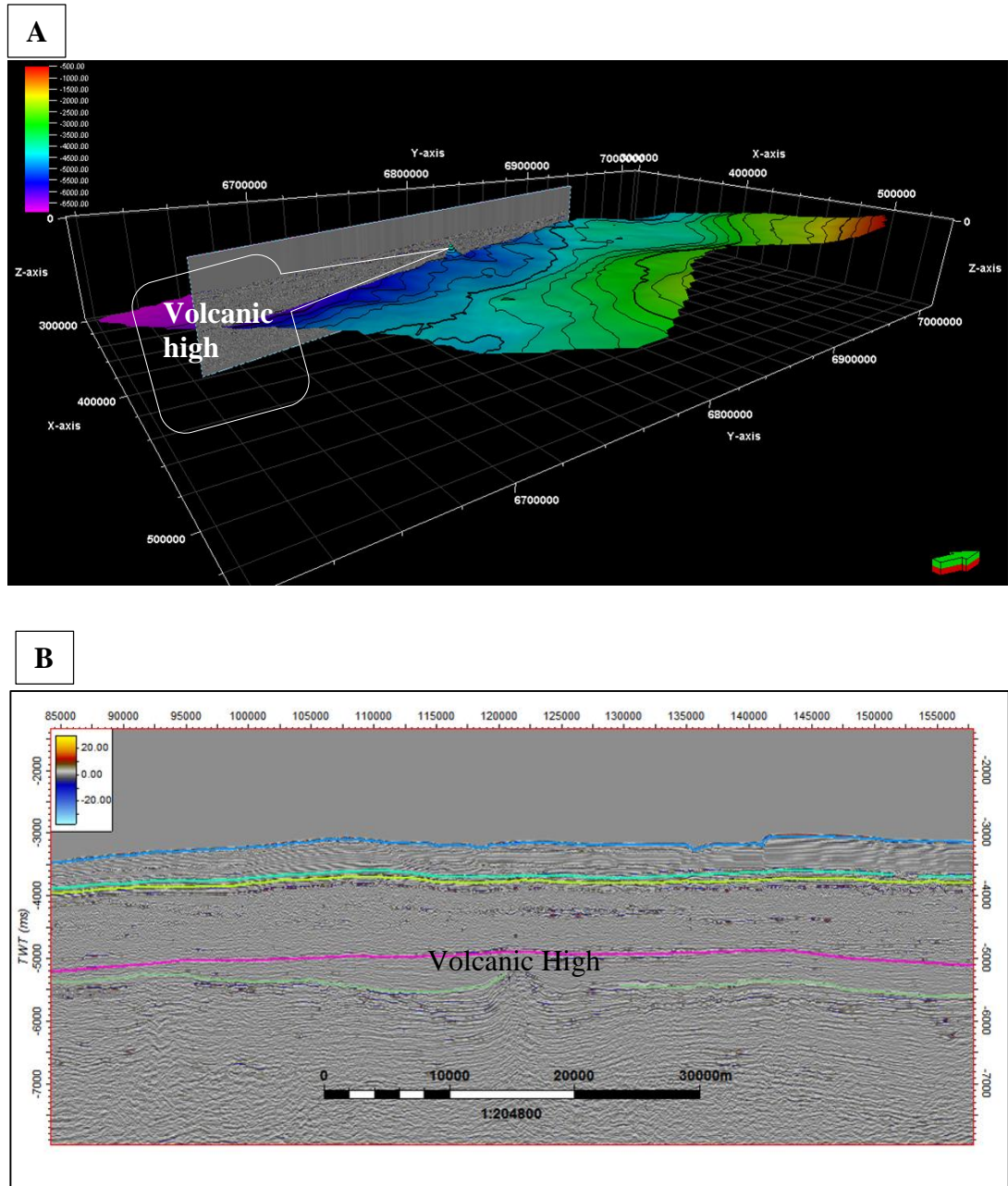


Figure 37: A) 3D view of Mid Aptian map in time showing the location of the volcanic high. B) Volcanic high on 2D seismic line, note that it does not penetrate through the mid-Aptian unconformity but pushes against this horizon forming a dome with approximately 4 km width.

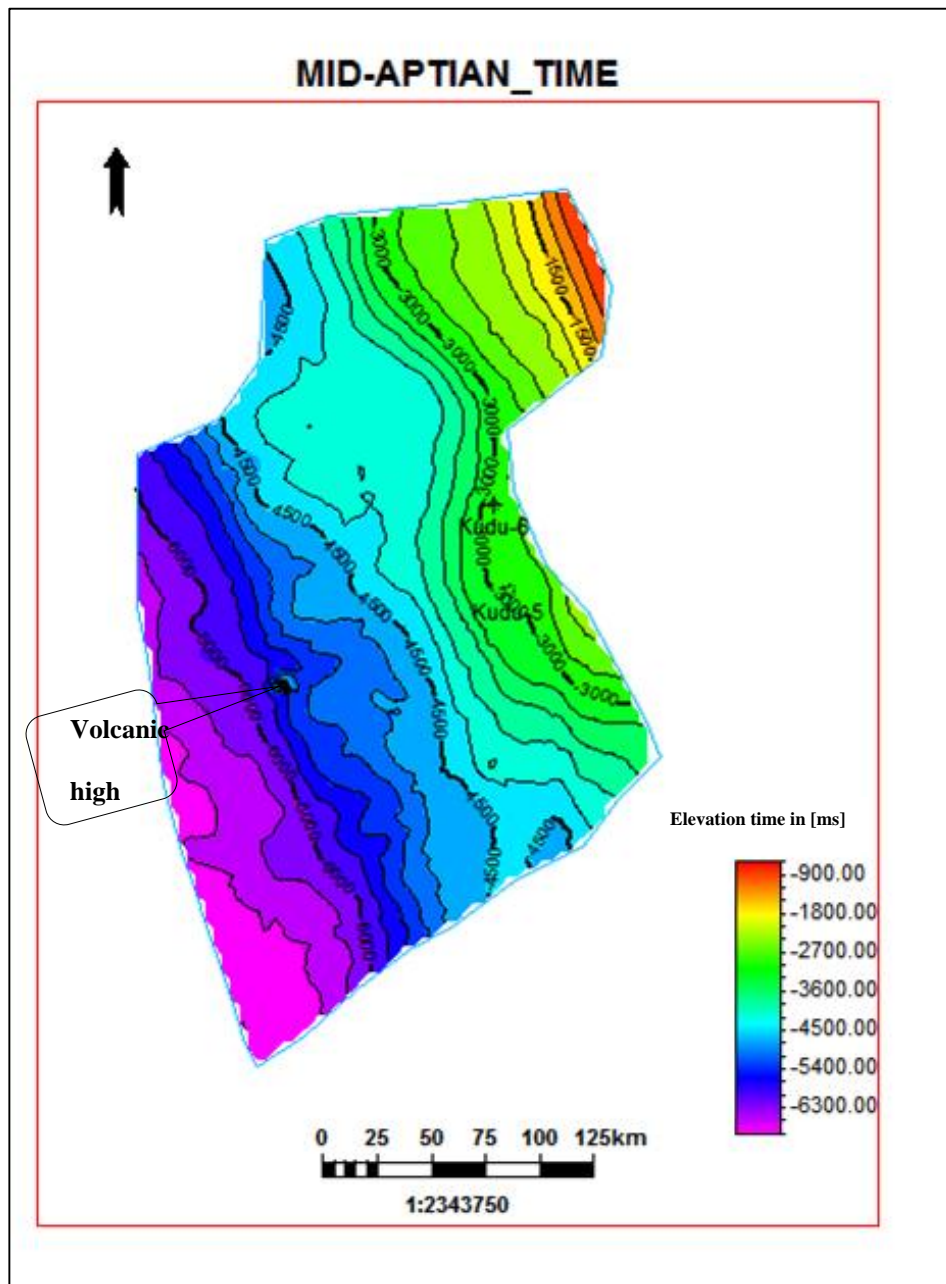


Figure 38 A: Mid-Aptian map in time, a volcanic high was observed at this stratigraphic level to the west of the Basin.

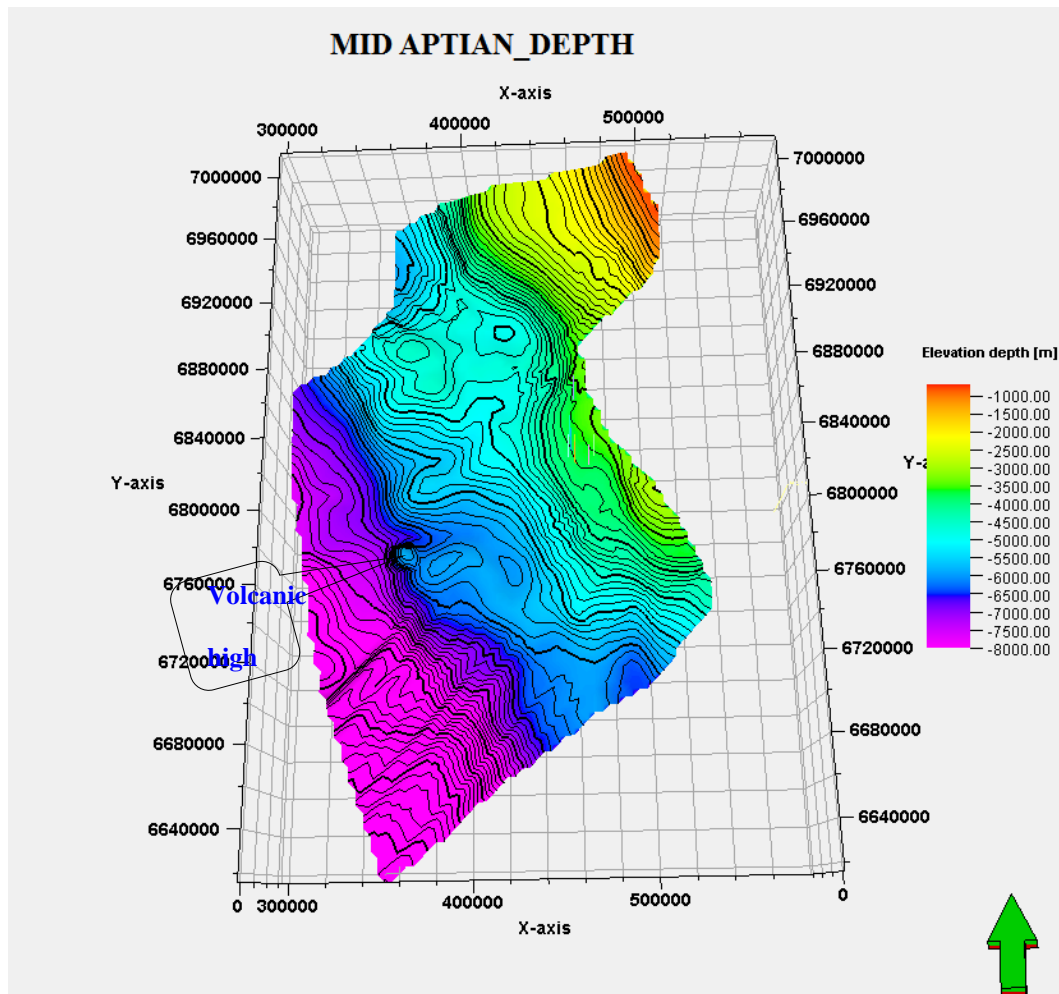


Figure 38 B) Structural depth map of Mid Aptian Shale unconformity displaying several major structural features including a volcanic high and closed contours in the middle of the Basin.

### **4.3.3 Turonian Unconformity**

The Turonian unconformity is very difficult to interpret as the reflectance of this horizon diminishes basin-ward. It has a stronger reflection over the shelf in the northern part of the Basin which becomes less visible at the shelf break and sea-ward. In the southern part of the Basin the Turonian unconformity has been eroded at the shelf (Figure 39). The sediment section between the Santonian and Turonian unconformity attains a maximum thickness of approximately 3000 meters. This sediment section consists of sediment slumps which appear to have been moved along the Turonian unconformity. The slumping becomes more distinct down-dip where toe thrust becomes more developed and major faults are clearly visible (Figure 40). Toe thrusts are clearly defined in the southern part of the study area, but the seismic reflections in this unit becomes chaotic moving north-ward. The Turonian maps in time shows minor closures, while the depth map displays several more distinct structural closures. However, Kudu wells revealed that this interval is mainly composed of shale and lacks good reservoir properties.

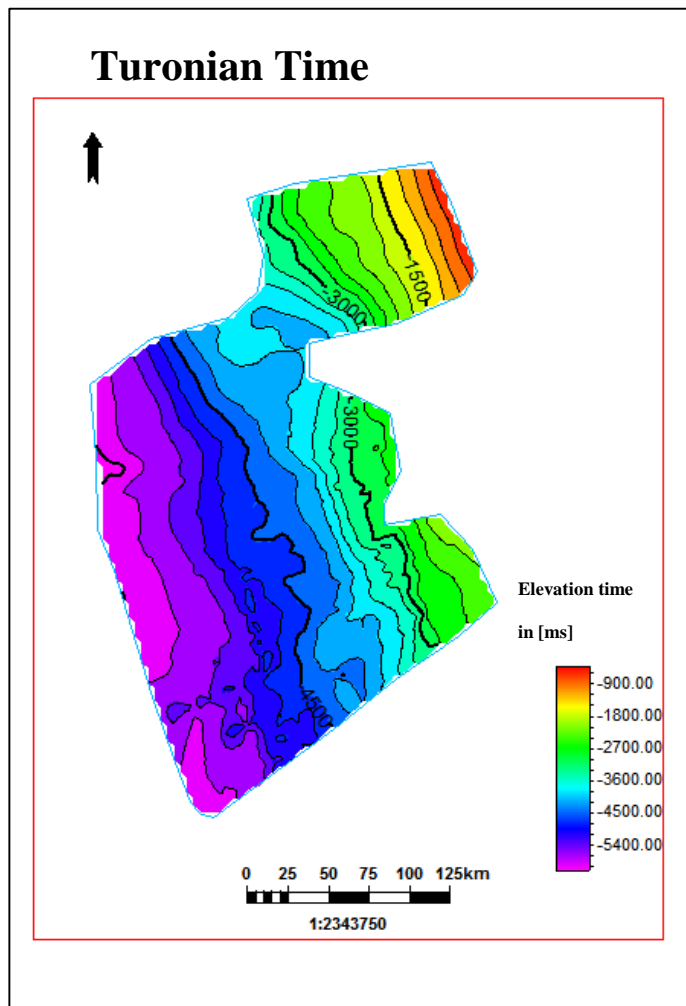


Figure 39A: Turonian map in time displaying small structural closures to the southern part of the Basin. Note that the Turonian unconformity has been eroded to the eastern and also to the north-western part of the Basin.

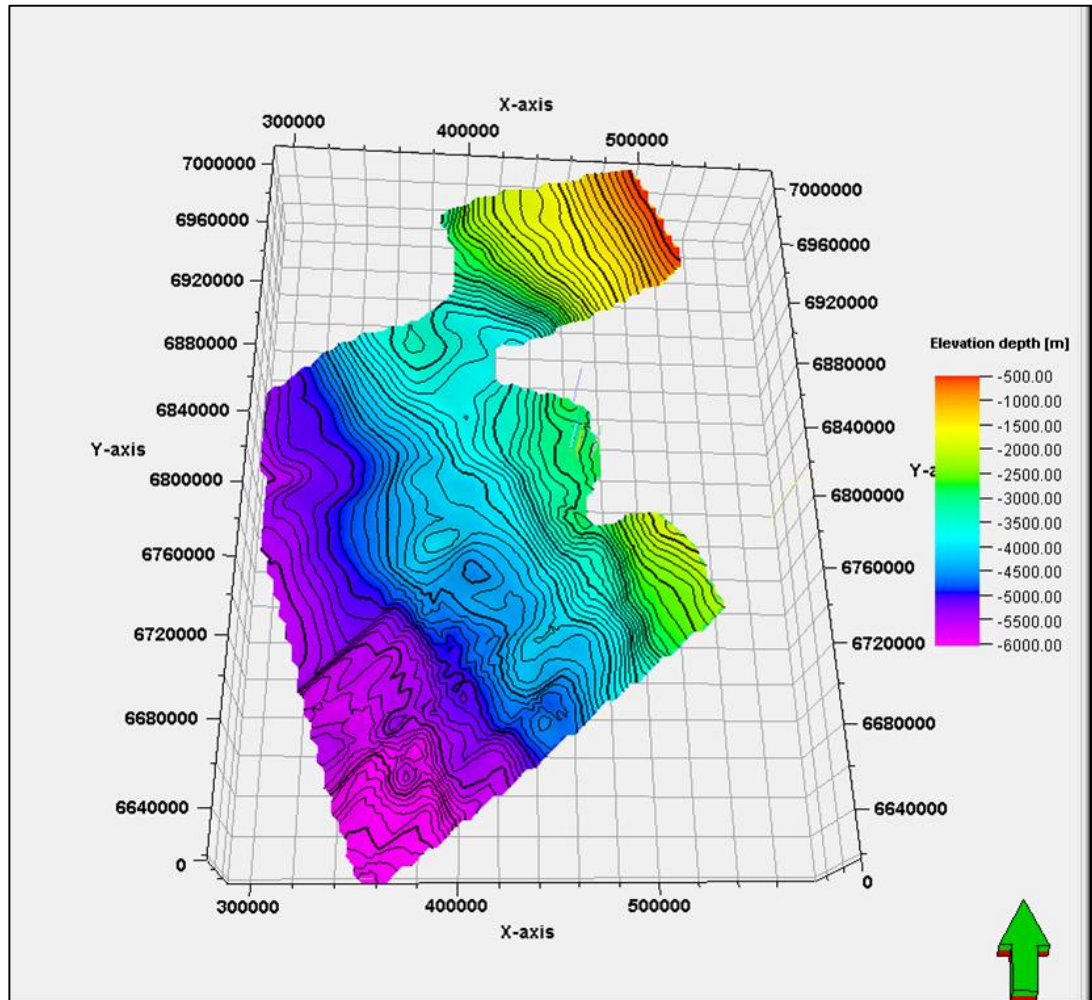


Figure 39B: Turonian map in depth displaying several structural closures in the middle of the Basin and to the southern part of the Basin.

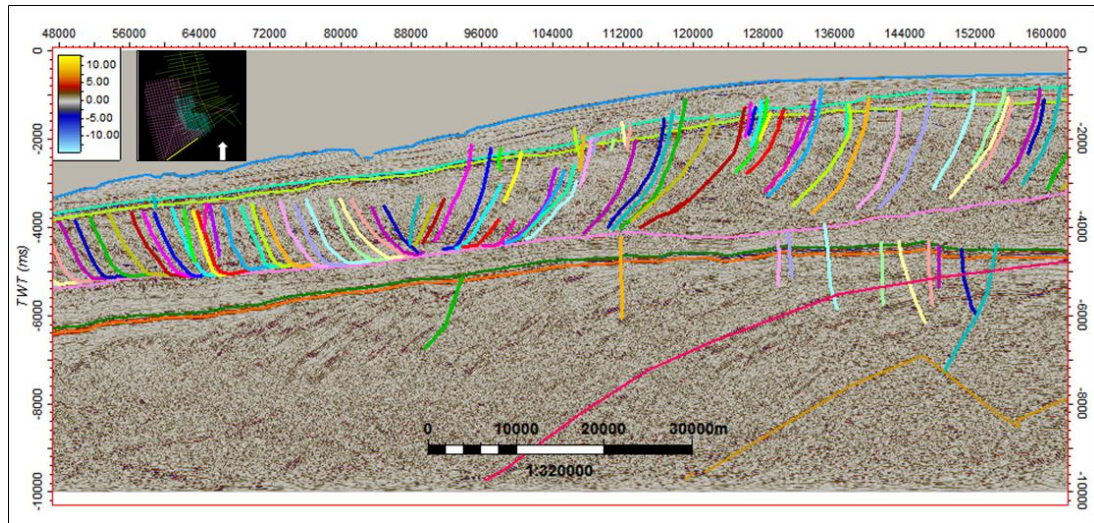


Figure 40: W-E seismic line showing toe thrusts terminating onto the Turonian unconformity. Toe thrusts become more prominent and better defined sea-ward. The Turonian unconformity is marked with a light purple line.

#### 4.3.4 Top Santonian Unconformity

A high amplitude marker delineates this horizon on seismic. It diminishes down dip. The Base Tertiary-Top Santonian interval is dissected by normal faults on the shelf which are prominent in the central area of the Basin (Figure 41 A & B). It becomes more prominent in central area with extensive slumping of the Late Cretaceous sediments, but problematic to interpret in zones within the propagating shelf edge. As a result, the Top Santonian unconformity could not be identified through-out the study area (Figure 42). The structural map shows that the Top Santonian thins towards the southern part of the study area where extensive slumping was observed.

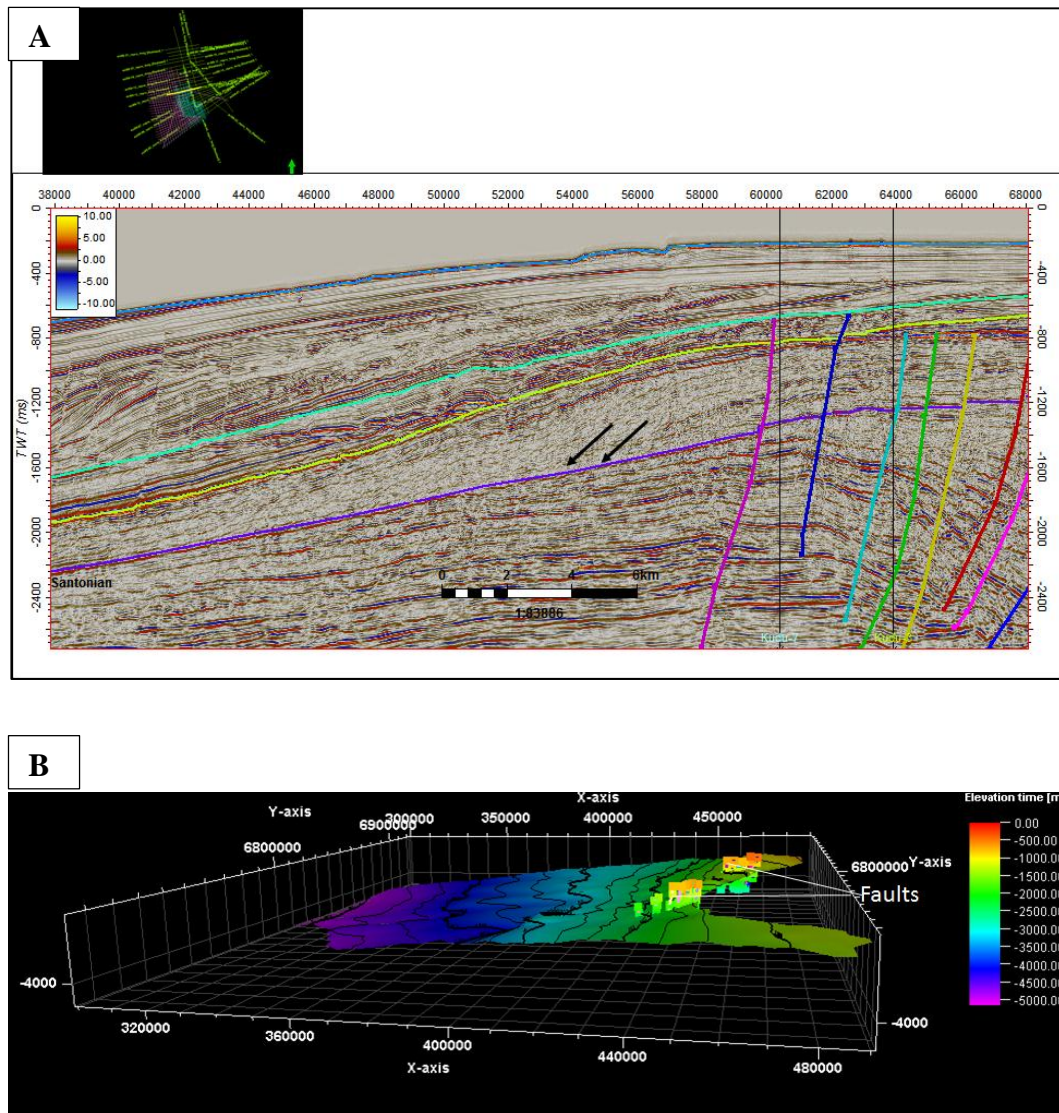


Figure 41: A) W-E seismic line showing Top Santonian unconformity (dark purple) located almost at the centre of study area. This section is heavily faulted to the east.

Figure 41 B) 3D view of the Top Santonian unconformity. Note that major faults were picked on the shelf close to shore which extends from the Turonian sequence through the Santonian and terminates just below Mid-Tertiary unconformity.

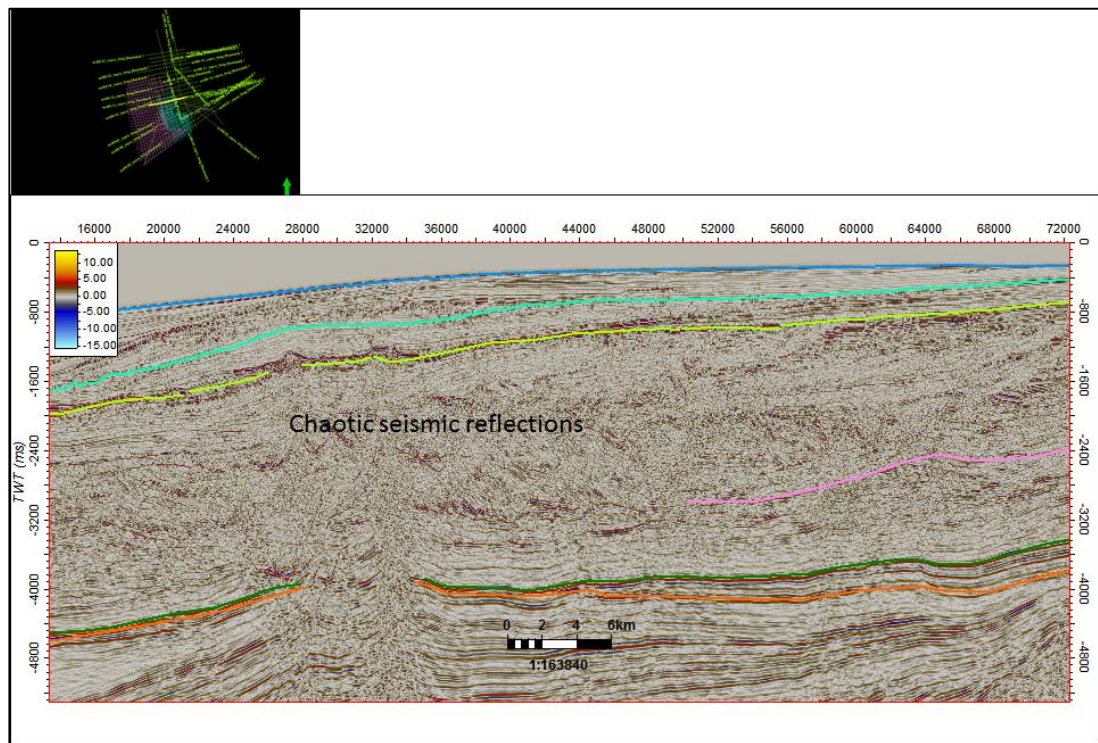


Figure 42: W-E seismic line displaying chaotic seismic reflection patterns which makes it difficult to pick the Top Santonian unconformity.

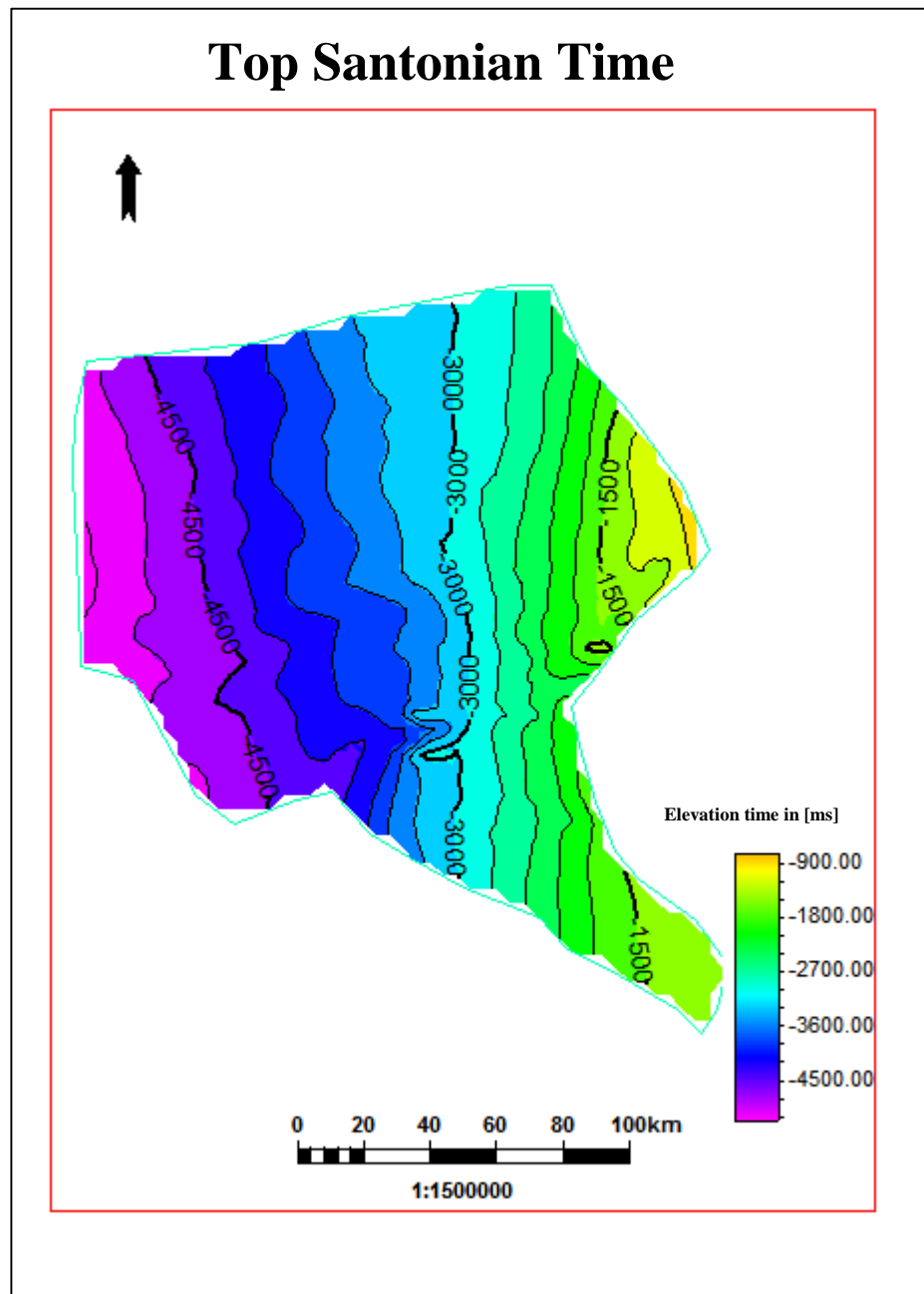


Figure 43A: Top Santonian map in time, note that this horizon was eroded to the southern part of the study area.

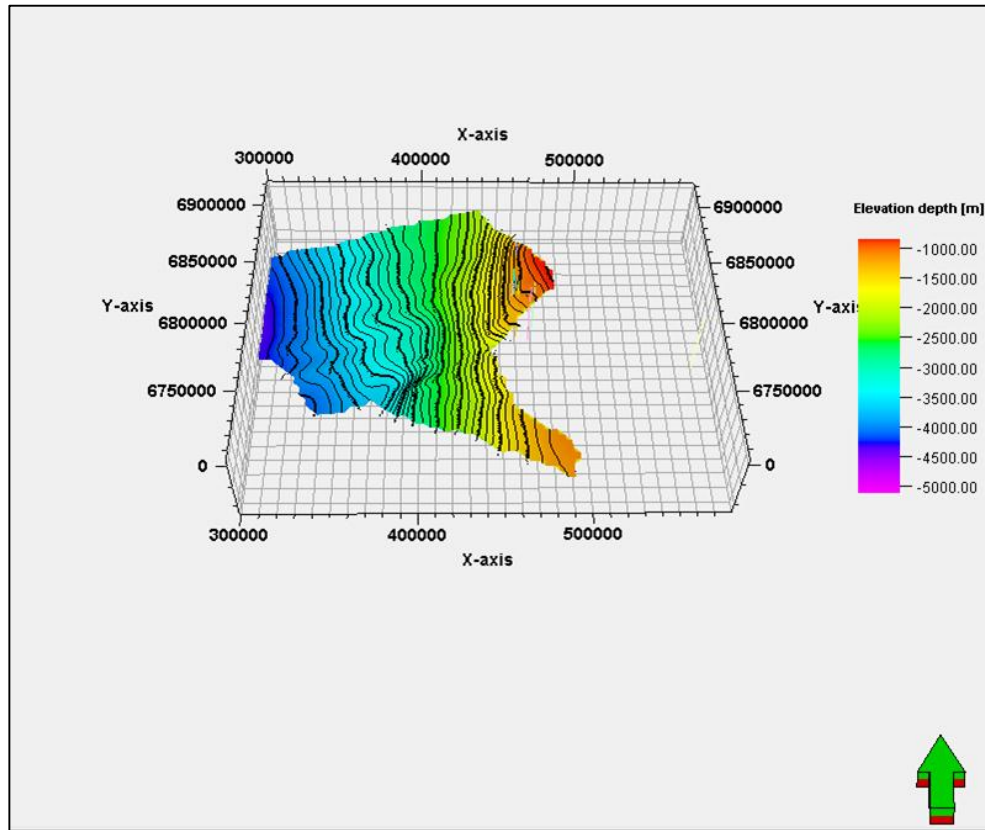


Figure 43B: Top Santonian depth map showing no structural closures.

#### 4.3.5 Base Tertiary Unconformity

This is a prominent unconformity which separates the Tertiary from the Cretaceous sequence. It was easily mapped almost in the entire study area apart from proximal zones to shore where it sub-crops beach sands (Figure 44). The upper section of the Tertiary sequence consists of channels which become more prominent to the west where it consists of shelves break clastics representing the most forward progression series of shelf breaks (Figure 45). Series of channels which were observed at this stratigraphic level deepen towards the southern part of the Basin (Figure 46A).

The Base Tertiary unconformity mirrors the palaeo shelf-continental slope topography; it slopes to the west becoming steeper at the shelf edge and eventually flattens down dip (Figure 47A and B). The mapping of this horizon revealed no significant closures (Figure 47B).

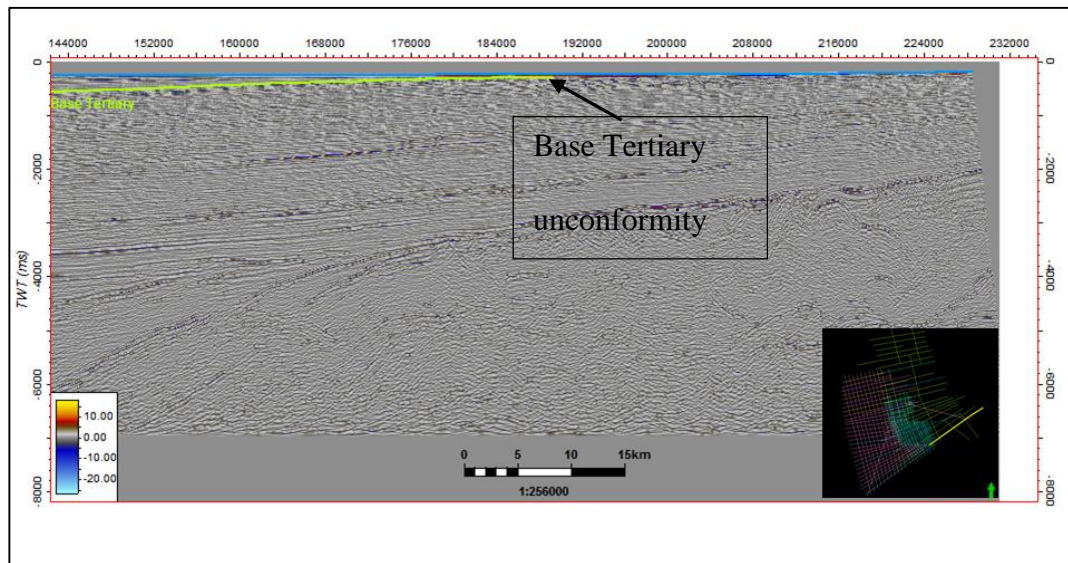


Figure 44: W-E seismic line showing the Base Tertiary unconformity (green) sub-cropping into beach sands to the east of the Orange Basin.

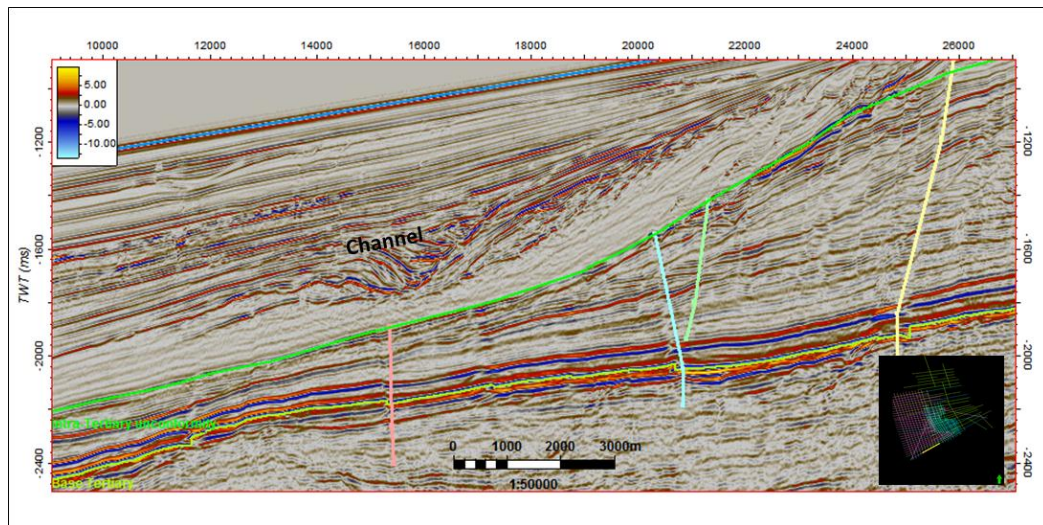


Figure 45: W-E seismic line showing channels in the Tertiary sequence. Note the mid-Tertiary unconformity (bright green) dividing the Tertiary sequence in two major units. Seismic reflection character changes significantly across the Mid-Tertiary unconformity indicating a significant change in lithofacies. The Base Tertiary is highlighted with the lime green line.

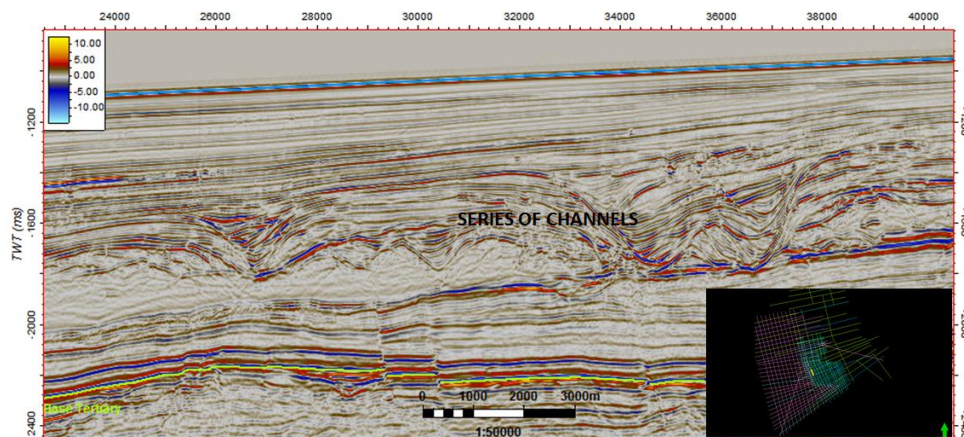


Figure 46A: N-S seismic line showing series of channel in the upper Tertiary section. Note that the channels occur at a deeper stratigraphic level towards the southern part of the Basin.

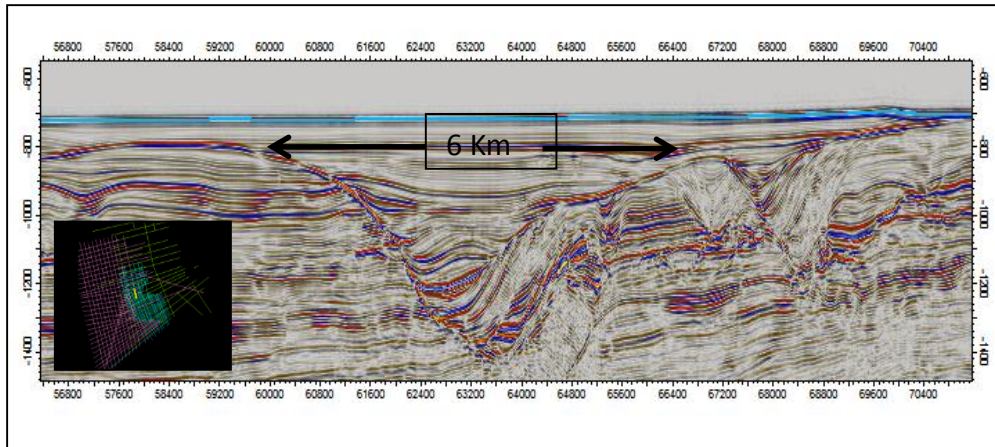


Figure 46B: N-S seismic line showing a conspicuous channel feature in the upper section of the Tertiary unit which attains a width of 6 km.

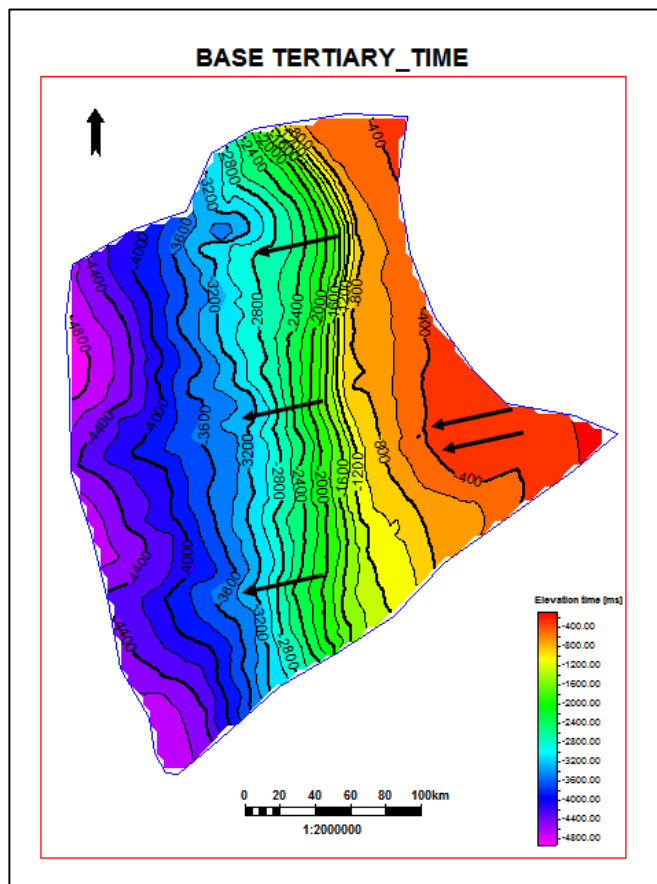


Figure 47A: Base Tertiary Map in time displaying series of channels indicated by black arrows.

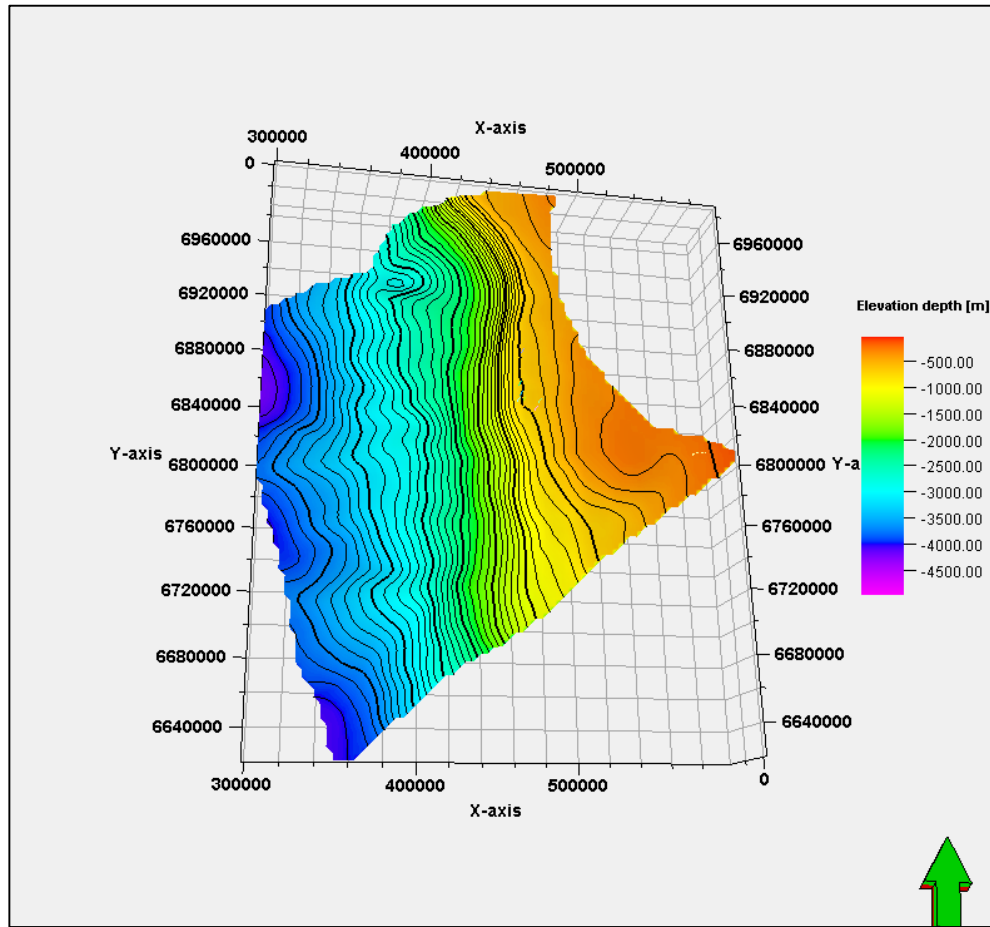


Figure 47B: Base Tertiary depth map displaying no significant closure, however a small closure was observed in the northern part of the Basin on the continental slope.

#### **4.3.6 Summary**

Structural mapping at a regional scale revealed that all sequences of the study area are dipping sea-ward and dissected by normal faults (Figure 48). The presence of major faults extending from the sequences below the Base Barremian and terminating just below the Mid Aptian unconformity indicates transitional fault zones. These faults can act as migration path for hydrocarbons generated at various stratigraphic levels.

The structural map of the Aptian shows geometries similar to that of the Base Barremian sequence in terms of structural distribution. Two broad structural highs were identified at Barremian and Aptian sequences (Figure 49). The Kudu high to the east and a deep water high which resembles the Kudu high. The Kudu high hosts gas as proven by the Kudu wells. For this reason the deep water may also represent a hydrocarbon reservoir.

The mid Cretaceous is extensive dissected by gravitational faults associated with graben structures. Those structures allow for possible traps with potential source and reservoir rock present in this interval. In fact, the structural map of the Turonian shows structural closures occurring mostly to the south-west part of the Basin. This coincides with the area of gravitational structures.

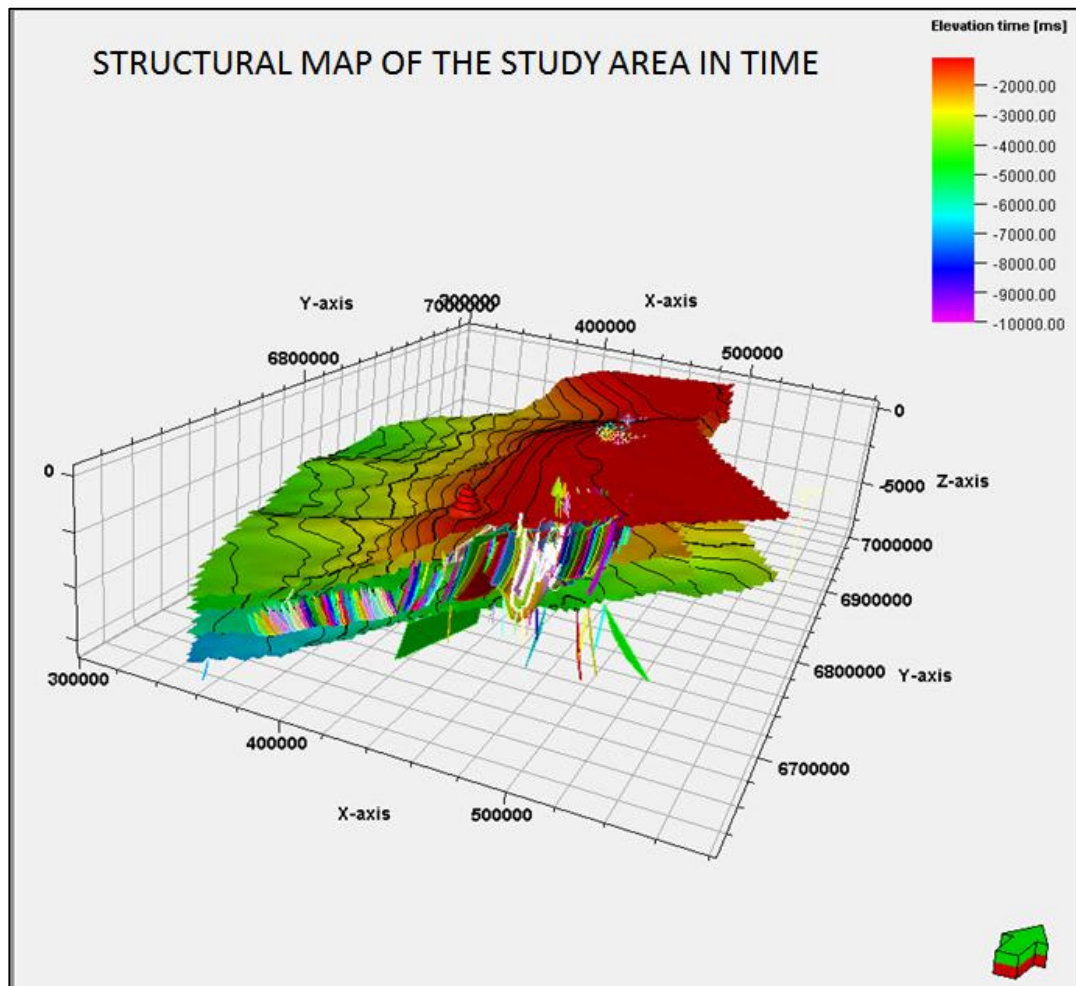


Figure 48: Structural model displaying the geometry of the Basin. Stratigraphic surfaces are dipping to the west. Major faults were mapped to the southern part of the Basin. Extensional faults within the mid Cretaceous associated with graben structures were identified on seismic.

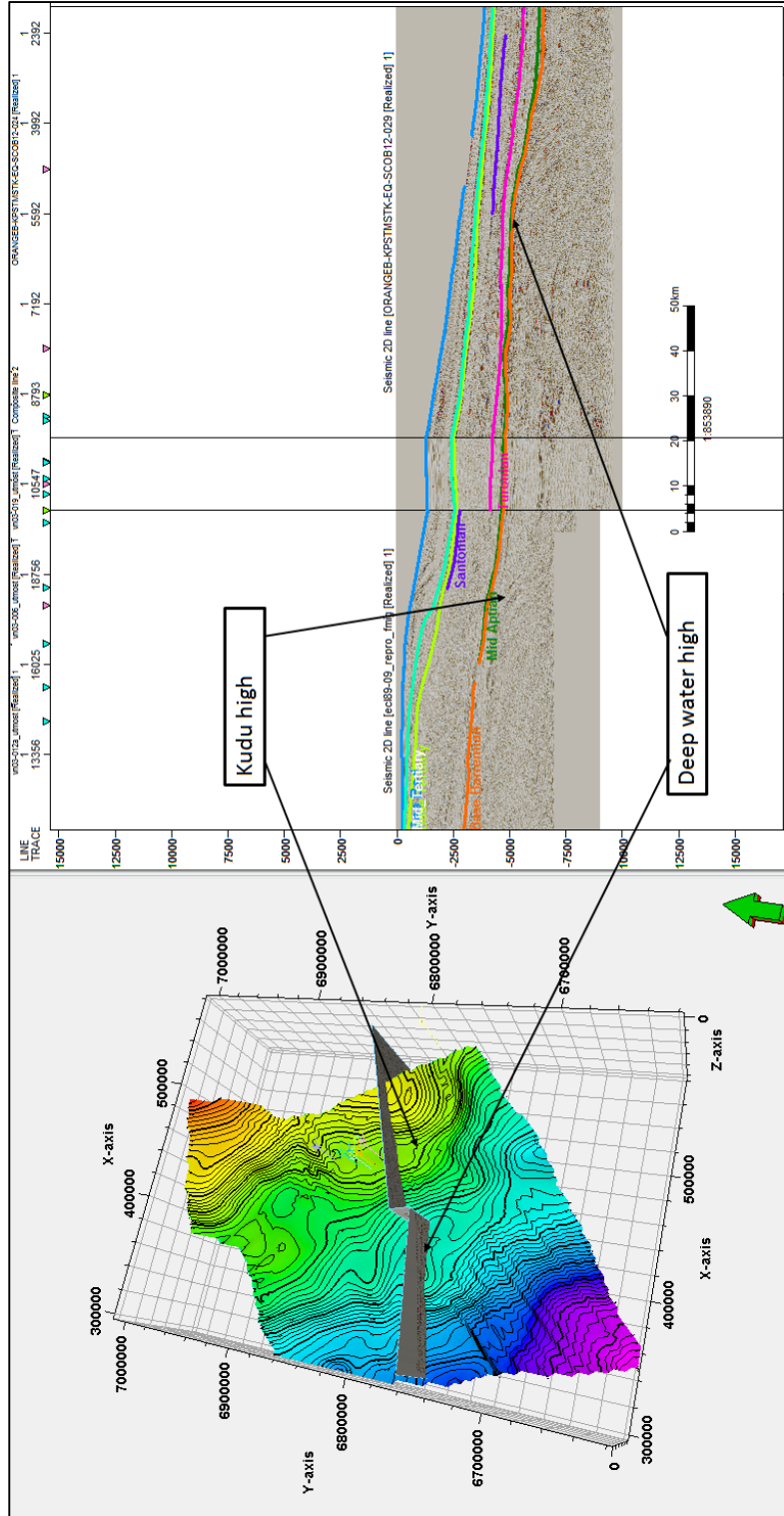


Figure 49: Two structural highs identified both on the seismic profile and structural map for transitional Early Cretaceous sequence.

Several structural closures were identified from the Base Barremian shale depth map up to the Turonian depth map. Those closures are considered as leads for hydrocarbon traps consisting of both reservoir and source rock (Figure 50). Major leads are located mostly at the center of the Basin and they were observed at all three stratigraphic levels (Base Barremian, Aptian and Turonian). The eastern part of the Basin did not show the presence of major structures.

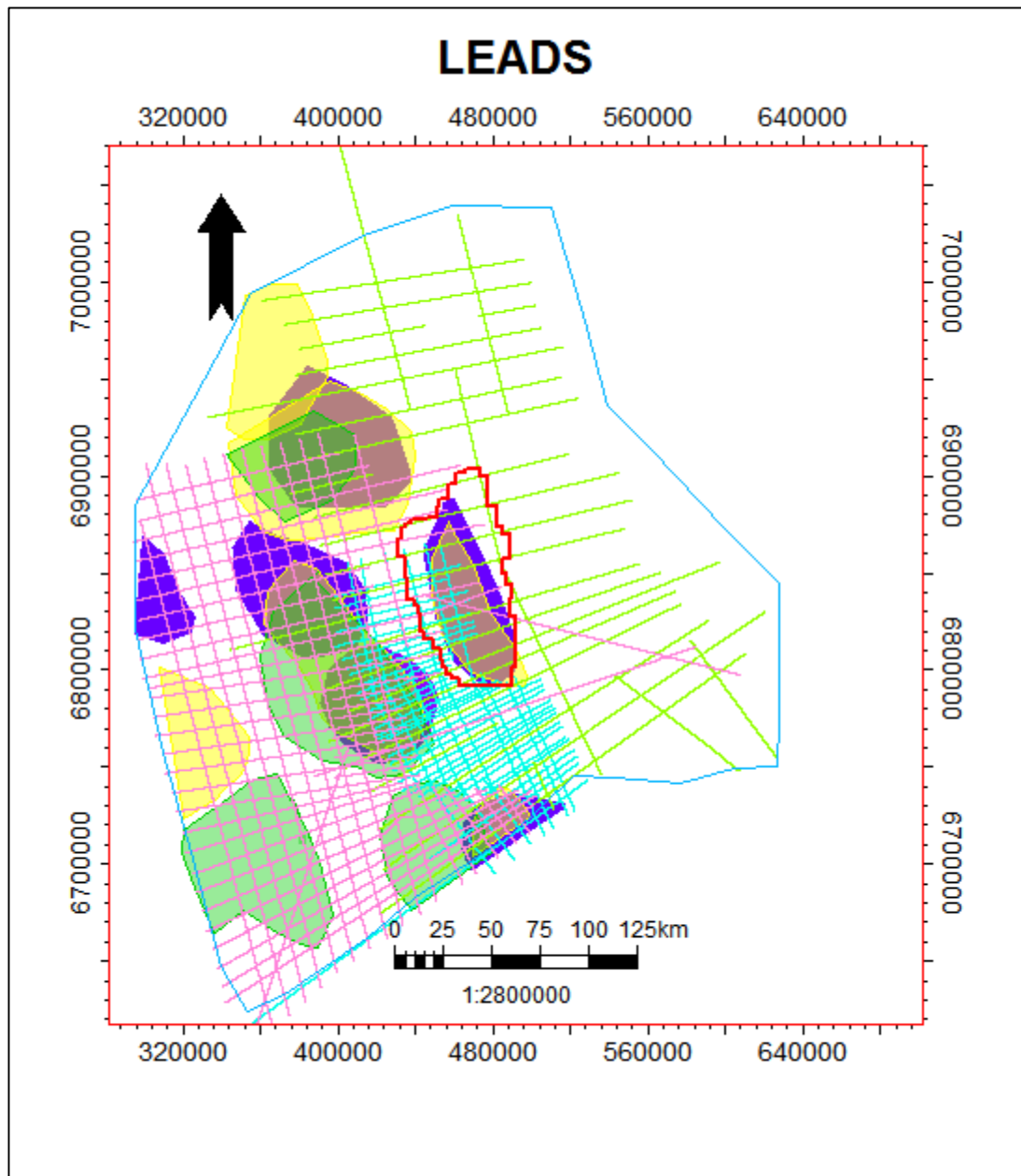


Figure 50: Map showing the location of leads identified in the study area. Base Barremian leads are indicated in purple, Aptian in Yellow and Turonian in green.

## **4.4 PETROLEUM SYSTEMS**

### **4.4.1 Source Rock Intervals**

Four source rocks intervals have been identified in the Orange Basin. Three of them have been encountered in the Kudu wells and A-J1 well in the South African part of the Orange Basin.

iiii. Pre-rift source rock

Since none of the wells offshore Namibia and Orange Basin South African has penetrated the Pre-rift, the prediction of source rock at this interval is solely based on onshore analogues. These are the late Paleozoic Whitehill Formation onshore Namibia and the correlative Irati Shales in Brazil. The Pre-rift source is considered to be oil-prone, since the rocks above the onshore analogues have proven to contain liquid hydrocarbon inclusions which might have migrated from the strata below. However, the deeply buried pre-rift offshore Namibia below 4 secs TWT on seismic profiles is expected to be over-matured. High temperature encountered in Kudu wells suggest that the temperature of deep strata was likely higher than the oil window (Bray et al., 1998).

ii. Syn-rift lacustrine source rock

This is a proven source rock that has been encountered in AJ-1 well. It has been characterized as type II, lacustrine, oil prone with TOC of > 10% and HI of > 600mg HC/g (Paton et al., 2007; Barton et al, 1993). This interval occurs in the late Haveterian to Barremian. The lacustrine oil prone source rock is hosted in graben structures (Figure 51). Toplap of Syn-rift strata indicates stagnant sea-level, promoting carbonate build-ups where sedimentation occurs at equilibrium with vertical accommodation space (Figure 52).

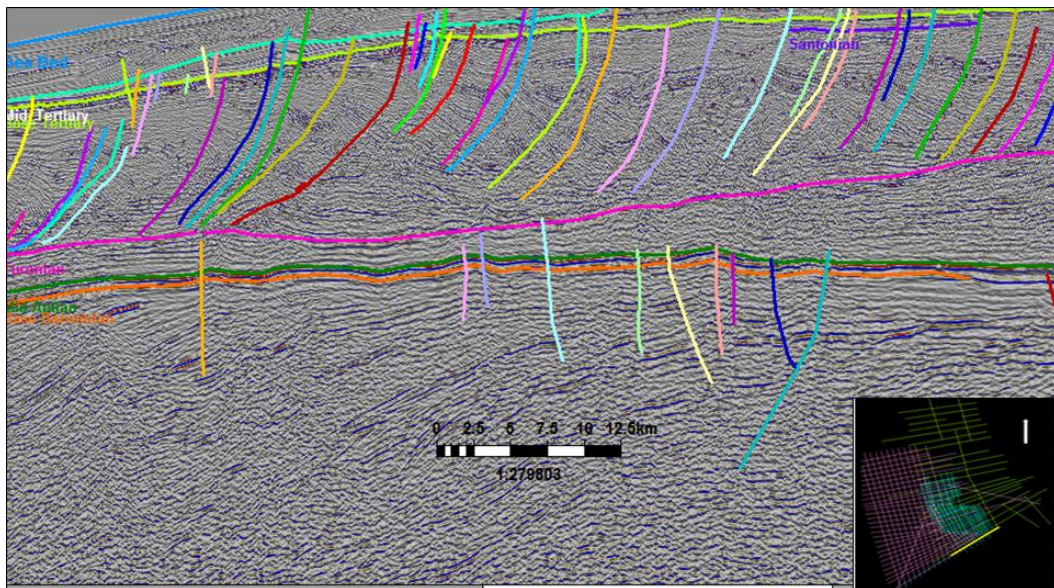


Figure 51: W-E seismic line showing graben structure with possible syn-rift source rock.

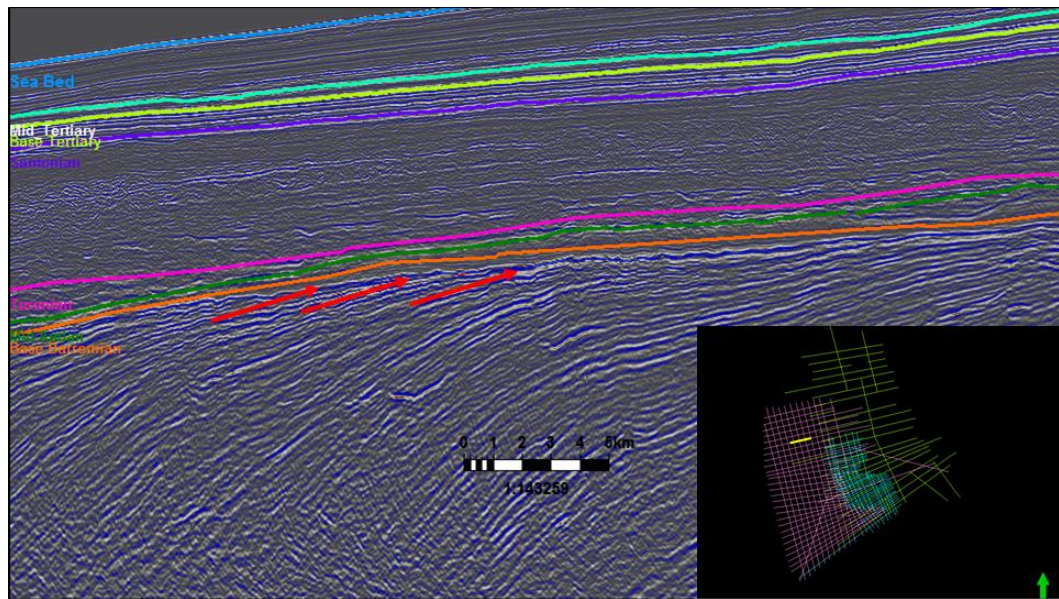


Figure 52: W-E line showing toplaps of Syn-rift strata towards the overlying unconformity indicated by red arrows.

### iii. Barremian to Early Aptian

The Barremian to Early Aptian interval has been well documented with the Kudu wells. There it consists of an approximately 500m thick black shale succession with approximately 2.0% TOC and HI of 180 to 200 mg HC/g (Veritas DGC Limited, 2004 and Schmidt, 2004). This interval gives the highest gamma ray values corresponding well with high TOC for a source rock. This source consists of Kerogen type II (Schmidt, 2004) even though both the TOC and HI appear low as it was significantly reduced by maturation (over-matured) and migration.

The interval was deposited during a general rise in relative sea level, but also during the time when the sediment supply from the Orange River system to the Basin commenced. The change in sediment supply to Basin result in basin-ward shift of the depocentre which provide sufficient burial possibly sufficient for source rock maturity.

The onlaps of strata on the mid-Aptian (Figure 53) confirms the drowning of this sequence resulting in further deposition of fine grained facies. The overall increasing sedimentation rate allowed for sufficient burial vital for source rock maturity. The Early drift to Sea Bed thickness map show that the thick successions are located at the southern part of the Orange basin Namibia where the kitchen is most likely located. (Figure 54A). The thick part of the Early Drift succession is located at the Southern flanks of the Basin (Figure 54B).

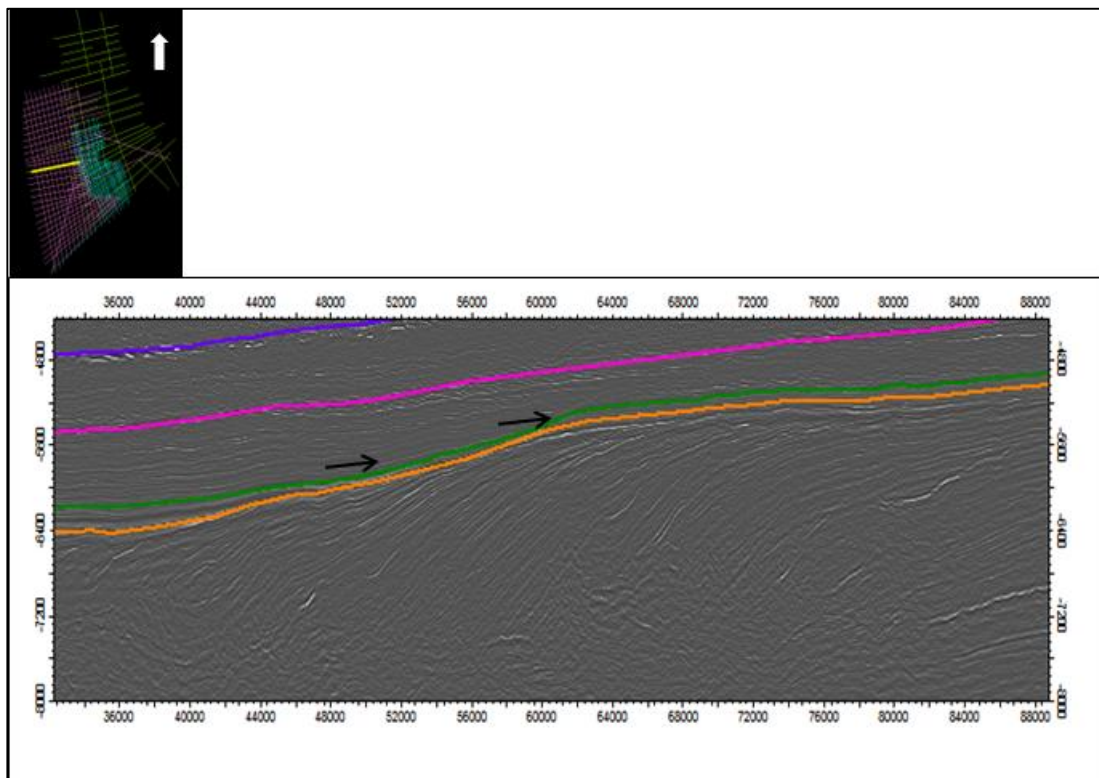


Figure 53: W-E seismic line showing onlapping of the upper Aptian sequence onto the mid-Aptian unconformity. The Barremian (orange) to mid-Aptian (green) interval contains the proven source rock for the Kudu Gas Field.

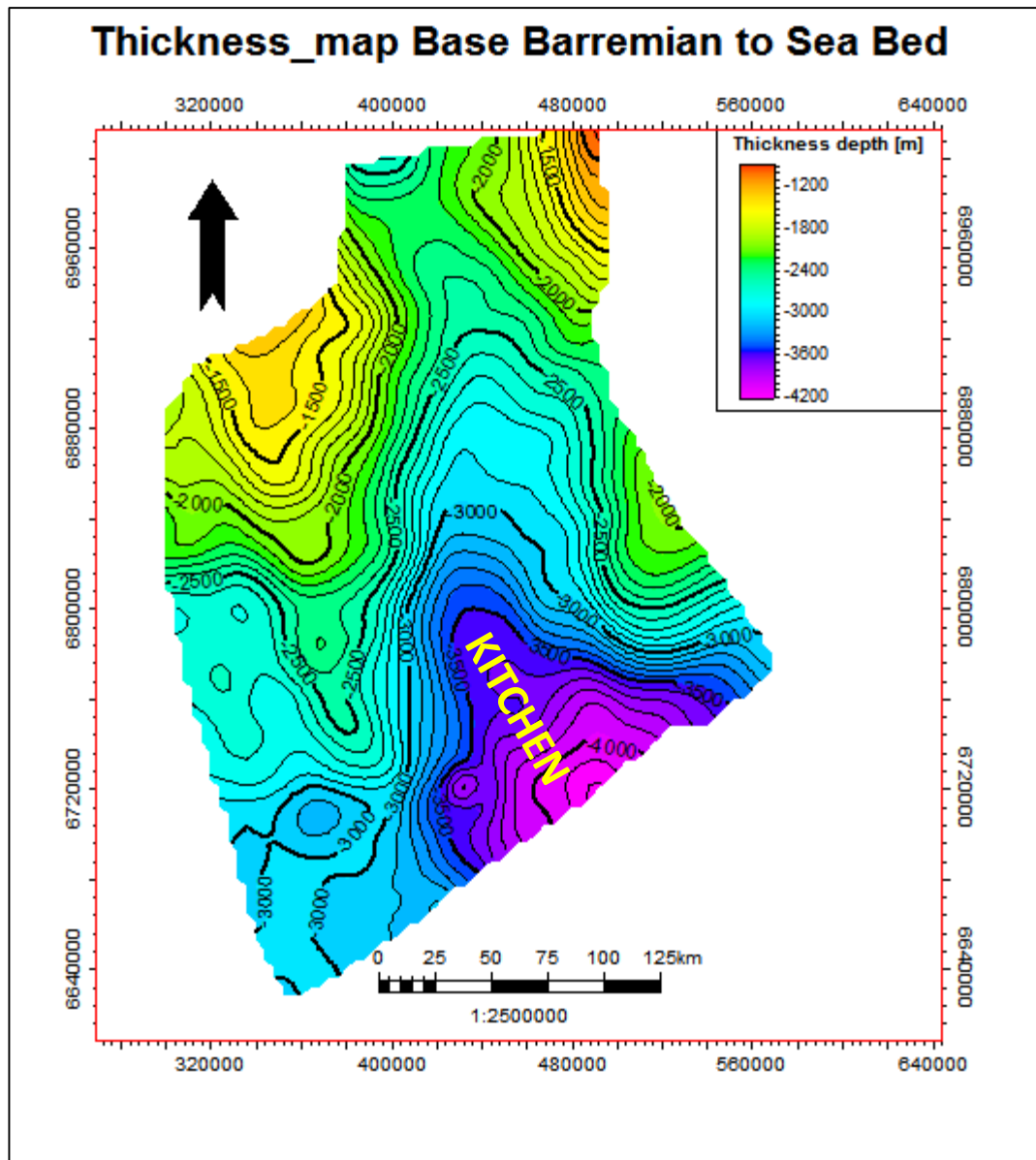


Figure 54A: Thickness map of the Base Barremian to Sea Bed indicating the location of kitchen at the southern edge of the Namibian Orange Basin which attains a maximum thickness of about 5000m.

### Thickness map Base Barremian To Turonian

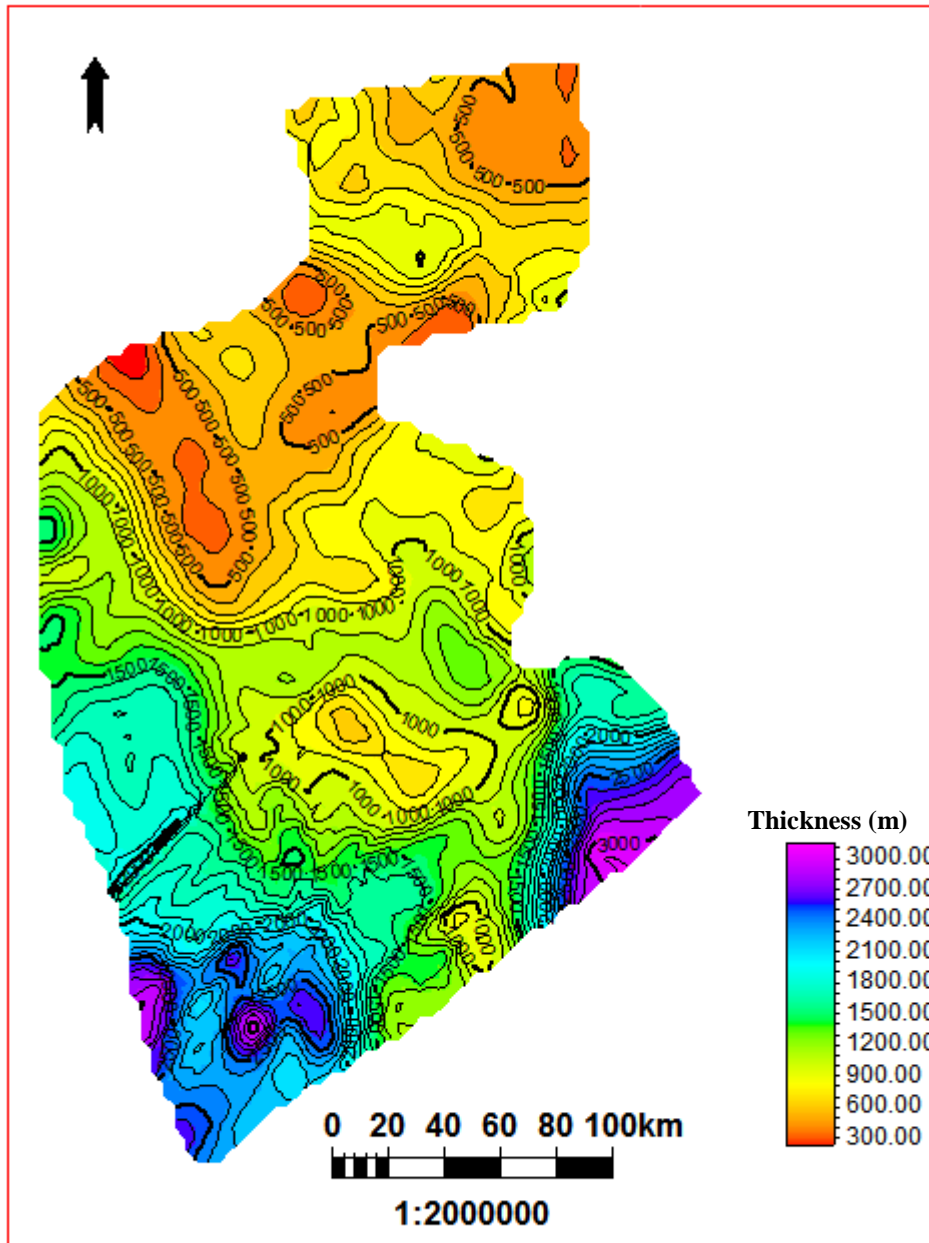


Figure 54B: Early drift thickness map showing the locations of the thick part of this unit to the southern part of the Basin reaching a maximum thickness of about 3000m.

#### iv. Cenomanian-Turonian

The Cenomanian-Turonian is the most speculative source rock. Gas has been encountered in the AJ-1 well and it may be oil prone at shallower depths further east in the Basin (Campher et al., 2009). The Turonian was also encountered in the Kudu wells and it was envisaged to be immature in that area. However, the Cenomanian-Turonian source encountered by the Kabeljou well in block 2714A drilled in the Orange Basin by Chariot in 2012 has been considered to be early mature (<http://investorshub.advfn.com>). The Turonian to Sea bed thickness map shows that the Kitchen is most probably located at the southern part of the Orange Basin offshore Namibia (Figure 55A).

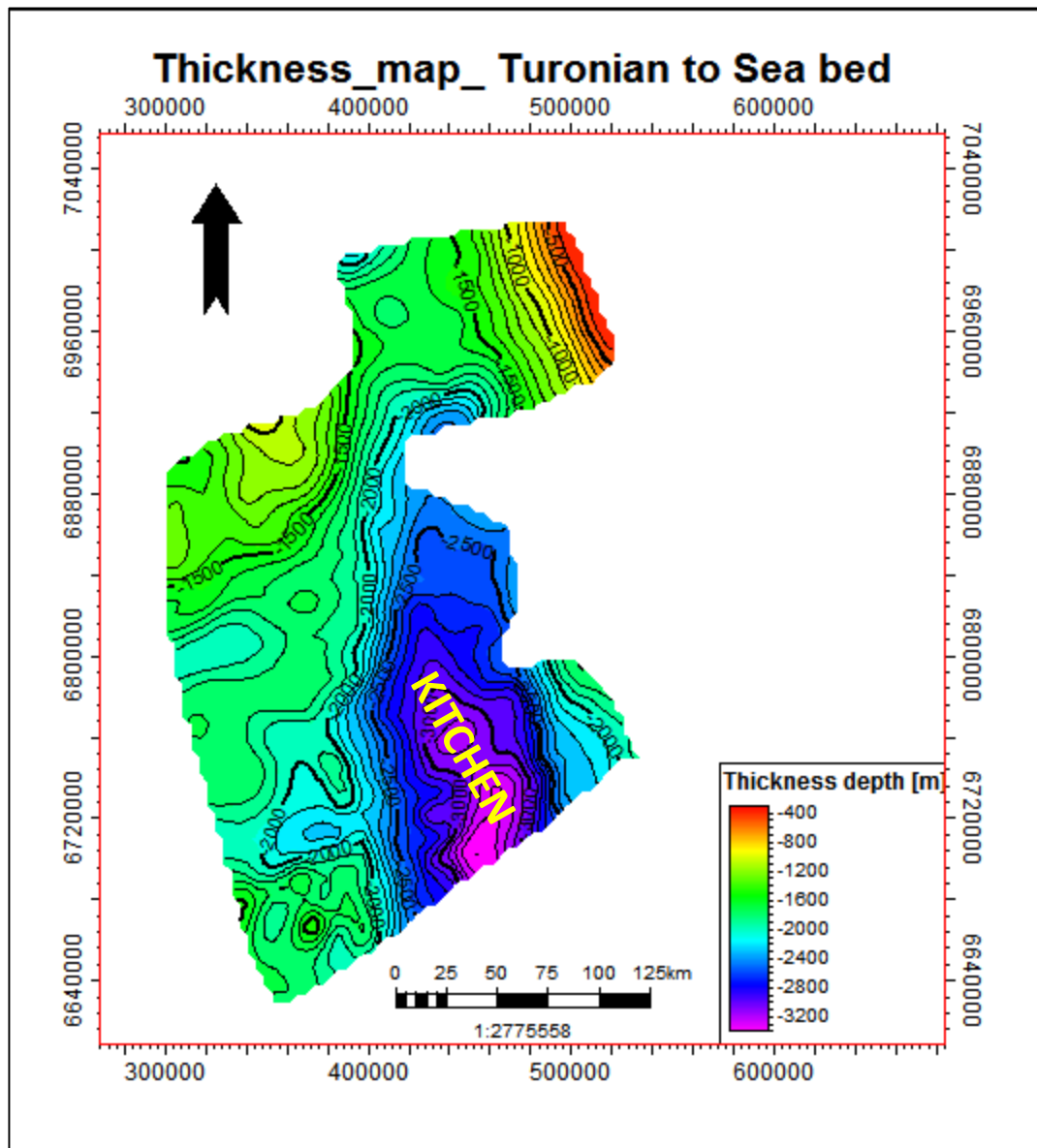


Figure 55A: Turonian to Sea bed thickness map indicating the location of kitchen at the southern part of the Namibian Orange Basin attaining maximum thickness of about 3400m.

### Thickness map Turonian To Base Tertiary

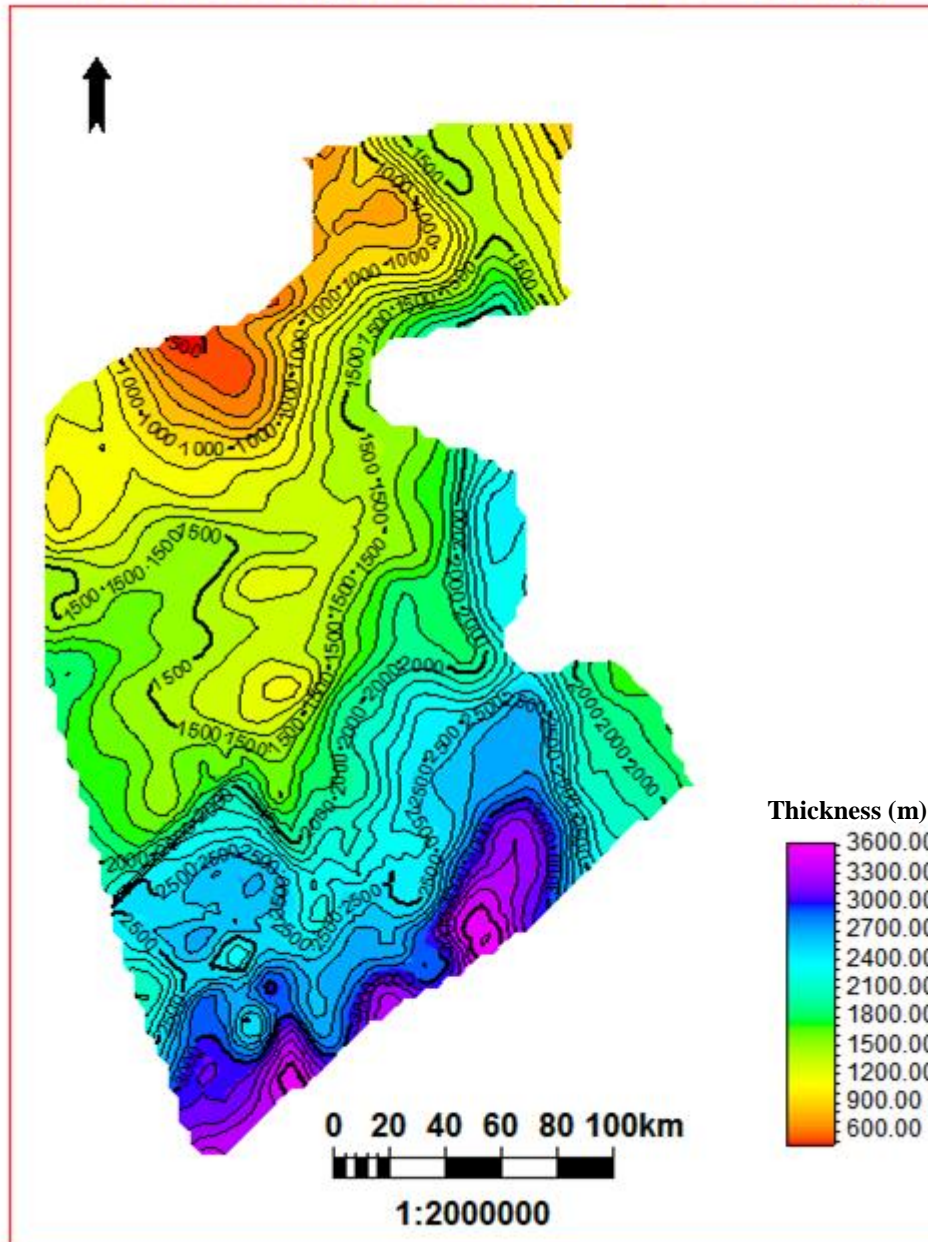


Figure 55B: Late drift thickness map indicating the thick part of this unit at the southern edge of the Namibian Orange Basin reaching a maximum thickness of 3300m.

#### **4.4.2 Reservoir Rock Intervals**

The inner graben lacustrine source rock encountered by AJ-1 well is interbedded with lacustrine sands which can act as reservoir rock. This well did not reach the graben floor, but it intersected lacustrine sandstones, conglomerates and breccias, interbedded with oil prone lacustrine source rock (Veritas DGC Limited, 2004).

The Barremian - Early Aptian source found in the Kudu wells are trapped stratigraphically in aeolian sand interbedded with volcanics. This essentially Barremian reservoir rock has poor porosity and permeability. It has been deposited during lowstand system tract (LST) followed by a transgressive system tracts (TST). These tracts typically exhibit overgrowths of quartz and authigenic minerals such as montmorillonite, the latter partially reduced to chlorite (Adeniyi et al., 2009). The overgrowth of quartz and cementation with authigenic minerals are likely responsible for the poor porosity and permeability at this stratigraphic level.

Up-section, the Late Cretaceous toe thrust structures in the western part of the Basin (Figure 56) are expected to contain deep sea turbidite sands which may be also possible reservoir rocks. The turbidite sands are envisaged to have been deposited in basin floor fans from periodical collapse of the Orange River delta and later deformed within toe thrusts.

In addition lowstand wedges are associated with the Late Cretaceous late sequence. Reservoirs are possibly associated with such prograding wedges. Good reservoir sands

might have supplied to the basin at this stratigraphic levels by channels, which have been identified at this interval (Figure 45 & 46).

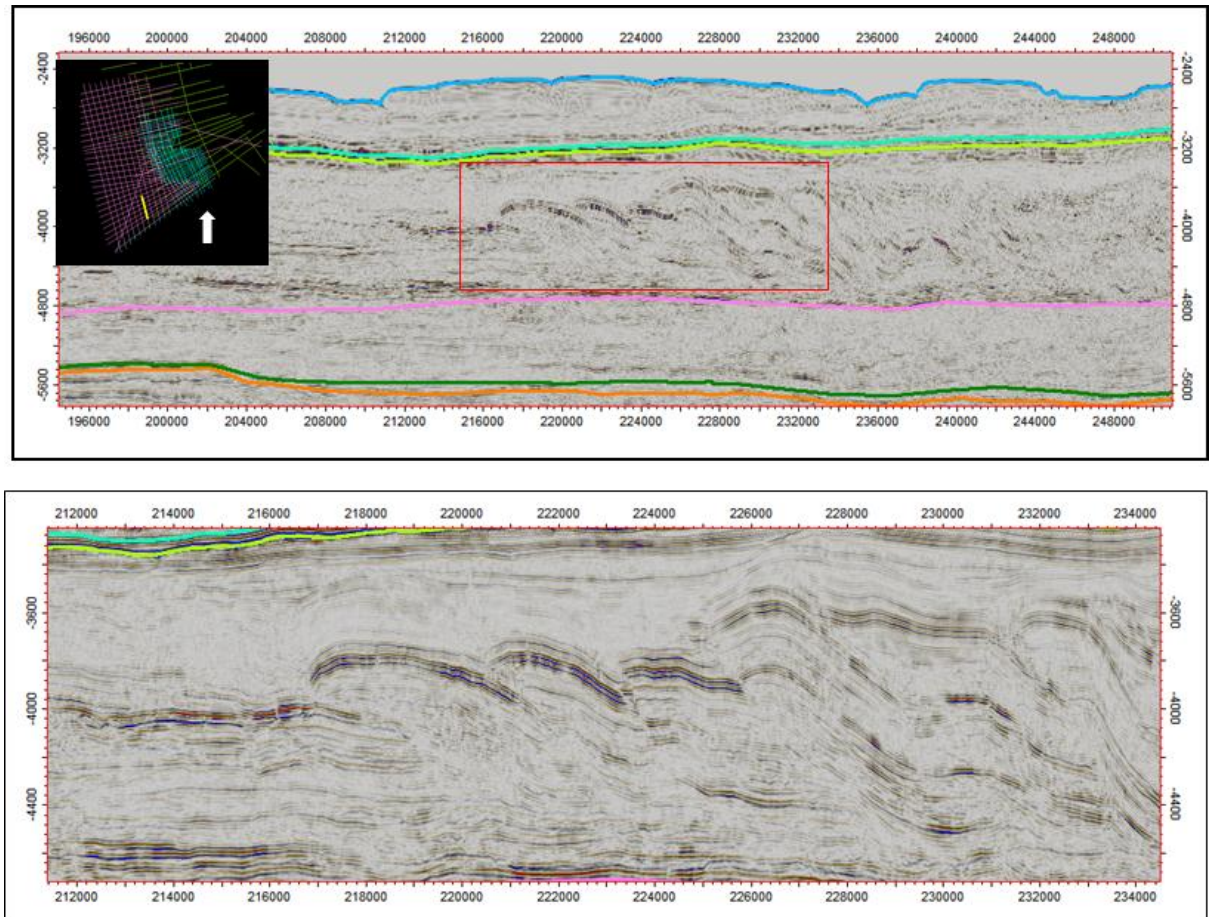


Figure 56: N-S seismic line showing toe thrusts just above the Turonian unconformity, the amplitude is brighter at the top of the thrust and dims down dip due to change in seismic facies.

#### **4.4.3 Traps and Migration Paths**

The pre-rift section has not been penetrated by any well in the entire Namibian margin, but it's presumed that the Pre-rift occurs in the eastern part of the Basin where tilted blocks might contain continental Karoo sediments of Late Paleozoic to Early Mesozoic age (Clemson, 1977).

Syn-rift Structural traps are characterised of half graben structures which has been proved in the Orange Basin offshore South Africa. The syn-rift pinch-outs observed on seismic profile in chapter 5 are possible traps. Those pinch-outs do probably contain similar lithologies as the syn-rift half graben structures (Veritas DGC Limited, 2004).

Early drift wedge-out traps have been proven by the Kudu wells in the Orange Basin offshore Namibia. They formed as early drift fans that provide possible stratigraphic traps as they are located immediately above the Aptian source rock and are overlain by thick marine shales acting as top seal. Structural highs bulging up over faults that cuts through the Early Cretaceous unconformity and terminates within this unit can be potential hydrocarbon traps. Another possible trap can be fault block plays in which faults extends from the Syn-rift and terminates in Early drift.

This play has been penetrated by The Kudu-1 well, but no reservoir was encountered presumably due to unsuitable location for the well. The well might have been drilled in the by-pass zone for sediments over the shelf break (Veritas DGC Limited, 2004). The reservoir for this play is expected to be located closer to the shore within channel systems.

Late drift toe-thrust traps have not been penetrated by any of the wells in the Orange Basin. Their occurrence is restricted to the deeper offshore. The presence of faults in the Basin may augment migration of hydrocarbons, preferably in updip direction.

#### **4.4.4 SEAL**

Thick shales were encountered by the Kudu wells within the Cretaceous in the entire drift section. These shales act as seal for the Kudu gas reservoirs. There is no proof for the presence of seals in the synrift offshore Namibia, since none of the Orange Basin wells offshore Namibia penetrated this section. However, the sequence overlying faults extending from the syn-rift might be considered as possible seal if it consists of a continuous package of mudstones.

#### 4.4.5 SUMMARY

The stratigraphic and structural analysis of the Orange Basin demonstrated the presence of a working petroleum system. The proof is the gas discovery in the kudu wells. The proven source rocks in the Orange basin are located in Barremian-Aptian and Turonian units, while the proven reservoir occurs in the Barremian and a potential reservoir interval was observed in Kudu wells at Maastrichtian (Figure 57). The Critical time for a complete petroleum system in the Basin is from Palaeocene to recent.

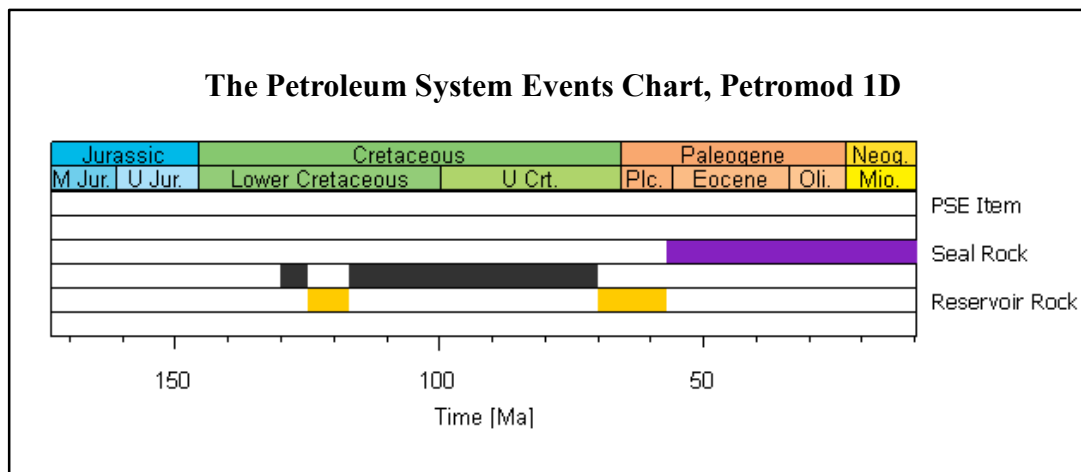


Figure 57: Petroleum system model showing reservoir intervals in yellow, source rock in black and seal in purple.

The hydrocarbon kitchen is rather located to the southern part of the Basin at all stratigraphic levels. The main argument for this location is increased sediment thicknesses. Apart from the proven petroleum systems the Basin has potential of

having plays at the Pre-rift and Syn-rift intervals. The Syn-rift play is considered to be most likely present offshore Namibia as it was proven in the Orange Basin of South Africa. For accumulation, the timing of maturation and the critical moment of secondary migration are crucial. The Aptian source rock has both, source and seal properties. Therefore hydrocarbon accumulation in the underlying Barremian reservoir sands must have happened either during or after source rock maturation. The fact that the reservoir is located beneath the source implies an overpressure driven downward migration (Schmidt, 2004). Tertiary (Eocene to recent) shales may act as seal for the Maastrichian potential reservoir sands.

## **CHAPTER 5: ONSHORE ANALOGUES**

Onshore analogues are exposures of rock strata that provide a 3D understanding of depositional architecture and hence with a better understanding of depositional dynamics. In contrast to well data that provides localized information only, outcrops provides spatial information by direct 3D exposure. Moreover, seismic data does not show small scale spatial architectures due to limited resolution which can be clearly identified on outcrops. Therefore an outcrop analogue reveals additional information on the geometric and depositional architecture of offshore rock units which improves the understanding of petroleum systems.

### **5.1 HUAB BASIN**

#### **5.1.1 Background**

The geological setting of the onshore aeolian /lava deposits of the Huab Basin (Figure 58) have been considered to be one of the Kudu reservoir analogues (Jerram et al., 1999). The geomorphology and lithological units of these deposits provides an insight on the depositional history of the kudu reservoir rock unit. The main objective of this section is to analyse the interaction of sediments and lava deposits which will enhance the understanding of Orange Basin sediment-lava reservoir rock unit.

The Huab Basin was developed during the Paleozoic (280-250 Ma) in an intra-cratonic thermal sag Basin. During this time 200m of mainly continental Karoo sediments were deposited in the Huab Basin (Mountney et al., 1998). The break-up of west Gondwana during Jurassic to early Cretaceous times resulted in north-south oriented extension of the Huab area. During this period accommodation space was created in the Huab area due subsidence in which aeolian and fluvial sediments of the Etjo Formation were deposited.

The stratigraphic unit of the Huab Basin indicates that the Karoo sediments unconformably overlie the Damara basement rocks (Figure 59). These Karoo rocks are alienated from the overlying basaltic lava and aeolian sandstone of the Etjo Formation by an angular unconformity. The Lower Awahab Formation overlies the Etjo sands and it's capped by the quartz latite (Figure 60). However, the Huab outliers in the study area are predominantly composed of Karoo and Etjo sediments interlayering with dolerite intrusives. The Etjo sandstones consist of medium grains of mainly quartz with abundant feldspars. Large foresets, grain flow structures and laminations that were observed in the Etjo sandstones correspond to an aeolian dune nature. These dunes attain a maximum thickness of appromately 100m (Regional Evaluation Report, 1998). Stollhofen 2000, renamed the the Etjo Formation in this area to Twyfelfontein Formation with an assumption that these lava-aeolian sandstone are younger than the Etjo sandstone found in the Waterberg area.

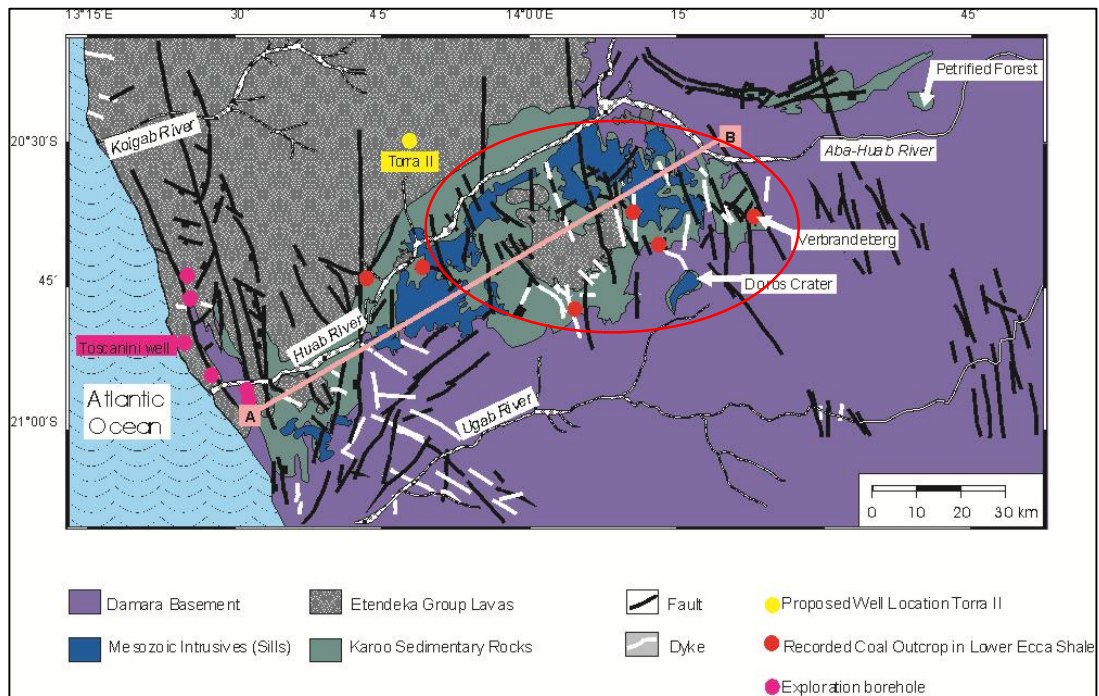


Figure 58: Geological map showing the location of the Huab Basin modified after Mountney et al., 1998. The study area is circled in red.

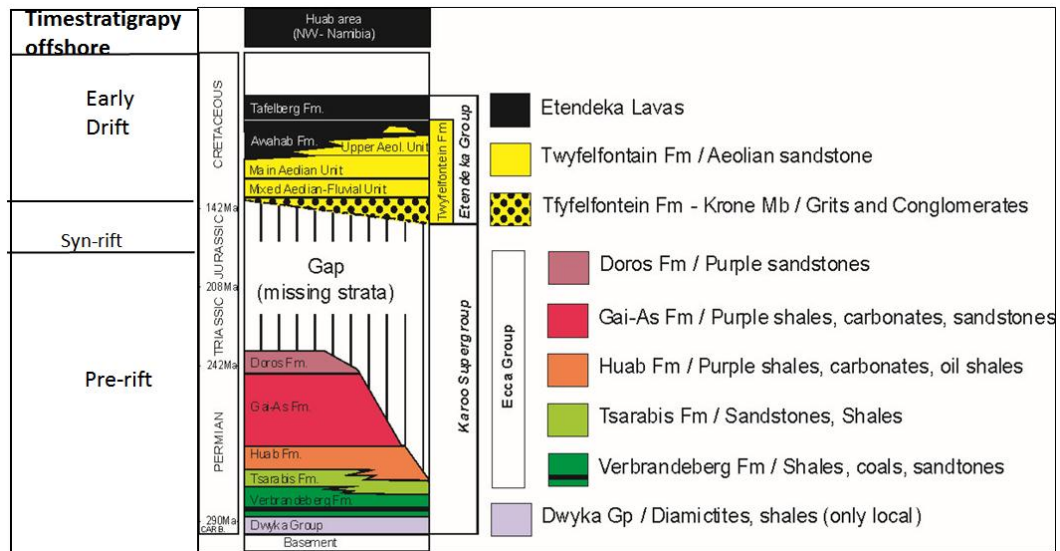


Figure 59: Timestratigraphic offshore and tectonostratigraphy framework of the Karoo Supergroup and Etendeka Group in the Huab Basin showing a link between offshore and onshore units, modified after Mountney et al., 1998.

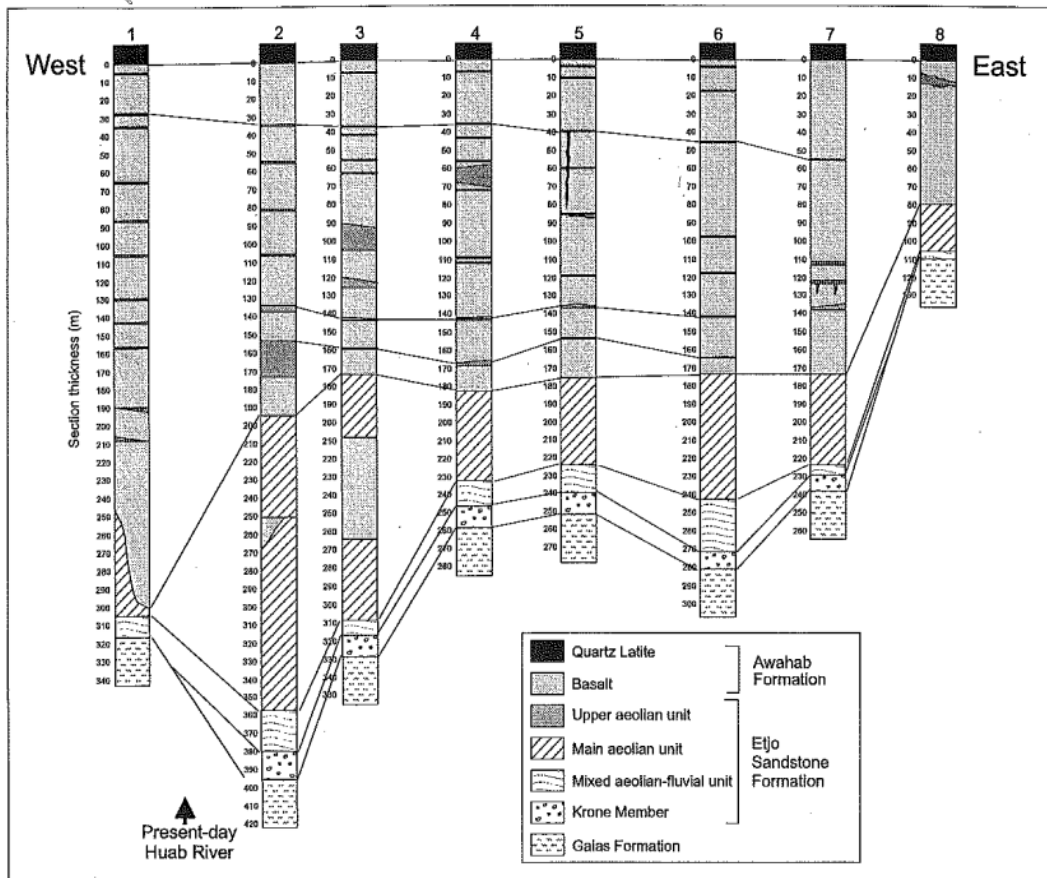


Figure 60: Lithological units across the Huab basin (Mountney et al., 1998). Note that the Etjo Formation has been sub-divided into four sedimentary units and the lower Awahab is capped by quartz latite.

## 5.1.2 Field Observation

### 5.1.2.1 Geometries in 3D Exposures

This analogue has been extensively studied and documented by several authors. Therefore the field work was mainly based on field observations and no measurement of geological features was conducted. The Neoproterozoic outcrops, Late Paleozoic to

Mesozoic Karoo rocks units, Cretaceous igneous complexes, Cretaceous volcanics and the Tertiary alluvial gravels of the Huab Basin are well exposed with little to no vegetation cover in most areas.

i. Krone Member

South of the aeolian-lava field lies an outcrop comprised Jurassic-Cretaceous aeolian-fluvial deposits unconformably overlying lower Permian shale unit of the Karoo Supergroup (Figure 61). The underlying Permian shale unit is locally known as the Gaias Formation (Mountney et al., 1999). Stratigraphically, the basal massive shale unit is unconformably overlain by fluvial deposit consisting of clast-supported pebble and cobble conglomerate of the Krone Formation. The clasts are mainly reworked meta-sedimentary rocks of the Damara sequence found at the edge of the Huab Basin margins. The fluvial clast-supported conglomerates are envisaged to have been deposited in a high energy flow environment subjected to flash floods and braided river flow systems (Mountney et al., 1999). The fluvial conglomerates are overlain by mixture of fluvial and aeolian sandstones which represents the change in depositional environment. This reflects a change from semi-arid environment with ephemeral fluvial flows system to more arid environment where aeolian sediments were deposited by wind. The fluvial drainage system is envisaged to have been shut-down due to the increase in aridity.

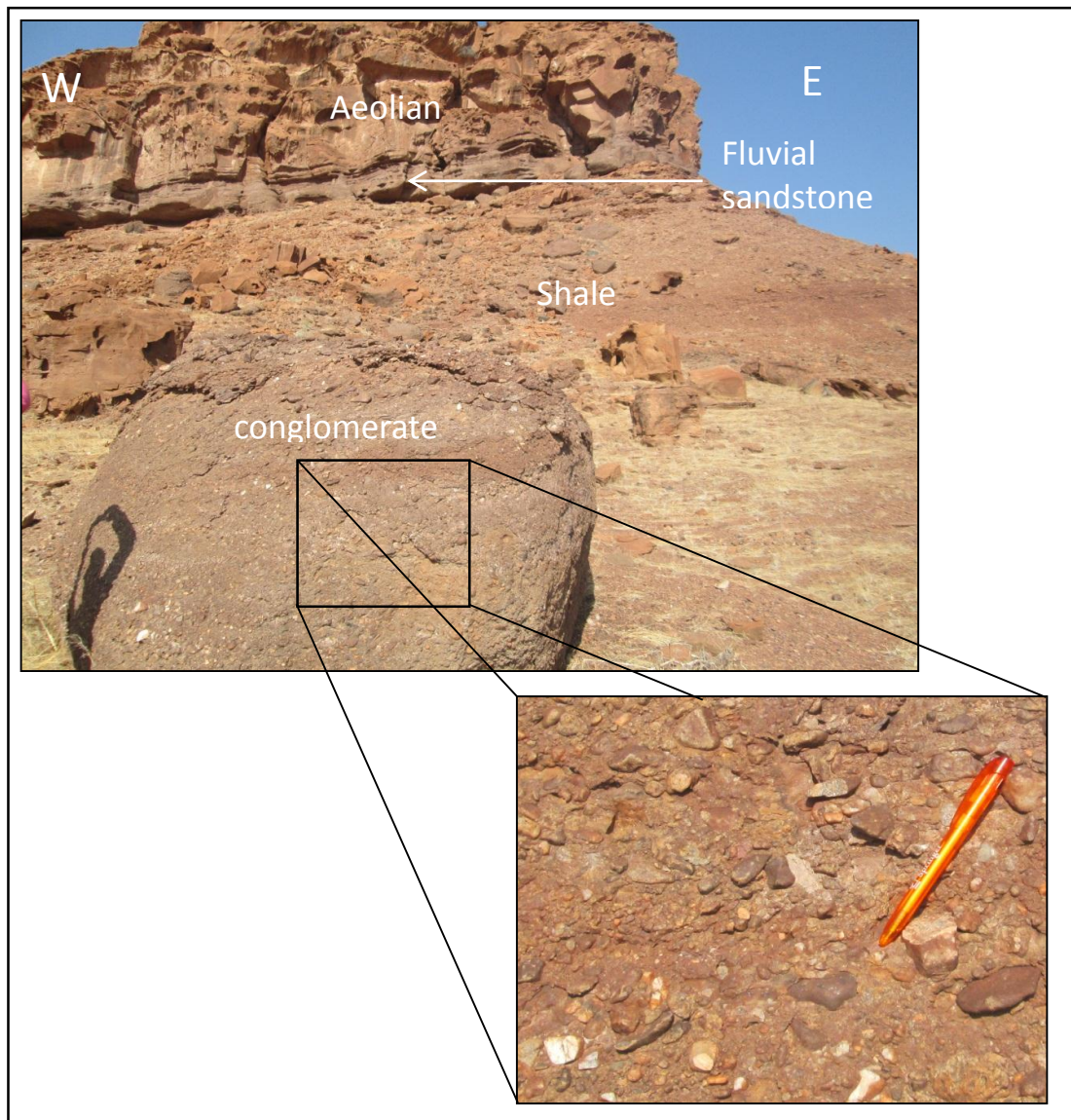


Figure 61: Outcrop showing different types of deposits which were deposited in a different environments. The bottom part is comprised of shales (Pre-rift time equivalent) which are overlain by fluvial deposits capped by aeolian deposits (Early drift time equivalent). The fluvial deposits consist of angular matrix supported material as shown in an enlarged picture. Eastern flank of tributary North of Huab River 14°07.432'E, 20°37.721'S.

An inclined north-south dolerite dyke cutting through fluvial sandstone of the Krone member was observed at 014°04.590'E, 20°37.640'S (Figure 62). The emplacement of the dyke displaced the sandstone block, moving it upward. The composition of this dyke is equivalent to the weathered basalt observed at the base of Awahab Formation which is mainly olivine-phyric. The olivine-phyric dykes in the Huab Basin show a high concentration of olivine phenocrysts at the centre of dyke which might have been caused by flow differentiation (Duncan et al., 1998).

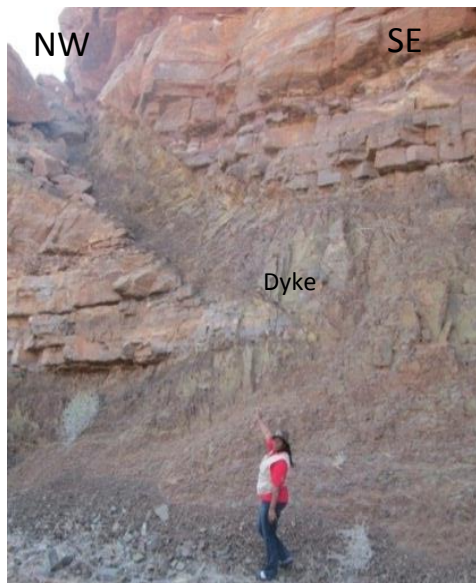


Figure 62: Inclined dolerite dyke cutting through Krone Formation sandstone (Syn-rift time equivalent). Eastern valley flank at 14°04.512'E, 20°37.568'S

ii. Aeolian Twyfelfontein

The Huab rock units are mainly comprised of sediments preserved under and within massive lava units. Climbing sequential aeolian bedforms are preserved one on top of each other in basalt (Figure 63). The highest preserved bedform observed attains a maximum height of 100m (Jerram et al., 1996). The geometry and size of the Twyfelfontein dunes is analogous to the present day barchan dunes observed at the skeleton coast.



Figure 63: Isolated barchans dune interbedded in basalt in the mid-section of the outcrop (Early drift time equivalent). Note that the identified isolated barchans dune in the picture is the only one observed in the middle section of this outcrop. View from 14°08.432'E; 20°39.940'S.

The Huab Basin olivine-phyric basalts were subjected to weathering unlike the interbedded aeolian sandstones which did not show any indication of weathering.

The sandstone contained no carbonate cementation since it did not react with the hydrochloric acid which indicates that these are silica cements sandstones.

#### iiv. Etendeka Volcanics

The lower Awahab outcrop at the geographic location of 14°09.377'E, 20°09.237'S is mainly comprised of basalt and sandstones interlayers (Figure 64 & 65). Layers of sandstones are embedded between basalt layers, whereas weathered basalts are situated at lower part of the outcrop and a massive basalt layers overlies the first sandstone layer. This is an indication that there was insufficient sand supply at this stage to allow dune forms to develop. Sand filled fissures were also observed in the lower weathered basalts.

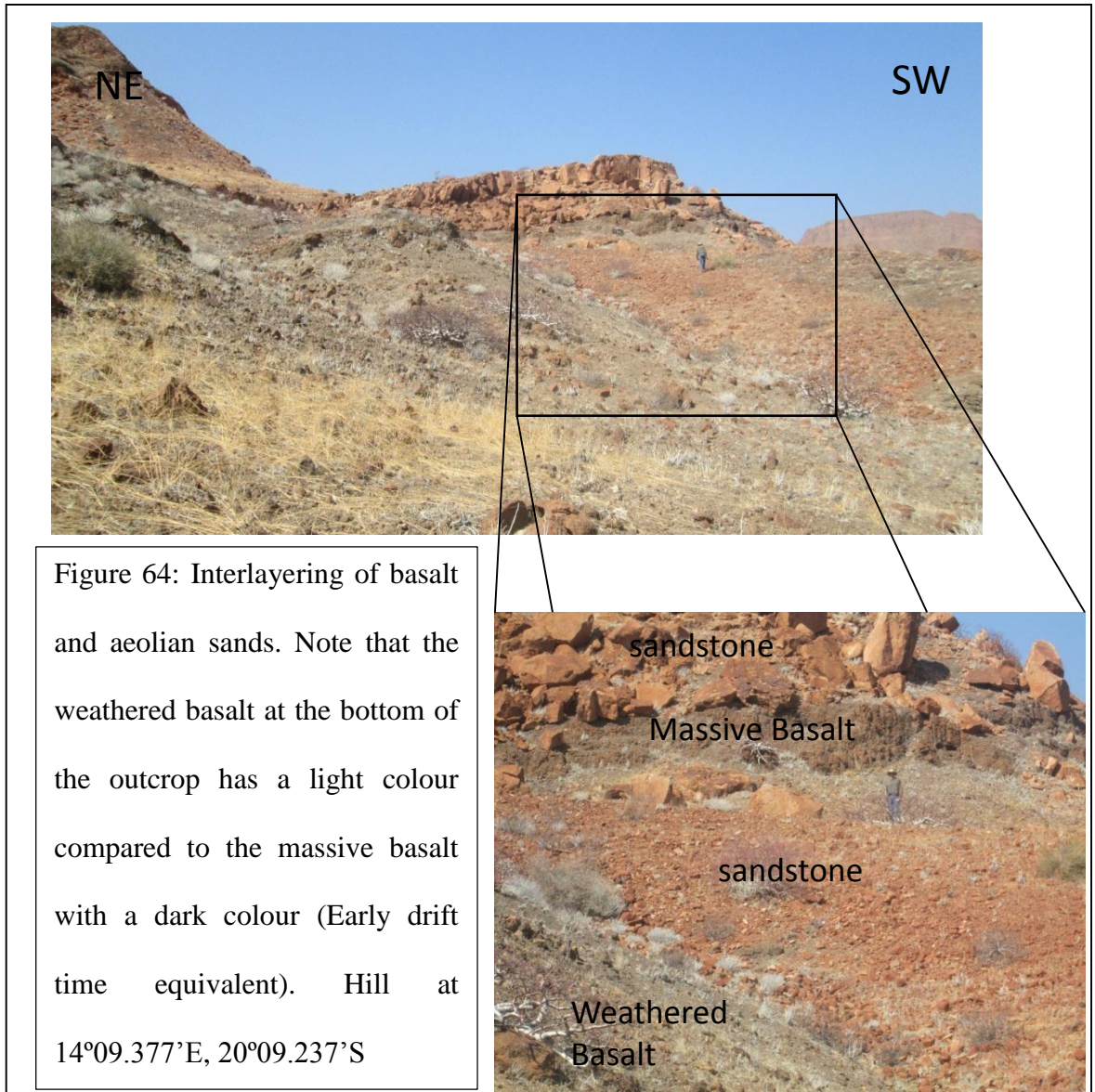




Figure 65: Red sandstone interbedded in weathered basalts.

#### iv. Isolated barchans

The isolated barchan dune is smaller compared to the isolated multidunes. The isolated multiple dunes attain a maximum thickness of about 20 m and width of approximately 1 km (Jerram et al., 1999). The multidunes in the outcrop (Figure 66) are found just below the isolated single barchans dunes and they are completely embedded in basalt rock. Foot of hill at  $14^{\circ}09.377'E$ ,  $20^{\circ}09.236'S$  .

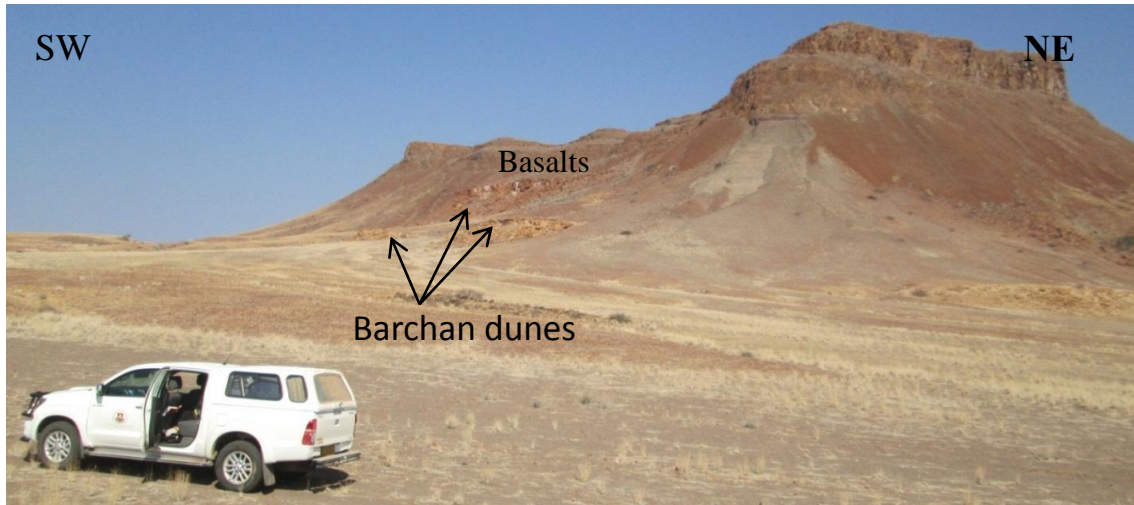


Figure 66: Series of barchanoid (multi-dunes) dunes preserved in volcanic unit in the lower part of the outcrop (Early cretaceous equivalent). View from 14°09.139'E; 20°39.978'S.

#### 5.1.2.2. Regional Scope

An outcrop with the geographical location of 14°06.443'E, 20°41.406'S within the Huab Basin mainly comprised of basalt subjected to minimal weathering which consist of small sand filled cracks (Figure 67). This is envisaged to have been resulted from wind-blown sand bypassing the lava surfaces settling and later preserved in cracks within basaltic rock unit. These bypass surfaces have been laterally correlated to large isolated barchans dunes buried within the lava. This signifies the dynamic system of the sand bodies which migrated over a lava field while preserved under a subsequent lava flow.

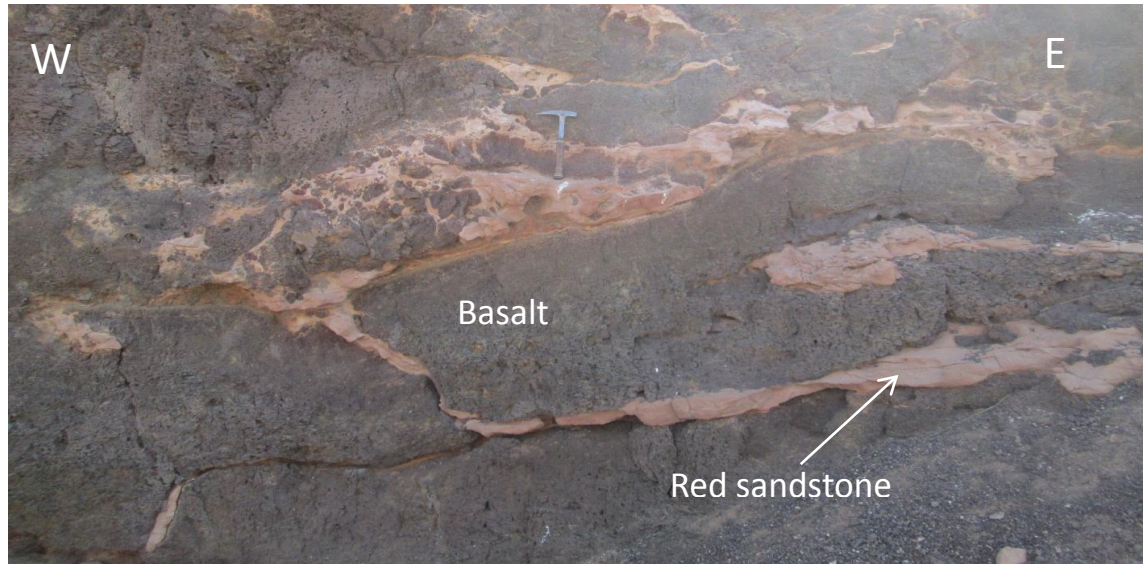


Figure 67: Bypass section showing aeolian sand preserved in small cracks within the basalt (Early drift time equivalent). Note that the basalt at this outcrop is subjected to minimal weathering. Valley flank at 14°06.478'E; 20°41.907'S.

Vertical sandstone filled crack embedded in highly weathered massive basalt rock was observed tributary towards the Huab River (Figure 68). The upper part of the vertical sandstone filled crack has been displaced few meters to the South East. The upper and middle part of this outcrop show very little sand-lava interaction.



Figure 68: Vertical cracks (fault) at the top of the basalt filled by aeolian sands (Early drift time equivalent). Outcrop close to exposure in Figure 67.

### 5.1.3 Summary

The Tweyfontein sediment/lava interaction deposition occurred as flood basalt lavas which erupted over large areas in which sedimentary deposition was active. These flood basalts are known as Parana in South America and Etendeka in Namibia. The stratigraphic correlation of flood basalts between South America and Africa indicates an Early Cretaceous age. The aeolian/lava deposits resulted from the initial basalt lava spilling into an active erg sedimentary system, with prevailing winds towards ENE (Figure 69). The deposition of the first lavas was controlled by the aeolian bed forms channeling lava flow to fill interdune areas. At this stage a significant amount of sand bodies were not buried in lava, resulting in the continued sedimentary deposition forming secondary dune fields and subsequent lava flows, with predominant wind direction towards SE (Figure 70). The topographic height of secondary dunes decreased due to less sand supply. The isolated barchans dunes preserved in basalt suggests that sand was blown across lavas as isolated sand bodies between episodes of lava eruptions. The deposition of sands ceased as a result of change in wind direction which might have shifted winds away the source area of aeolian sands, explains the absence of aeolian sand bodies capping the basalts. Alternatively, the deposition of sand might have stopped by the deposition of basalts on top of the dunes sealing the sand source. The preserved dunes show little sign of deformation caused by deposition of lavas on top of the Tweyfontein sands. This implies a remarkable passive emplacement mechanism of the basalts which resembles the present day Hawaii flow generally used to measure the flow rates and emplacements of ancient lava flows

(Jerram et al., 1996). Sand filled cracks and fissures observed on top of the basalt is the record for the pathway of bedforms.

The difference between the Huab Basin aeolian/lava deposits and the Kudu reservoir is the lava distribution that is controlled by sand topography in Huab compared to the high volume of lava and less sand composition in Kudu which promotes a pure control of sediments by lava geometries. The depositional architecture of the Huab Basin sedimentary deposits differs from that of the Kudu reservoir unit. The aeolian rock unit overlies the fluvial deposits in the Huab Basin as opposite to the Kudu reservoir where the fluvial deposits overlies aeolian /lava deposits.

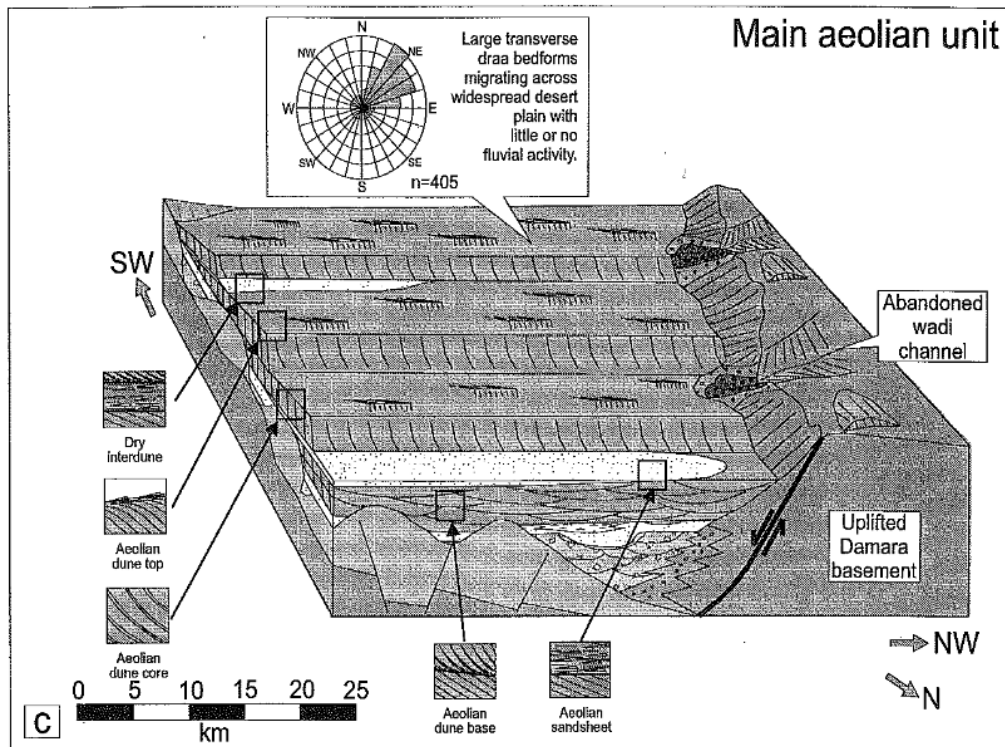


Figure 69: Depositional model for main aeolian unit in the Huab region, in which the orientation of aeolian bedforms indicates that the prevailing wind was blowing towards ENE (Mountney et al., 1998).

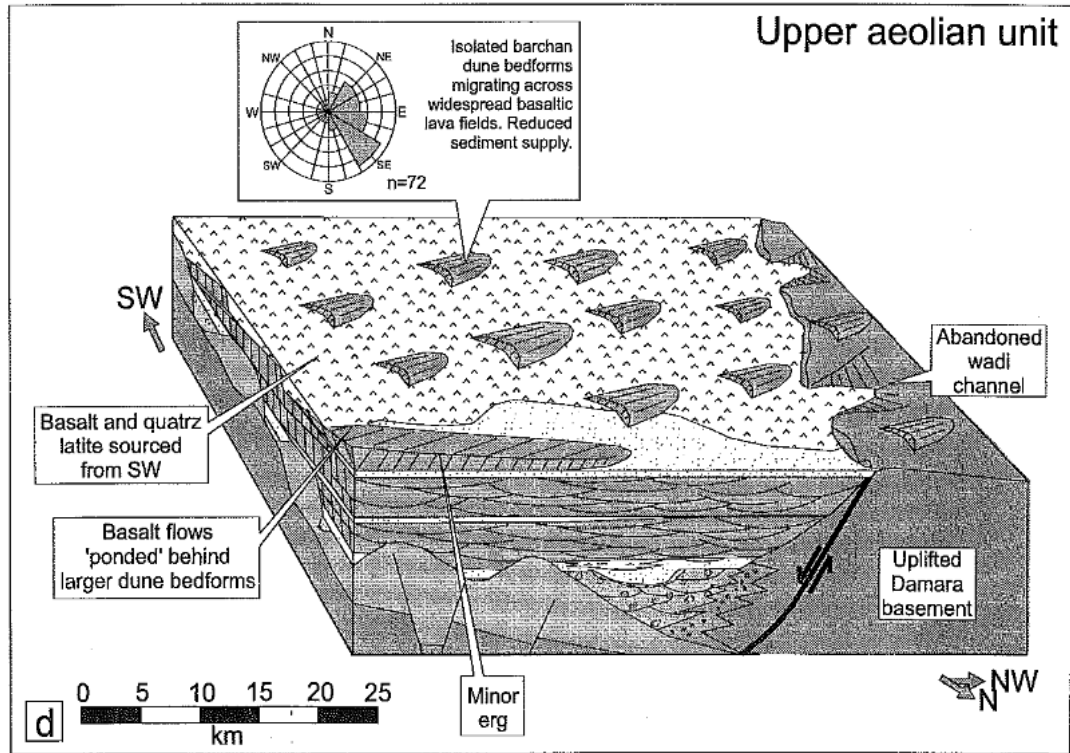


Figure 70: Depositional model for upper aeolian unit in the Huab region, in which the orientation of aeolian bedforms indicates that direction of prevailing wind changed to SE (Mountney et al., 1998).

## **5.2 Southern Namibia Fieldtrip**

### **5.2.1 Background**

The main objectives of this field excursion was:

- To study the Kalkrand Formation as Kudu reservoir analogues in order to understand the factors controlling the deposition of potential reservoir.
- To compare the Hardap Shale member and Whitehill Formation to Kudu source rocks in the Orange basin Namibia and also source rocks encountered in AJ-1 well offshore Orange Basin South Africa.
- To study the outcrops at the Orange River Mouth, with the aim of enhancing the understanding of depositional dynamics in the Orange Basin during episodes when deltaic systems were feeding the rift graben structures with sediments.

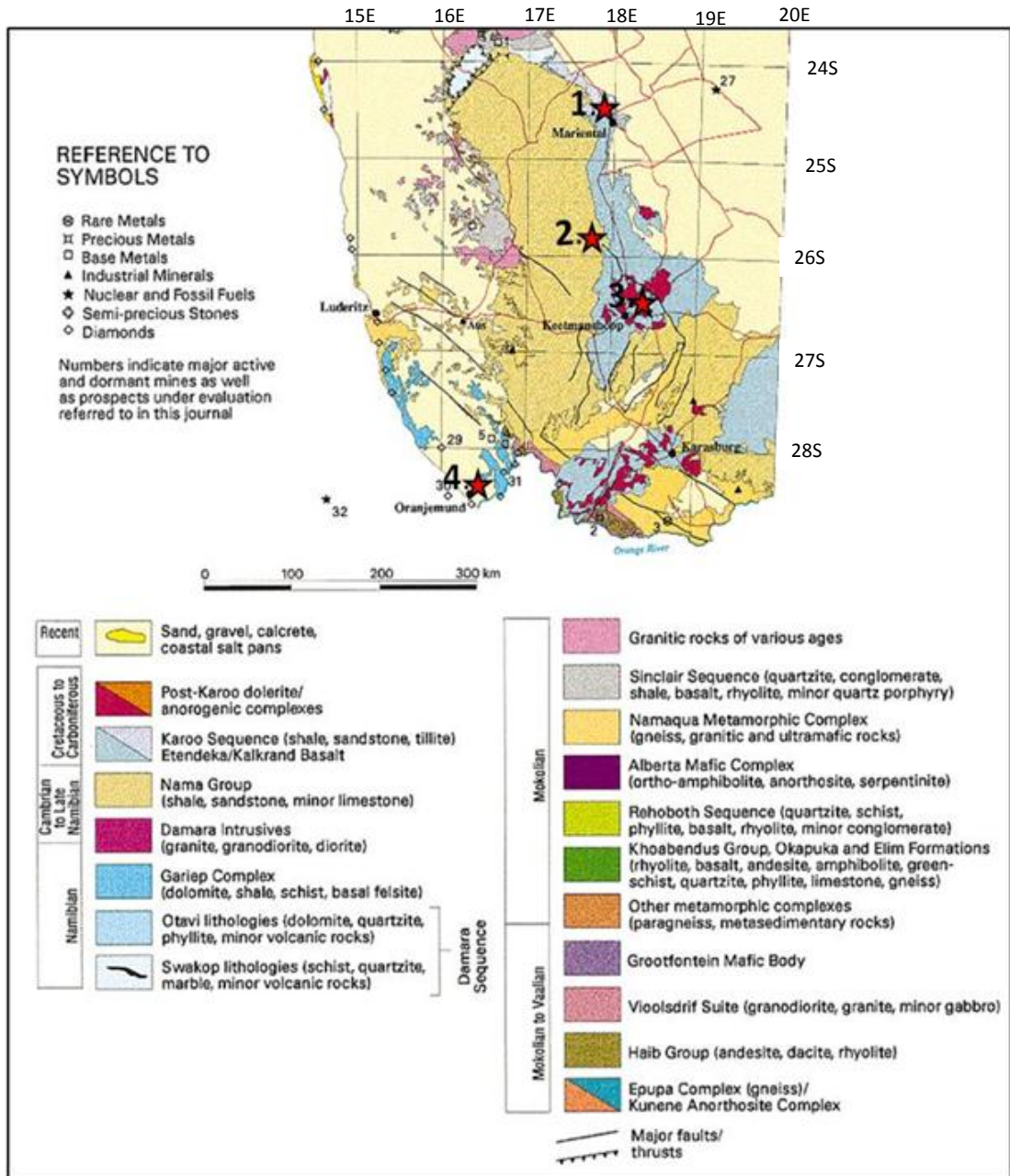


Figure 71: Generalized Geological Map of Southern Namibia (modified after Geological Survey of Namibia). Note that the red stars marked 1 to 4 represents the outcrop visited during the field excursion. Kalkrand Formation is marked with a red star marked 1, Ganigobis shale member (Star marked 2), Whitehill Formation on farm Spitzkoppe (star marked 3) and Oranjemund (Star marked 4).

### 5.2.2 Ganigobis Shale Member

The dark grey laminated Ganigobis Shales located 018°00.524'E, 25°49.660'S with an elevation of 929 m above sea level lies on the west bank of the Fish River capped by Kalahari sediments which protects the shales from erosion (Figure 72). The Ganigobis Shale Member belongs to the uppermost section of the third glaciation sequence of the Dywka Group. Cone shaped calcareous concretions and volcanic tuff ash were observed at this outcrop which demonstrates that this rock unit was deposited in anoxic environment (Figure 73).

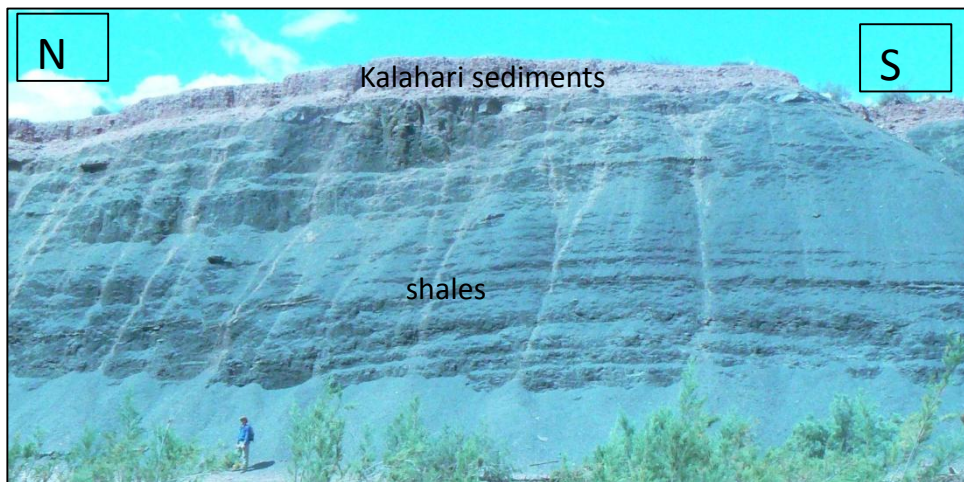


Figure 72: Dark grey shales of the Ganigobis Shale Member capped by Kalahari sediments.

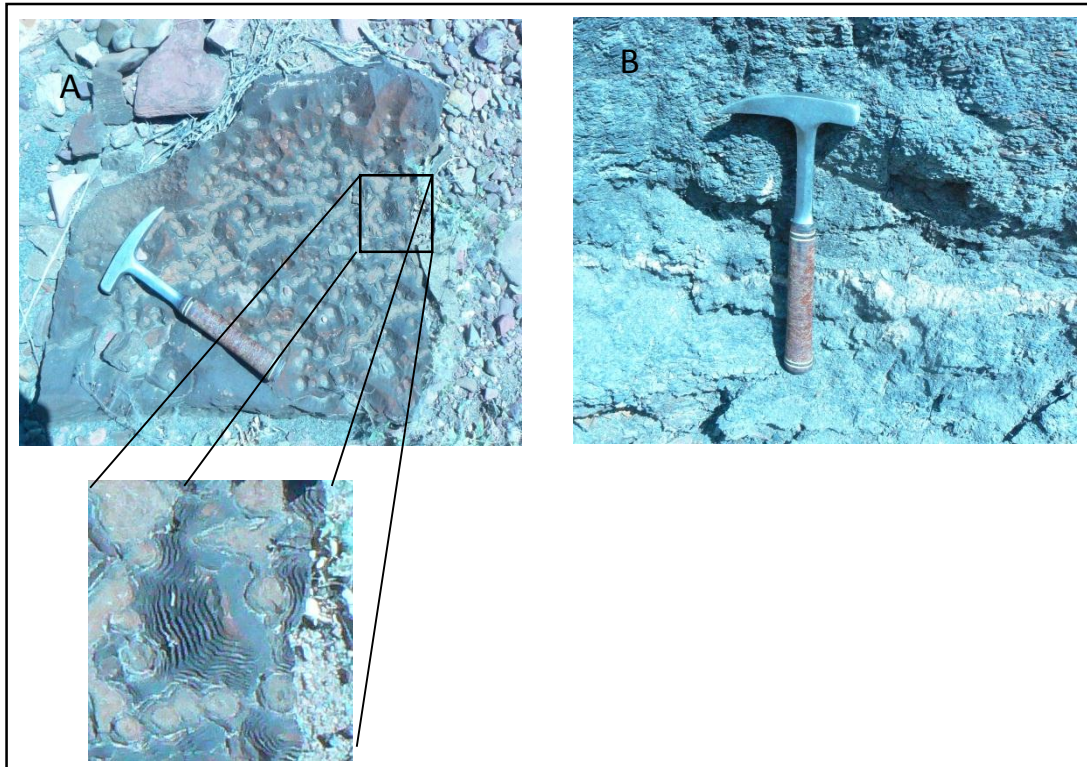


Figure 73: A) Cone shaped calcareous concretions observed in Ganigobis area.

B) Light coloured thin layer of volcanic ash in the Ganigobis shale outcrop.

### 5.2.3 Whitehill Formation

The light grey Whitehill shales located 018°30.504'E, 26°24.026'S on farm Spitzkoppe north east of Keetmanshop with an elevation of 1012 m belongs to the Karoo Supergroup (Figure 74A). The boreholes drilled in this area show that the shale rock units which are not exposed to the surface are completely black in colour. *Mesosaurus tenuidens* fossils were observed preserved in the shale (Figure 74B).

Therefore, the age of the Whitehill Formation can be deduced from the presence of the Mesosaurus, which is a free-swimming neotonic reptile that existed during the lower Permian period (Miller, 2008). The Whitehill Formation has a lower gamma ray compared to the overlying and underlying shales, it also has a lower density due to high hydrocarbon content with an average TOC of 4.3% (Miller, 2008). The Whitehill Formation in the Karoo Supergroup is oil-prone and tiny black inclusions of liquid oil were observed in clear quartz crystals on farm Ausserkjer 147 by Miller, 2008.

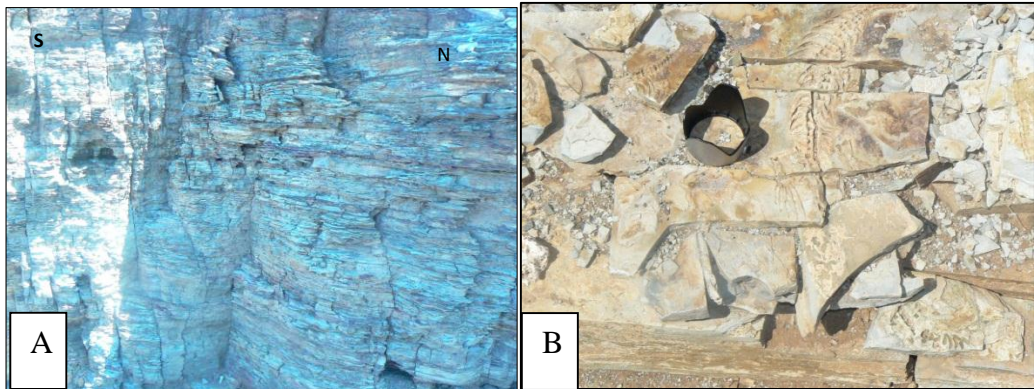


Figure 74: A) Jointed weathered light grey shales of the Whitehill Formation . B) Mesosaurus fossil preserved in sandstone.

#### 5.2.4 Kalkrand Formation

The outcrop located at 017°50.430'E, 24°28.809'S in the Hardap Dam area comprises of red sandstones interbedded with Kalkrand weathered flood basalts of mid-Jurassic age (180 Ma). The sandstones show sets of boudinage and planar lamination (Figure 75). These are medium grained (0.5 to 0.8 mm) sandstones which are mainly quartz dominated with minor feldspar grains indicating that it was deposited from a near source. Foresets beds within the sandstone are dipping at 140° South East at a dip angle of 22°. The fine sets of laminations and the absence of wave ripples at this outcrops symbolizes that it's an aeolian deposit. A thin layer of red sandstone interlayered with basalt dipping to the north east was also observed (Figure 76).

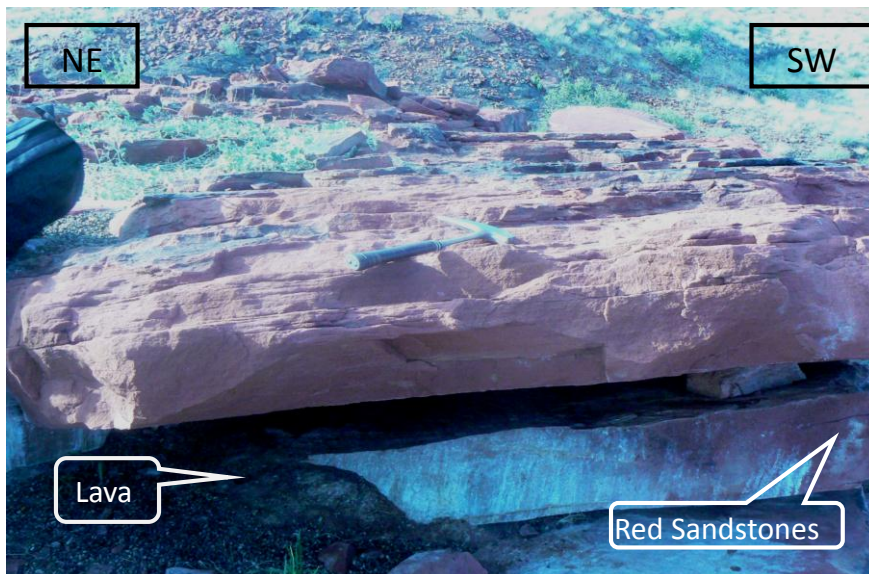


Figure 75: Planar laminated red sandstone interbedded with kalkrand flood basalts.

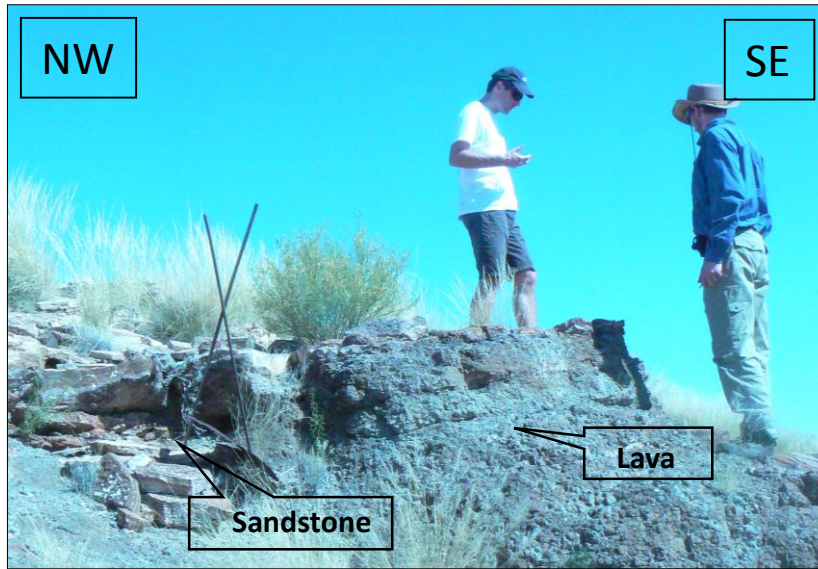


Figure 76: Thin layers of red sandstone interbedded with basalts dipping to the north east.

### 5.2.5 Orange River System

The Perennial Orange River is situated along the border of South Africa and Namibia and it originated from the Lesotho highlands, an area with high rainfall (Figure 77). The predominantly braided and meandering Orange River overlies the Precambrian bedrock.



The Orange River Mouth is located at GPS location of 28°37.092'S, 06°26.922'E South East of Oranjemund Mine Town with an elevation of 6m above mean sea level.

The Orange River system has been supplying sediments to the Orange Basin during the post-rift evolution which is from Mid-Aptian to present day which is also evident on seismic profile. The uplift of the Southern African subcontinent during the Early Cretaceous to late Early Miocene times greatly influenced the onshore sediment supply to the Orange Basin. The Kudu wells has shown that the Tertiary unit dominantly consist of claystones (shales) which indicates that the Orange River was eroding low quantity of rocks during this time , as result little sand was deposited offshore. The evidence for decreasing in the rate of the uplift and erosion during Tertiary is evident on seismic profiles which show that the Cretaceous sediments are thicker than the preserved Tertiary sediments.

The Tertiary sediments thickens in the deeper offshore, this is an indication that the accumulation of sediments during this time was influenced by the accommodation space.

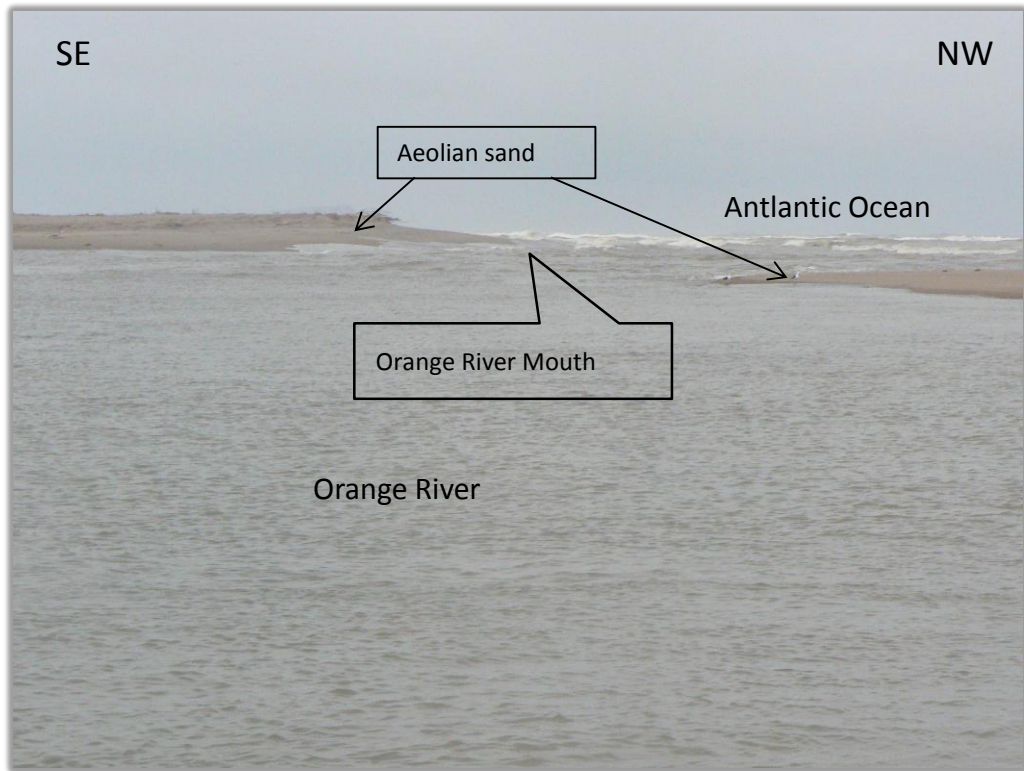


Figure 78: Picture showing the Orange River Mouth.

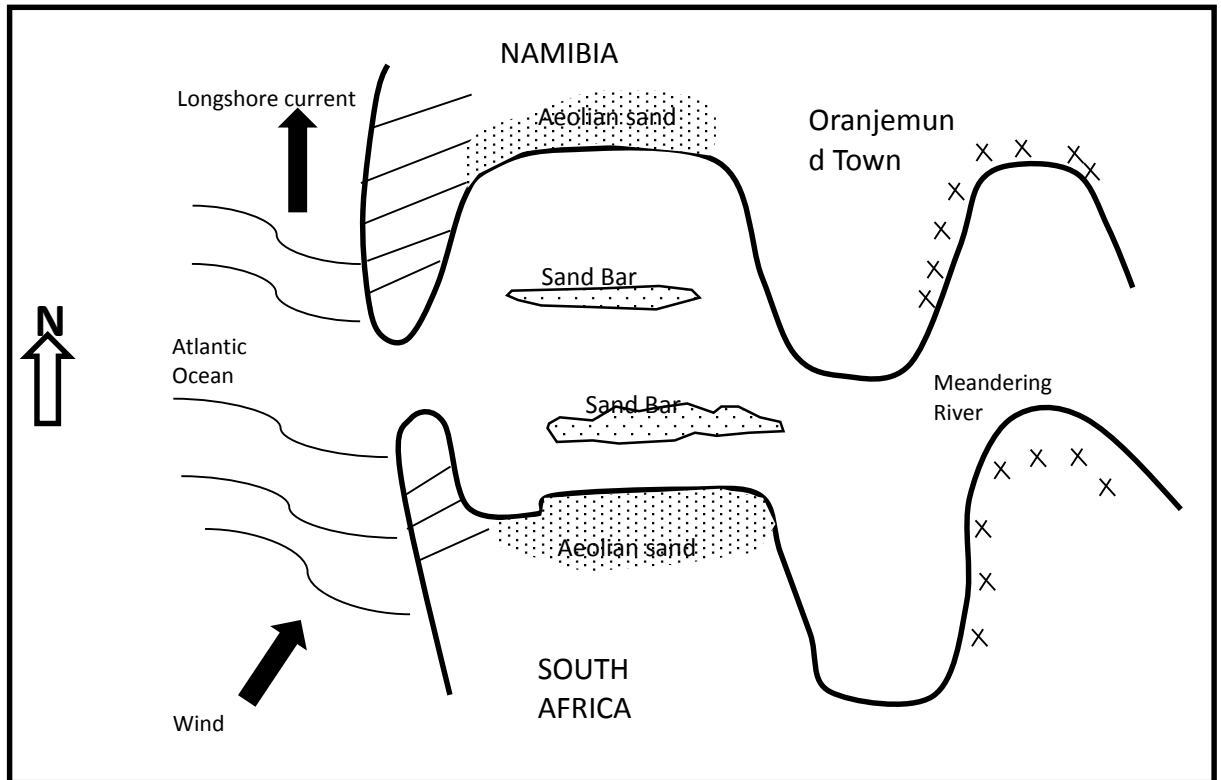


Figure 79: Schematic diagram of the Orange River system.

The geology of Orange River Mouth is mainly a mixture of unconsolidated fluvial and aeolian deposits. The aeolian sands consist of thin layers of coarse high (<2mm) energy sand interlayering with thick layers of fine grained material (Figure 80 D & E). The interlayering of coarse and fine grained materials resulted from wind erosion of fine material leaving behind coarse material (Figure 80A).

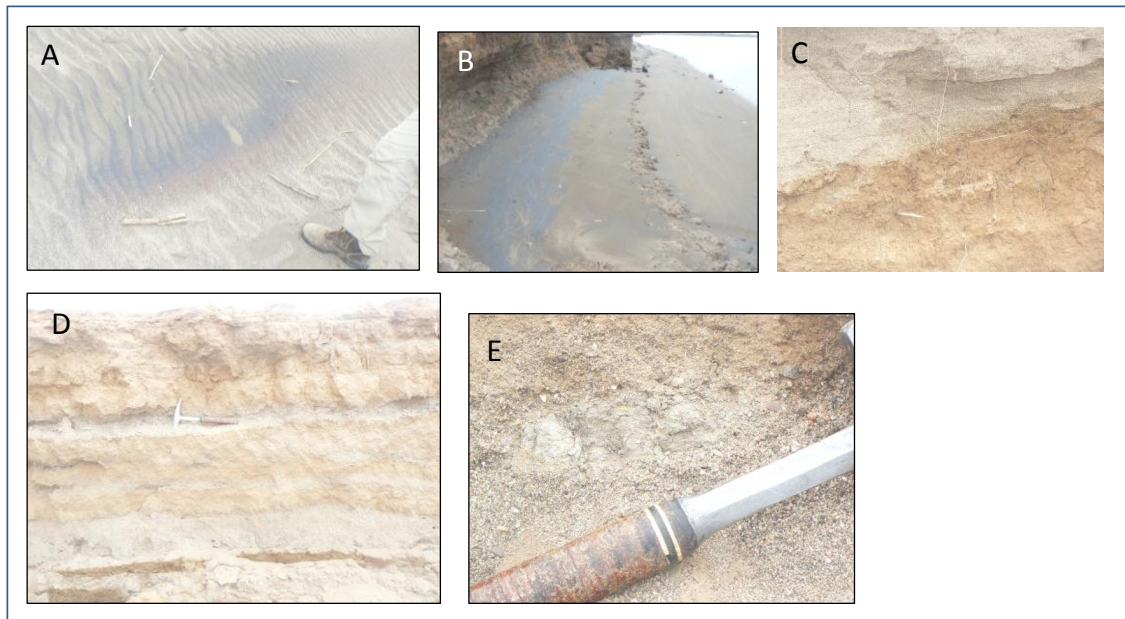


Figure 80: A. Heavy minerals sand deposits in Aeolian sand along bank of the Orange River, B. Heavy minerals deposited on the bank of the river in fluvial sand, C. mixture of fluvial and Aeolian sand at the bank of the Orange River, D. interbeds of high energy (coarse) and low energy (fine) material.

### 5.2.6 Summary

In general, the onshore analogues resemble the depositional environments of the offshore source and reservoir units, but are not exact time-stratigraphic equivalents.

The interlayering of Kalkrand sedimentary rock units and volcanic is similar to that of the Kudu Reservoir. However, the presence of feldspar grains in the sandstone indicates that these sediments were deposited from a near source or dry environment retarding chemical weathering. However the environment of deposition for the Kalkrand sands differs from that of the Kudu reservoir. Since, the presence of current ripples within the Kalkrand sandstone confirms a fluvial system at work during sediment deposition. While the Kudu reservoir is considered to be aeolian sand deposits.

The depositional environment of the Ganigobis Shale Member is similar to that of the Aptian source rock of the Orange Basin. They were both deposited in anoxic environment.

The Whitehill Formation of the Karoo Supergroup is considered to be equivalent to the pre-rift Karoo oil-prone source rock in the Orange Basin (Bray et al., 1998). The study of the Whitehill Formation can provide an insight in the characteristics of the Pre-rift source rock of the Orange Basin. Since, none of the wells in the Orange Basin have penetrated the pre-rift section. Therefore, Orange Basin pre-rift source rock is expected to have low gamma ray and density similar to that of the Whitehill Formation, since it expected to have high hydrocarbon content.

The Orange River has been supplying sediments to the Orange Basin offshore since early Cretaceous, which is evident on seismic profiles. The sediment supply to the Orange Basin was enormous during Cretaceous time and deteriorated during Tertiary times. This is also evident on seismic as the Cretaceous section is much thicker compared to the Tertiary section. Therefore, uplift and subsequent massive sediment supply resulted high volumes of sediments being deposited offshore during Cretaceous. The Base Tertiary marks the period at which the rate of sediment supply began to subside. The decreasing sediment supply during Tertiary is due reduced uplift in the Orange River catchment.

## **CHAPTER 6: CONCLUSIONS**

The geometry of the Orange Basin is controlled by tectonic evolution, sediment supply and eustasy. The initial Basin development involves onset rifting during the Late Carboniferous to Mid-Jurassic (Pre-rift phase). The rifting continued during Syn-rift phase coupled with regional lava eruptions during Early Jurassic and Early Cretaceous, regional uplift and then block rotation. This was followed by drifting of the South American and the African plate during Early Cretaceous time (Barremian to mid-Aptian) marking the initial opening of the Atlantic Ocean. This phase also marks the transition from non-marine to marine environments in the Basin. The pinch-outs occurring at the stratigraphic level just below the Early Cretaceous sequence indicates end of the Syn-rift phase. The onlapping strata on the Early Cretaceous unconformities implies drowning of topography during a transgressive system tract.

The Orange River has been supplying sediments to the Orange Basin since the Early Cretaceous and it still contributes significantly to sediment deposition in the Basin. During the Aptian to Turonian sediments were largely deposited to the area near shore (shelf) compared to younger stratigraphic levels which show large sediment thickness at the basin slope. The uplift of the Basin margins and associated block rotations occurred during the late drift phase. The herewith enhanced Basin topography resulted in rapid sedimentation in the Turonian-Santonian interval, collapse of the Cretaceous delta, a mass transportation of sediments downslope, with a detachment evident at the Turonian unconformity on seismic profiles. Table 5 summarizes stratigraphic levels of depositional environments and associated source and reservoir facies.

Table 5: Outline of depositional environments and associated source and reservoir facies in the Orange Basin.

<b>SEQUENCE</b>	<b>AGE</b>	<b>DEPOSITIONAL ENVIRONMENT</b>	<b>POTENTIAL SOURCE &amp; KEROGEN TYPE</b>	<b>RESERVOIR TYPE</b>
Pre-Rift	Late Carboniferous-Mid Jurassic	Mostly continental (assumption based on onshore analogues)	Oil; Type I and II	unknown
Syn-Rift	Late Hauterivian and Early Barremian	Lacustrine	Oil; Type I & II	Lacustrine sandstone
Early Drift	Early-Barremian-Aptian	Anoxic, restricted marine	Gas & oil; Type II	Aeolian sandstone inter-fingering with volcanics.
Late Drift	Cenomanian-Turonian	Anoxic, restricted marine	Gas & oil; Type II and III	Fluvial sands

The basin hosts both, stratigraphic and structural plays which were identified from pre-rift up to the Tertiary. Source rock intervals were predicted at Pre-rift, syn-rift, Barremian-Aptian and Turonian. However, only the syn-rift, Barremian-Aptian and Turonian have been proven by offshore wells. All of these source rocks are matured

except for the Turonian. The reservoir intervals occur in the syn-rift sequence, in the Barremian (early-drift), furthermore potentially in mid-Cretaceous sandstones possibly hosted in graben structures, as well as in Late Cretaceous prograding wedges. The southern Etendeka province exposes possible onshore analogues to the Kudu reservoirs. There occur sandstone-lava inter-fingering types of reservoir of analogues, including sections of good reservoir continuity but also isolated reservoir units. In the Huab Basin of the southern Etendeka province thickest and lateral continuous aeolian sands of good reservoir quality (main erg of Jerram et al, 1999) occur directly beneath the base of the lava succession. This is an important observation in terms of potential reservoir sands that may also occur beneath the lava succession in the Orange Basin. So far none of the exploration wells has penetrated the lava succession.

The Orange Basin contains a number of large structural closures at Turonian to Barremian stratigraphic levels which potentially represent hydrocarbon traps. Stratigraphic traps, such as wedge-outs, onlaps, unconformity trap types, have also been identified within various levels in this Basin.

The southern part of the Basin is more prospective compared to the northern part, because it attains thick sediment accumulation which augments source rock maturity. It also consists of toe thrust plays similar to that of a producing field in Brunei. Several stratigraphic and structural closures occur at this part of the Basin.

## RECOMMENDATIONS

- Improved and updated maturity modelling of Orange Basin source rocks is required to effectively locate more prospective areas in the Basin. Enhanced knowledge on the maturity of the Basin will be achieved with the incorporation of recently drilled wells in the Basin once they become non-proprietary. The 2012 Moosehead well located to the west of the Kudu will enhance the knowledge on the geology of the Basin to the west of Kudu, providing insight in deep water plays. While the 2012 Kabeljou well drilled to the North-East of Kudu will provide insight on the shelf plays north of Kudu.
- A Basin modelling study is also required to identify source kitchens and migration pathways.
- In order to identify prospects on block size level more 2D seismic survey should be incorporated in the study.
- The upcoming study of Orange Basin well cores will reveal the architecture of the Kudu reservoir rock including information on the porosity and permeability of reservoir rocks at different stratigraphic intervals. This will also give information the TOC,  $R_0$ , and rock-eval parameters, seal strength and composition of different rock strata.
- The integration of magnetic and gravity data will enhance the identification rocks types present in area with little well control, especially in deep waters.
- Exploration companies undertaking search for hydrocarbons in this Basin should be encouraged to drill deep wells to test the syn-rift plays. Those wells

could encounter possible reservoir sands underlying the volcanic succession as observed onshore in the Huab Basin.

## REFERENCES

- Abreau V. dos santos, (1998): Geological Evolution of Conjugate Volcanic Passive Margins: Pelotas Basin (Brazil) and Offshore Namibia (Africa); Implication for Global Sea-level changes. *A Thesis submitted in partial fulfilment of the requirements for the degree Doctor of Philosophy*, Rice University, Houston, Texas, USA.
- Adeniyi, A.S, Akinsehinwa, A. & Oluwasen, F.A. (2009): Source Rock Potential of Selected Shale Samples from Orange Basin, South Africa. *Online Journal for E & P Geoscientists*, University of Western Cape, South Africa.
- Allen, P.A. & J.R. Allen (2013), Basin Analysis – Principles and Applications to Petroleum Play Assessment, 3<sup>rd</sup> edition, Wiley-Blackwell, 619pp.
- Ashcroft w. (2011): A petroleum Geologist's Guide to seismic Reflection, Wiley-Blackwell.
- Aizawa,M., Bluck, B, Cartwright, J., Milner, S., Swart, R & Ward, J. (2000): Constraints on the geomorphological evolution of Namibia from offshore stratigraphic record. *Communications of the Geological Survey of Namibia*, 12, 337 – 346.
- Baker Hughes INTEQ (1996): Final Well Report, Shell Exploration and Production, Well Kudu 4, Offshore Namibia.
- Bagguley, G. J. (1996): The Application of Seismic and Sequence Stratigraphy to the post-rift Megasequence Offshore Namibia. *Unpublished doctoral dissertation*, Oxford Brooks University, Oxford, UK.

- Bagguley, G. J. (1997): Sequence Stratigraphy of the Namibian passive margin. A thesis submitted in the partial fulfillment of requirements of Oxford Brookes University, for Degree of Philosophy, UK.
- Bagguley J & Prosser S. 1999. The Interpretation of Passive margin depositional processes using seismic stratigraphy: examples from offshore Namibia. The Oil & Gas Habitats of the South Atlantic. *Geological Society Special Publications*, 153, 321-344.
- Barnes, A. E., (2007): A tutorial on complex seismic trace analysis: *Geophysics*, Vol. 72, No.6, W33 – W43 p.
- Barton, K.R., Muntingh, A. & Noble R. D. P. (1993): Geophysical and Geological Studies Applied to Hydrocarbon Exploration on the West Coast Margin of South Africa. *Extended Abstract of the Third International Congress of Brazillian Geophysical Soiciety*, Rio de Janeiro, Brazil, Nov 7-11.
- Bisaso, I., (2011): Calibration of Seismic and Well Data: Improved quantitative seismic reservoir characterization of the Triassic to middle-Jurassic Gullfaks reservoir units of the northern North Sea, *Masters of Science Thesis*, University of Bergen.
- Bluck, B.J., De Wit, M.C.J., Ward, J.D (2005): Diamond mega-placers: Southern Africa and the Kaapvall craton in a global context. *Mineral Sources and Earth Evolution, Geological Society, London, Special publication*, 248, 213-245.
- Bray R., Lawrence S. & Swart R. (1998): Source Rock, maturity data Indicate Potential off Namibia. *Oil and Gas Journal*.10, 84-89.
- Brown, L.F. & Fisher, W.L. (1977): Seismic Stratigraphy interpretation and Petroleum Exploration, *AAPG Continuing Education Notes*.

- Craeney, S. and Passey, O.R., 1995, Recurring patterns of total organic carbon and source rock quality within a sequence stratigraphic framework, *AAPG Bulletin* 77, 386-401.
- Campher, R.C., di Primio, R., Domoney, R. & Van der Spuy D. (2009): Geological Modelling of the offshore Basin, Est Coast of South Africa, *2<sup>nd</sup> Edition*, Cape Town, South Africa.
- Cartwright, J., Corner, B. & Swart, R. (2002): *Volcanic Passive Margin of Namibia, a Potential Fields Perspective*. Geological Society of America, Special Paper, 362, 203 – 220.
- Cartwright, J., Corner, B. & Swart, R. (2005): Conjugate Margins of the South Atlantic. Unpublished Report, Namibia-Pelotas, Windhoek, Namibia.
- Catuneanu, O. (2006): Principles of Sequence Stratigraphy, Elsevier, 375pp.
- Chevron, (1974): Geological Final Report – Kudu 1, Offshore block 9A, South-West Africa.
- Clemson, J. (1997): Segmentation of the Namibian Passive Margin. A Thesis submitted for the Degree of Doctor of Philosophy, University of London (Imperial College of Science, Technology and Medicine), Uk.
- Clemson, J., Cartwright, J. & Swart, R. (1999): The Namib Rift – a rift of possible Karoo age, Offshore Namibia, *Geological Society, London*, Special publication, 153, 381 – 402.
- Corbett, I. & Burell, B. (2001): The Earliest Pleistocene (?) Orange River fan-delta: an example of successful exploration delivery aided by applied Quaternary research in diamond placer sedimentology and palaeontology, Oranjemund, Namibia.

- Corner C., Shaw J.H. & Suppe J. (2005): Seismic Interpretation of Contractional Fault-Related Folds – *An AAPG Seismic Atlas, Studies in Geology #55*. The American Association of Petroleum Geologists, Tulsa, Oklahoma, USA.
- Dow, W.G. & Leslie, B.M. (1994): The Petroleum System from Source to Trap. *American Association of Petroleum Geologist, Memoir, 60, 7 - 75*.
- Duncan, A.R., Milner, S.C. & Jerram, D.A. (1998): International Volcanological Cogress, Magmatic Diversity: Volcanoes and their Roots, Field Excursion C4, Southern Volcanism, northwestern Namibia, Cape Town, South Afrca.
- Duncan, R.A., Hooper, P.R., Rehacek, J., Marsh, J.S., Duncan, A.R., (1997). The timing and duration of the Karoo igneous event, southern *Gondwana*. *Journal of Geophysical Research* 102, 18127-18138.
- Frimel, H. E., Basei, M.S. & Gaucher, C. (2010): Neoproterozoic Geodynamic Evolution of SW-Gondwana: A Southern African Perspective, *Int J Earth Sci* (Geol Rundsch, 2011), 100, P323-354.
- Fugro Robertson, (2010): Southern Africa Petroleum Geological Evaluation-Namibia Report. Llandudno, North Wales,UK.
- Gearhart Geodata Services, (1988): Well Completion Report - Kudu-3 prepared for SWAKOR, Orange Basin, West Coast, South West Africa/Namibia.
- Geological Survey of Namibia: Generalised Geological Map of Namibia.
- Gerschütz, S. (1996): Geology, volcanology, and petrogenesis of the Kalkrand Basalt Formation and the Keetmanshop dolerite complex, southern Namibia. *Unpublished doctoral dissertation*, University of Würzburg, Würzburg, Germany.

- TP., Hinz K., Eldholm O., Meyer H., Neben S. & Skogseid J. (1997): South Atlantic Volcanic Margins. *Journal of The Geological Society*, 154, 465-470.
- Gladchenko TP, Skogseid J & Eldhom O. 1998. Namibia Volcanic Margin. *Marine Geophysical Researches*, 20 (4), 313-341.
- Green, P.F. (1988): Offshore Namibia Thermal History Reconstruction, Burial/uplift History and Hydrocarbon Generation History Assessed using *AFTA® and Vitrinite Reflectance Data from the Kudu 9A-2, Kudu 9A-3, 2012/13-1 and 2213/6-1 Wells and two DSDP sites*, Geotrack Report #707, Victoria, Australia.
- Hirsch, K.K. (2008): Integrating structural and Sedimentological observations with numerical lithospheric models to assess the 3D evolution of the South African Continental passive margin, *Scientific Technical Report STR08/13*, Berlin.
- Holzförster, F., Stollhofen, H. & Stanistreet, I.G. (1999): Lithostratigraphy and depositional environments in the Waterberg-Erongo area, central Namibia, and correlation with the main Karoo Basin, South Africa.- *J. African Earth Sci.*, 29, 105-123.
- Houghton, M.L. (1993): Summary of Play Concepts, License 2815, Offshore Namibia. Unpublished report, National Petroleum Corporation of Namibia (NAMCOR), Windhoek, Namibia.
- Howell, J. & Fitzsimmons, R. (1997): An Introduction to Clastic Sequence Stratigraphy, BSRG Short Course, *Notes on seismic stratigraphy by Sarah Prosser*, Saga Petroleum Research Lab, Oslo, Norway.
- HRT Petroleum, (2008): Competent Person's Report, prepared for Chariot Oil & Gas Limited. Rio de Janeiro, Brazil.

- Hubbard, R.J. (1988): Age and Significance of Sequence Boundaries on Jurassic and Early Cretaceous Rifted Continental Margins. *Bulletin American Association Petroleum Geologists*, 72, 49-72.
- Hyne, N.J (2001): Non Mechanical guide to Petroleum Geology, Exploration, Drilling and Production, Second Edition, Tulsa, Oklahoma, USA.
- Jerram, D.A., Mountney, N. & Stollhofen, H. (1999): Facies Architecture of the Etjo Sandstone Formation and its Interaction with the Basal Etendeka Flood Basalts of Northwest Namibia – Implication for Offshore Prospectivity. *Geological Society, London, Special Publications*, 153, 367 – 380.
- Khan S.,(2005): Evolution of thr Orange Basin Rift Zone, Offshore Namibia. Independent Msc Petroleum Geoscience Project. Imperial College, London.
- Koopman, H., Franke, D., Schreckenberger, B. Schulz, H. Hartwig, A., Stollhofen, H & Di Promio, R (2013): Segmentation and Volcano-Tectonic Characteristics along the SW Africa Continental Margin, South Africa, as derived from Multichannel Seismic and Potential Field Data. *Marine & Petroleum Geology*, **50**, P22-39.
- Light M.P.R., MaslanyinJ. & Banks N.L., (1992): New Geophysical Evidence For Extensional Tectonic On The Divergent Margin Offshore Namibia. (eds) Magmatism and the causes of continental Break-up, *Geological Society Special publication*, **P 257-270**.
- Marsh, J.S., Swart, R.S. & Phillips, D (2003): Implications of a new  $^{40}\text{Ar}/^{39}\text{Ar}$  age for a basalt flow interbedded with the Etjo Formation, Northeast Namibia, *South African Journal of Geology*, 106, p. 281-286,

- Miller R. McG. (2008): The Geology of Namibia - Volume 1, 2 & 3. *Ministry of Mines and Energy, Geological Survey, Windhoek, Namibia.*
- Miller R. McG. (2008): Namibia Hydrocarbon Exploration Terms and Opportunities. *Proceedings of SADC Energy Sector Petroleum Conference, Windhoek, Namibia P113-135,*
- Ministry of Mines and Energy (1990): Communication of Geological Survey of Namibia, The Kudu Offshore Drilling Project, **6.**
- Mitchum, R.M., Vail, P.R. & Thompson, S. (1977): Seismic stratigraphy and global changes in sea level. Part 2: the depositional sequence as a basic unit for stratigraphic analysis. In: C.E. Payton: *Seismic Stratigraphy – Applications to Hydrocarbon Exploration* (pp. 53-62), *American Association of Petroleum Geologist Memoir, 26.*
- Mitchum Jr, R. M., Vail P. R, and Sangree J. B. (1977b): Seismic stratigraphy and global changes of sea level, part 6: Stratigraphic interpretation of seismic reflection patterns in depositional sequence, in C. Payton, ed., *Seismic stratigraphy – Application to hydrocarbon exploration: AAPG Memoir 26, 49-212 p.*
- Mountney, N., Howell, J., Flint, S & Jerram, D. (1998): Aeolian and alluvial deposition within the Mesozoic Etjo sandstone Formation, northwest Namibia. *Journal of African Earth Sciences, 27(2), 175-192.*
- Muntling a., & Brown, Jr L.F. (1993): Sequence Stratigraphy of the Petroleum Plays, Post-rift cretaceous Rocks (Lower aptian to Upper Maastrichtian), Orange Basin, West Offshore, South Africa. *AAPG Memoir.*
- Nichols G. (1999): *Sedimentology & Stratigraphy, Second Edition, Wiley-Blackwell.*

- Nopec A.S (1991): The Hydrocarbon Potential of the Sedimentary Basins offshore Namibia, prepared for Nopec directors and Ministry of Mines and Energy-Namibia.
- Norsk Hydro Namibia (1998): Regional Evaluation Report, Namibia Licencing Round 008 prepared for NAMCOR.
- Paton, A.P., Primio, R., Kuhlmann, G., Van der Spuy, D & Horsfield, B. (2007): Insights into the Petroleum Systems - Evolution of the Southern Orange Basin, South Africa. *South African Journal of Geology*, 110, 261 – 274.
- Petroleum Agency SA (2007): Petroleum Exploration Information and Opportunities-The Orange Basin, P11- 15
- Petroleum Agency SA (2003): South African Petroleum Exploration Opportunities – The Orange Basin, P11 – 15.
- Quad Consulting Ltd./EPI (1996): Seismic Interpretation and Petroleum Prospective Review of the Luderitz Basin, offshore Namibia.
- Roux, J., Van der Spy, D. & Singh, V. (2004): Deep Drilling on the Way Offshore South Africa. *Unpublished Report, Petroleum Agency of South Africa (PASA)*, Parow, South Africa.
- Seranne, M. & Anka, Z.: South Atlantic Continental Margin of Africa, A comparison of the tectonic vs climate interplay on the evolution of equatorial West Africa and SW Africa margins. *Journal of African Earth Sciences*, 43(1), 283 – 300,
- Shenk H.J. et al. (1997) Kinetics of petroleum formation and cracking, in: Welte D.H. et al. (editors) *Petroleum and basin evolution*, Berlin, Springer, 233-269.
- Shell, (1999): Well 2814/11-4 (Kudu 5) Petroleum Engineering – *End of Well Report* SEPN/DGL/SDT.

- Shell, (2002): Subsurface Evaluation of the Kudu Licence, Block 2814A, Offshore Namibia.
- Schmidt, S. (2004): The Petroleum Potential of the Passive Continental Margin of the South-Western Africa – Basin Modelling Study. *Unpublished report, National Petroleum Corporation of Namibia (NAMCOR)*, Windhoek, Namibia.
- Schümann, T.K. (2002): The Hydrocarbon potential of the Deep Offshore along the Argentine Volcanic Rifted Margin - a numerical simulation. *Unpublished doctoral dissertation*, University of Aachen, Aachen, Germany.
- Simon Petroleum Technology Training Centre, (1994): Play Fairway Definition (Basin Analysis for Explorationists). Unpublished Course Book, Havana, Cuba.
- .
- Stanistreet, I.G. & Stollhofen H. (1999): Onshore Equivalents of the Kudu Gas Reservoir in Namibia. In Cameron, N.R., Bate, R.H. & V.S Clure (Eds.), *The Oil and Gas Habitats of the South Atlantic* (pp. 345-365). *Special Publication Geological Society of London*, 153.
- Soekor, (1989): Summary of Wellsite Data – Kudu 9A-2, Orange Basin, West Coast, South West Africa/Namibia.
- South African Committee for Stratigraphy (SACS) 1980, Part I (Comp. Kent, L.E): Lithostratigraphy of the Republic of South Africa, South West Africa/Namibia and Republic of Bophuthatsana, Transkei and Venda., *Handbook of Geological Survey of South Africa*, 8, PP660.

- Stewart, J., Watts, A.B. & Bagguley J.G. (1999): Three-Dimensional subsidence analysis and gravity modeling of the continental margin offshore Namibia, *Geophysical Journal International*, 141 (3), 724-746.
- Stollhofen, H., (1999): Karoo synrift-deposition and its tectonic control at the evolving continental margin of Namibia. *Dtsch. Geol. Ges.*149, p. 519-632.
- Timetrax, (2000): A Biostratigraphic Study of the Kudu 9A-3 Well, Orange Basin, Offshore Namibia.
- Uliana, M.A., Biddle, K.T. & Cerdan, J. (1989): Mesozoic Extension and the Formation of Argentine Sedimentary Basin. In: *Extensional Tectonics and Stratigraphic of the North Atlantic Margins*. Eds. Tankard A.J & Balkwill, H.R. *AAPG Mem.*46, P599-614.
- Vail, P.R., Audemard, F., Bowman, S.A., Eisner, P.N. & Perez-Cruz, C. (1991): The stratigraphic signatures of tectonics, eustasy and sedimentology - an overview. In Einsele, G., Ricken, W. & A. Seilacher (Eds.), *Cycles and events in stratigraphy* (pp. 617-659). Berlin: Springer.
- Van der Spuy, D. (2005): Prospectivity of the Northern Orange Basin, Offshore South Africa- *World Petroleum Congress*, South Africa.
- Van der Spuy, D (2000): Organic Maturity and Burial History Modelling in Petroleum Exploration, Offshore, South Africa.
- Van Wogoner, J.C., Mitchum, R.M., Campion, K.M. & Rahmannian, V.D. (1990): Siliclastic Sequence Stratigraphy in well Logs, Core and Outcrop: concepts for high resolution correlation of time and facies. *AAPG Methods in Exploration Series* (7) P55.

- Veritas DGC Limited (2004): Regional Interpretation Report of the Orange Basin 2004 Licensing Area, Namibia.
- Ward, J.D. & Bluck, B.J. (1998): The Orange River: 100 Million Years of Fluvial Evolution.
- Walter, M., Swart, R. & Summons, R. (1996): Oil and Gas Shows Numerous in Nama Basin, Southern Africa, *Oil & Gas Journal*, 94(48), PP 76-80.
- Wickens, H. de V & McLachlan ,I.R (1990): The stratigraphy and sedimentology of the reservoir interval of the kudu 9A-2 and Kudu 9A-3 boreholes. *Communications of the Geological Survey of Namibia*,6, 9-22.

### **Electronic References**

www.chariotoiland gas.com, September 2012

<http://www.galpenergia.com/EN/agalpenergia/Noticias/Paginas/Moosehead1exploracionwellresults.aspx>, September 2013).

[www.cgg.com/downloads/flyers](http://www.cgg.com/downloads/flyers)

[www.namcor.com.na](http://www.namcor.com.na) and [www.sunbirdenergy.com.au](http://www.sunbirdenergy.com.au)

<<http://kids.britannica.com/elementary/art-107400>>. *Africa: Orange River basin.*

Map/Still. *Britannica Online for Kids*. Web. 12 Dec. 2014.

## APPENDIX A: GLOSSARY

“**2D seismic**” data acquired in a grid of lines that is relatively broad spaced and is processed in two dimensions.

“**Albian**” geological stage between 112 and 99.6 million years ago. Albian is present in lower Cretaceous (USGS geological time scale).

“**Aptian**” geological stage between 125 and 112 million years ago. Aptian is present in lower Cretaceous (USGS geological time scale).

“**Barrel**” unit of volume measurement used for petroleum and its products, which is a volume of 42 U.S. gallons equivalent to 157 litres.

“**Barremian**” geological stage between 130 and 125 million years ago. Barremian is present in Lower Cretaceous (USGS geological time scale).

“**Basin modelling**” term generally applied to a group of geological disciplines that can be used to study quantitatively the formation and evolution of sedimentary basins, often but not exclusively to aid evaluation of potential hydrocarbon reserves.

“**Biostratigraphy**” branch of stratigraphy which focuses on correlating and assigning relative ages of rock strata by using the fossil assemblages.

“**Block**” commonly used to describe contract areas or tract, as in “Block of land”.

“**Cenomanian**” geological stage between 99.6 and 93.5 million years ago. Cenomanian is present in Upper Cretaceous (USGS geological time scale).

“**Conjugate Margin**” used to describe continental margins (i.e. South Atlantic Margin) which were spreadable in the geological past and at present day shown structural and Bio/Cronostratigraphic correlation.

“**Cretaceous**” geological period between 145.5 and 65.5 million years ago. It is present in Mesozoic (USGS geological time scale).

“**Depocentres**” an area of maximum thickness in a sedimentary basin caused by caused by maximum deposition during a specific geological time frame.

“**Depositional environment**” the area in the Earth’s surface where sediments are deposited and undergo the action of different physical processes such as wind, water or ice; and by the conditions of the location and its climate, such as desert, swamp or river.

“**Discovery**” petroleum having been detected in an exploration well.

“**Eolian**” (*in rocks*) the sedimentary deposits formed by the action of winds.

“**Exploration well**” a well drilled in an attempt to determine conclusively the presence or absence of hydrocarbons.

“**Facies**” the characteristics of a rock unit that reflect its origin and permit its differentiation from other rock units around it.

“**Fault**” a break in the earth’s crust where there has been displacement of one side relative to the other. Sometimes a layer of non-porous rock may be next to an oil-bearing porous interval along a fault and form a trap for the oil.

“**Field**” geographical area under which an oil or gas reservoir has been discovered.

“**Formation**” a certain succession of sedimentary layers that predominantly describe one type or combination of them.

“**Graben**” fault-elongated trough or Block of rock, down-thrown on both sides.

“**Jurassic**” geological period between 199.6 and 145.5 million years ago. It is present in Mesozoic (USGS geological time scale).

“**Lacustrine**” the sedimentary environment of a lake.

“**Lead**” a project associated with a potential hydrocarbon accumulation that is currently poorly defined and requires more data acquisition and analysis in order to be classified as a prospect.

“**Listric faults**” a geological normal fault that is characterized by a curved shape in a 2D section.

“**Maastrichtian**” geological stage between 70.6 and 65.5 million years ago. It is present in Upper Cretaceous (USGS geological time scale).

“**Marine anoxic** (in formation of source rocks) the condition that occurs when the Earth’s oceans become completely depleted of oxygen (O<sub>2</sub>) below the sea surface. These conditions are favourable for the preservation of marine source rocks.

“**Mature source rock**” it is the thermal state that is favorable to the formation of hydrocarbons from the organic matter of a source rock.

“**Mesozoic**” geological era between 251 and 65.5 million years ago. Includes Cretaceous, Jurassic and Triassic periods (USGS geological time scale).

“**Miocene**” geological Epoch between 23.03 and 5.33 million years ago. It’s in Neogene period (USGS geological time scale).

“**Migration pathways**” preferential passageways in sedimentary rocks along which hydrocarbons move due to higher permeabilities and porosity.

“**mmbbl**” million barrels of oil.

“**Neocomian**” geological stage between 145.5 and 136.4 million years ago.

“**Normal faults** a discontinuity that separates Blocks (upper and lower Blocks) that have been displaced with respect to the other. They form under a tensional force field.

“**OM**” Organic matter

“**Oil prone**” the quality of a source rock that makes it more likely to generate oil than gas.

“**Operator**” company that has legal authority to undertake petroleum operations.

“**Palaeoenvironments**” is a terminology that refers to the past setting of a given area that comprised several physical conditions that occurred naturally on earth.

“**Permian**” geological period between 250 to 295 million years ago.

“**Petroleum system**” it is a terminology that includes reservoirs, seals, source rocks, traps and processes such as timing; petroleum generation and migration that define the characteristics of a hydrocarbon accumulation.

“**Pinch-out**” a geometrical description of sedimentary layers whose thickness change laterally in a way that the rocks form wedges inside bedding.

“**Play**”: a geological situation in which a complete petroleum system operates including matured source rocks, migration paths, reservoir rocks and trap.

“**Progradation**” the accumulation of sequences by deposition in which beds are deposited successively basinward because sediment supply exceeds accommodation.

“**Prospect**” a geological or geophysical feature has been characterized with the aid of geological and geophysical data to potentially contain hydrocarbon accumulation.

“**Quasi-Isochronous surface**” surfaces with similar stacking patterns.

“**Reserves**” the amount of economically recoverable oil or gas in a particular reservoir that is available for production.

“**Reservoir**” the underground Formation where oil and gas has accumulated. It consists of a porous and permeable rock to hold the oil or gas, and a cap rock that prevents its escape

“**Sandstone**” sedimentary rock composed mainly of sand-size mineral or rock grains.

“**Santonian**” geological stage between 85.8 and 83.5 million years ago. It is present in Upper Cretaceous (USGS geological time scale).

“**Seal**” a relatively impermeable rock, commonly shale, anhydrite or salt, that forms a barrier or cap above and around reservoir rock such that hydrocarbons cannot migrate beyond the reservoir.

“**Shale**” a fine-grained sedimentary rock whose original constituents were clay minerals.

“**Stratigraphic trap**” way of trapping hydrocarbons which is not dependent on structural entrapment but mostly on lateral changes in rock properties that can seal a reservoir.

“**Structural high**” area where rocks have been elevated due to tectonic activity.

“**Source rock**” a rock rich in organic matter which, if heated sufficiently, will generate oil or gas. Typical source rocks, usually shales or limestones, contain about 1 per cent organic matter and at least 0.5 per cent total organic carbon (TOC), although a rich source rock might have as much as 10 per cent organic matter.

“**TCF**” volume measurement used by the oil and gas industry

“**TD**” is total depth of a well, when drilling has finished.

“**TOC**” (*Total Organic carbon*) the mass of carbon with respect to the total mass of source rock. It is specifically the amount of carbon covalently bonded in organic molecules.

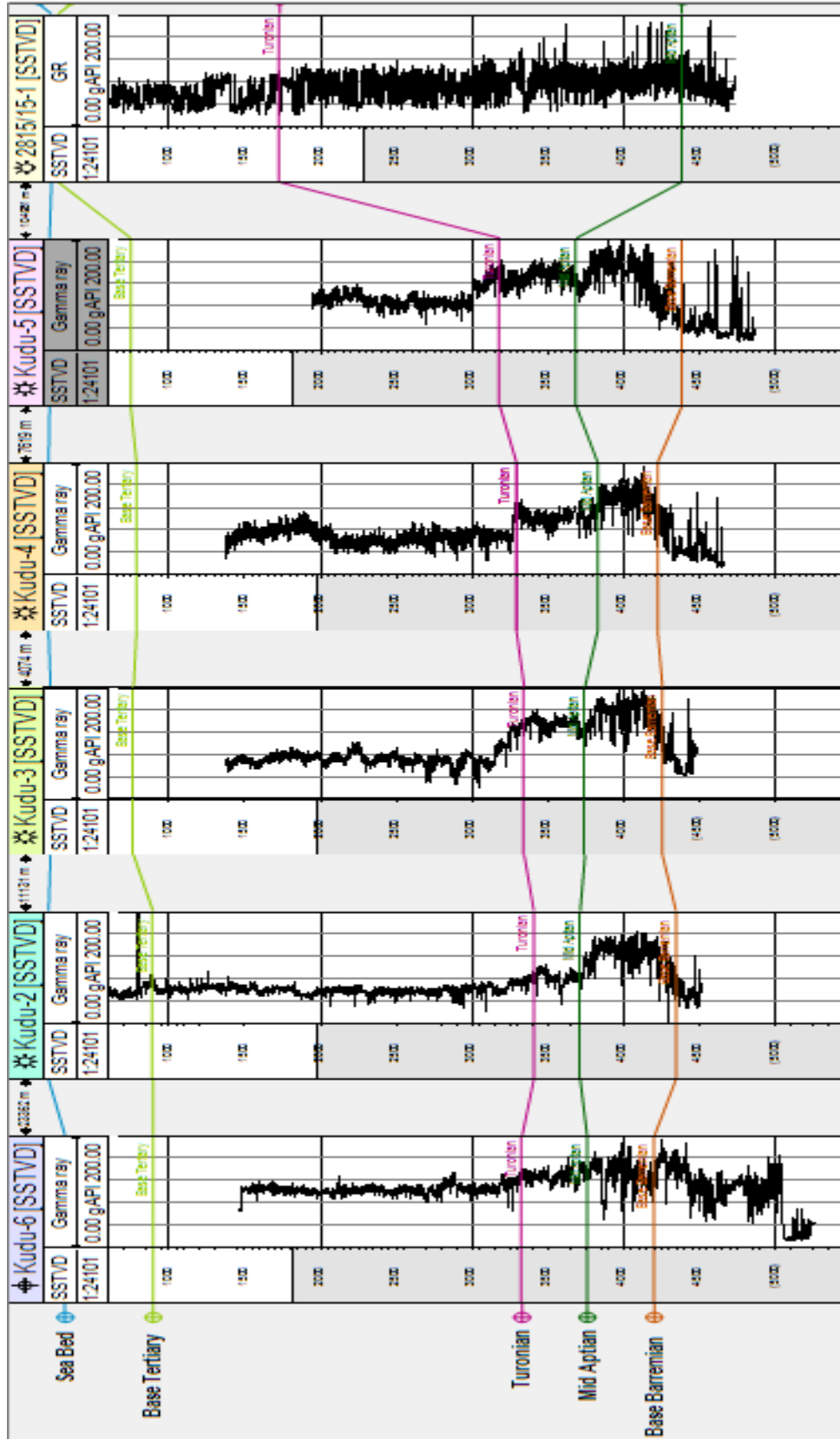
“**Trap**” a configuration of rocks suitable for containing hydrocarbons and sealed by a relatively impermeable formation through which hydrocarbons will not migrate.

“**Turbidite**” sedimentary deposits formed by turbidity currents in deep water at the base of the continental slope and on the abyssal plain.

**“Turonian”** geological stage between 93.5 and 89.3 million years ago. It is present in Upper Cretaceous (USGS geological time scale)



**APPENDIX C: Correlation of Orange Basin wells.**



**APPENDIX D: Well panel correlation for the main kudu field wells (Kudu-1, Kudu-3 and Kudu-4)**

